UNIVERSITY OF CALIFORNIA, SAN DIEGO

Induced pluripotent stem-cell-derived models of sporadic and familial Alzheimer's disease

A dissertation submitted in partial satisfaction of the requirements for the degree Doctor of Philosophy

in

Biomedical Sciences

by

Mason Arthur Israel

Committee in charge:

Professor Lawrence S. B. Goldstein, Chair
Professor Don W. Cleveland
Professor Sylvia M. Evans
Professor Christopher K. Glass
Professor Bing Ren

2011

The dissertation of Mason Arthur Israel is approved, and it is acceptable in quality and form for publication on microfilm and electronically:

_____

_____

_____

_____

_____
Chair

University of California, San Diego

2011

TABLE OF CONTENTS

LIST OF FIGURES AND TABLES

Chapter 1.

Chapter 2.

ACKNOWLEDGEMENTS

I thank Larry Goldstein for his mentorship. I thank past and present members of the Goldstein lab for scientific advice and contributions to an excellent work environment. Lab members who contributed most substantially to my work include Shauna Yuan, who co-developed our differentiation method; Emily Davis, who pioneered the use of the MSD machine; Sol Reyna, who provided experimental assistance; Angels Almenar-Queralt, who let me exploit her wide breadth of scientific knowledge; and Jessica Flippin and Cheryl Herrera, who both excellently managed our lab's stem cell operations. I thank all members of my dissertation committee, and in particular Don Cleveland, for scientific advice and inspiration. I thank the UCSD Alzheimer's Disease Research Center, and in particular Doug Galasko, Mary Sundsmo, Deborah Fontaine, Christina Gigliotti and Judith Rivera, for patient biopsies and data. I thank Ben Yu for teaching us biopsy methods. I thank all biopsy participants for donating a small part of themselves to the pursuit of knowledge. I thank Steve Dowdy and Naohisa Yoshioka for reprogramming vectors. I thank Mark Lawson for statistical advice. I thank BD Biosciences, and in particular Ben Balderas and Christian Carson, for reagents and methods. I thank the California Institute of Regenerative Medicine for offering me a predoctoral fellowship. I thank Hans-Willem Snoeck, my mentor before graduate school, who first introduced me to the world of stem cells. I thank my family and friends for years of support, especially my parents, Michael Israel and Bonnie Schnitta.

Chapters 1, 2 and 3 contain work submitted for publication by authors: Mason A. Israel, Shauna H. Yuan, Sol M. Reyna, Yangling Mu, Christian T. Carson, Fred H. Gage, Anne M. Remes, Edward H. Koo, Lawrence S. B. Goldstein. The dissertation author was the primary investigator and author of this material.

VITA

Education

2003 Sc.B. with honors, Biology, Brown University

2011 Ph.D., Biomedical Sciences, University of California, San Diego

Publications

Israel M.A., Yuan S., Reyna S., Mu Y., Carson C., Gage F., Remes A., Koo E., Goldstein L.S. Induced pluripotent stem-cell-derived models of sporadic and familial Alzheimer's disease. In revision.

Gore A., Li Z., Fung H., Young J., Agarwal S., Antosiewicz-Bourget J., Canto I., Giorgetti A., **Israel M.A.**, Kiskinis E., Lee J., Loh Y., Manos P., Montserrat N., Panopoulos A., Ruiz S., Wilbert M., Yu J., Kirkness E., Belmonte J., Rossi D., Thomson J., Eggan K., Daley G., Goldstein L.S., Zhang K. (2011). Somatic coding mutations in human induced pluripotent stem cells. *Nature* 471(7336): 63-7.

Yuan S., Martin J., Elia J., Flippin J., Rosanto I., Paramban R., Hefferan M., Vidal J., Mu Y., Killian R., **Israel M.A.**, Emre N., Marsala S., Marsala M., Goldstein L.S., Carson C. (2011). Cell-surface marker signatures for the isolation of neural stem cells, glia and neurons derived from human pluripotent stem cells. *PLoS One* 6(3): e17540.

Kim J., O'Sullivan M., Sanchez C., Hwang M., **Israel M.A.**, Brennand K., Deerinck T., Goldstein L.S., Gage F., Ellisman M., Ghosh A. (2011). Investigating synapse formation and function using human ES and iPS cell-derived neurons. *Proc. Natl. Acad. Sci. USA* 108(7): 3005-10.

Lian I., Kim J., Okazawa H., Zhao J., Zhao B., Yu J., Chinnaiyan A., **Israel M.A.**, Goldstein L.S., Abujarour R., Ding S., Guan K. (2010). The YAP transcription co-activator in regulating stem cell self-renewal and differentiation. *Genes and Development*. 24: 1106-1118.

Kumar R., Fossati V., **Israel M.A.**, Snoeck H.W. (2008). $Lin^{-}Sca1^{+}Kit^{-}$ bone marrow cells contain primitive lymphoid-committed precursors that are distinct from common lymphoid progenitors. *J. Immunol*. 181(11): 7507-13.

Patent filings

U.S. filing 61/443,311. Filed February 16, 2011. Alzheimer's Disease Cellular Model for Diagnostic and Therapeutic Development Methods. L. S. B. Goldstein and M. A. Israel.

Invited Lectures

The Stem Cell Meeting on the Mesa, 2010.

UCSD Alzheimer's Disease Research Center Data Blitz, 2010.

UCSD Cellular and Molecular Medicine In-house Seminar, 2009.

The Salk Institute Stem Cell Interest Group Seminar, 2009.

The Alzheimer's Association, San Diego Chapter, Young Scholar Awards, 2008.

UCSD Alzheimer's Disease Research Center Lunch and Learn Seminar, 2008.

Awards

Best poster at retreat, Biomedical Sciences PhD Program, 2009.

Young Scholar Award, San Diego Alzheimer's Association, 2008.

Predoctoral fellow, California Institute of Regenerative Medicine, 2008.

Best grades in first year classes, Biomedical Sciences PhD Program, 2006.

Magna Cum Laude, Brown University, 2003.

ABSTRACT OF THE DISSERTATION

Induced pluripotent stem-cell-derived models of sporadic and familial Alzheimer's disease

by

Mason Arthur Israel

Doctor of Philosophy

University of California, San Diego, 2011

Professor Lawrence S. B. Goldstein, Chair

Our understanding of Alzheimer's disease (AD) pathogenesis is currently limited by difficulties in obtaining live neurons from patients and the inability to model the sporadic form of AD. It may be possible to overcome these challenges by reprogramming primary cells from patients into induced pluripotent stem cells (iPSCs). I reprogrammed primary fibroblasts from patients with familial AD (caused by a duplication of *APP*, APP^{Dp}), sporadic AD (sAD), and non-demented control individuals into iPSC lines. iPSC lines were then differentiated and neurons were purified by flow cytometry. Purified neurons were capable of generating action potentials and spontaneous currents. No significant differences were detected between patients and controls in the ability of iPSCs to differentiate into neural precursor cells (NPCs) or the ability of NPCs to differentiate into neurons. I observed

that iPSC-derived neurons from both APP^{Dp} patients and one sAD patient exhibited significantly higher levels of secreted $Aß^{1-40}$, phospho-tau^{Thr231} and active GSK3ß, relative to control neurons. Treatment of APP^{Dp} neurons with ß-secretase inhibitors, but not γ-secretase inhibitors, caused significant reductions in phospho-tau and active GSK3ß levels. These results suggest a direct relationship between APP proteolytic processing and tau phosphorylation in human neurons. Additionally, I observed that neurons with the genome of one *sporadic* patient exhibited the phenotypes seen in familial AD samples. More generally, I demonstrate that iPSC technology can be used to observe phenotypes relevant to AD, even though it can take decades for overt disease to manifest in patients.

CHAPTER 1.

Generation and characterization of induced pluripotent stem cells from familial and sporadic Alzheimer's disease patients, and non-demented control individuals

ABSTRACT

Our understanding of Alzheimer's disease (AD) pathogenesis is currently limited by difficulties in obtaining live neurons from patients and the inability to model the sporadic form of AD. It may be possible to overcome these challenges by reprogramming primary cells from patients into induced pluripotent stem cells (iPSCs). Here I report the generation of fibroblasts and patient-specific iPSC cultures from patients with familial AD (caused by a duplication of *APP*), sporadic AD and non-demented control individuals. Multiple lines of evidence suggest that these "AD-iPSCs" are high-quality pluripotent stem cell lines, such as expression of pluripotency markers, silencing of transgenes, maintenance of karyotype and differentiation into cell types of all three embryonic germ layers. Because of their stem cell properties and unique patient-specific genetic backgrounds, AD-iPSCs have the potential to be powerful tools for the elucidation of AD pathogenesis and serve as novel platforms for therapeutic development.

BACKGROUND AND SIGNIFICANCE

Alzheimer's disease (AD) is a fatal, incurable form of dementia that currently afflicts more than 35 million people worldwide (1). The primary neurological feature of AD is global cognitive decline, including deterioration of memory, orientation, judgment and reasoning (2). With the increasing longevity and aging of our population, the devastation caused by AD on patients, families, societies and economies is growing. Currently, there is no approved treatment with a proven disease-modifying effect (3).

Two hallmark pathologies are used to diagnose AD and are both thought to be critically involved in disease pathogenesis. The first, amyloid plaques, are cerebral extracellular deposits primarily composed of Aß peptides (2, 4). Aß peptides are aggregate-prone protein fragments cleaved from the Amyloid Precursor Protein (APP), a process that involves the proteases ß-secretase and γ-secretase. Amyloid plaques are often present in the brains of individuals who die without dementia, but an unknown proportion of these individuals would have developed AD at a later timepoint.

The second hallmark pathology, neurofibrillary tangles, are filamentous accumulations of hyperphosphorylated tau protein located in the somatodendritic compartment of neurons (1). The abundance in brain autopsies of tangles or phosphorylated tau correlates with the severity of dementia better than the abundance of plaques (5, 6). In its normal state, tau is a microtubule associated protein primarily localized to the axonal compartment and has a well-characterized role in maintaining axonal microtubule stability (7, 8). Under disease conditions, tau is hyperphosphorylated by kinases such as GSK3ß and CDK5 (9), which causes its detachment from microtubules, its mislocalization to the somatodendritic compartment, microtubule instability, synaptic dysfunction, and possible disruption of axonal transport (10, 11). The mechanism responsible for activation of tau kinases is poorly understood. Although the predominant hypothesis is that Aß is the initial culprit, several lines of evidence suggest that other cleaved products of APP, especially the C-terminal fragments (CTFs), play a role (12-15).

AD can be subdivided into two categories: sporadic AD (sAD) and familial AD (fAD). The vast majority (~99%) of AD is sAD (16). sAD is heterogeneous on both the

genetic level, with a non-Mendelian pattern of inheritance, and on the pathological level. Although called *sporadic*, sAD has a clear genetic contribution (17). Age of onset is generally late (> 65 years of age), but a high degree of variability also exists in this aspect. The rare fAD cases have fully penetrant, dominantly inherited forms of AD that are usually early onset (< 65 years). Although tau pathology more closely associates with disease severity, it is the Aß pathology that associates with fAD genetics (2). All known mutations that cause fAD involve either the *APP* gene, or the *Presenilin* genes, which encode proteolytic components of γ-secretase activity necessary to cleave Aß (and other derivatives) from APP. fAD caused by *APP* aberrations can either involve specific point mutations within the gene or a single duplication of the *APP* locus (18, 19). Since *APP* is located on chromosome 21, individuals with Down's syndrome invariably develop AD pathologies in an early onset fashion. Despite detailed knowledge of the genetic causes of fAD and the pathological culmination of fAD and sAD, mechanistic understanding of pathogenesis and effective therapies remain elusive. A major reason for this is the failure of animal models to fully recapitulate AD pathogenesis.

Animal models harboring mutations found in fAD, although they have invaluably contributed to our current understanding of AD, do not recapitulate important pathological and neurological features of the disease (20). For example, the most common animal models of AD are mice that overexpress fAD mutant *APP* and/or fAD mutant *Presenilin*. Despite these extremely aggressive genetic paradigms, mice only develop plaque pathology and mild cognitive deficits, and escape tangle pathology and neurodegeneration. Our current inability to model important aspects of AD is a major barrier separating us from a more complete understanding of AD and

the development of novel therapies. Furthermore, the sporadic form of AD cannot be modeled in mice due to complex and unidentified genetics.

One obvious explanation for the shortcomings of animal models is species-specific differences. Indeed, Geula, *et al.* observed differences between rodents and primates in response to injected amyloid preparations, as well as between two different primate species (21). Additionally, important differences exist between rodent and human tau. An accurate *human* model of AD is therefore of extreme value. Unfortunately, human central nervous system biopsies are too limited in quantity and autopsy samples, though less limited, cannot be used to study live neurons or the critical early stages of pathogenesis. Human peripheral cells, such as skin fibroblasts, have been used as models for many years because they secrete Aß peptides into the culture media (22), but are incomplete models because they do not express tau and many other neuronal proteins. Additionally, fibroblast models have not been highly useful in elucidating the causes of sAD. Live, human, patient-specific neuronal models of AD, although of tremendous potential value, have not been reported.

In addition to the two hallmark pathologies, multiple additional defects have been observed in AD autopsies. Some, such as accumulations of endocytic and axonal vesicles, have been observed very early in disease pathogenesis (23, 24). Other pathologies detected more frequently in AD autopsies than control samples include reduction in synapse number, reduction in neurotrophin levels, damage to mitochondria, aberrant cell cycle reentry, calcium signaling dysregulation, and activation of astrocytes and microglia (1). Another class of AD pathologies, including vascular disease, cholesterol dysregulation, and reduction of insulin-pathway

components, are only observed in subsets of AD patients (1). Since animal models fail to fully recapitulate disease pathogenesis and AD autopsies represent endpoints of disease, the relative importance of all these pathologies to disease initiation and propagation, though of extreme interest, remains unclear. An abundant source of live, patient-specific neural cells could allow researchers to probe the contributions of these pathologies to overall pathogenesis.

The recent development of induced pluripotent stem cell (iPSC) technology has allowed the creation of live, patient-specific models of disease and the investigation of disease phenotypes *in vitro* (25-28). Currently, iPSCs are most commonly made by overexpressing the transcription factors *OCT4, SOX2, KLF4* and *cMYC* in primary fibroblasts, followed by culturing the transformed cells in human embryonic stem cell (hESC) culture conditions. Amazingly, the resultant *reprogrammed* cell lines, if high quality, are patient-specific stem cell lines that appear to divide indefinitely and can differentiate into theoretically any cell type of the human body. IPSC technology has been touted as a method to create “diseases in a dish,” as well as novel platforms for therapeutic development (29, 30).

Though the first report of human iPSCs occurred less than four years ago, a handful of research groups have already reported successful use of iPSCs in disease modeling, including neurodevelopmental diseases. Ebert, *et al*. found that iPSC-derived motor neurons from two spinal muscular atrophy patients had a decreased survival rate relative to control neurons, and the undifferentiated iPSCs from affected patients had an increased number of intracellular gem structures, which have been previously shown to be increased in SMA cells (28). Lee, *et al*. reported defects in neural differentiation and cellular migration using iPSCs derived from patients with

familial dysautonmia (31). Both studies reported that specific drugs could be used to partially rescue phenotypes.

Very recently, iPSCs have been made from a wide variety of diseases, including neurodegenerative diseases. For example, iPSCs have been generated from individuals with amyotrophic lateral sclerosis (ALS), Parkinson's disease (PD), Huntington's disease (HD), and Down's syndrome (32-35). However, the ALS, PD and Down's publications did not report identification of cellular phenotypes. The HD study reported activation of caspases in iPSC-derived neural stem cells but did not report phenotypes in neurons. Urbach, *et al*., in their attempt to model the developmental disorder Fragile-X syndrome with iPSCs, reported that they failed model the syndrome with iPSCs even though hESCs could be successfully used (36). This study strongly argues that it is important to show recapitulation of disease phenotypes for disease-specific iPSC lines. It currently remains unreported if iPSC technology can be used to model AD or the sporadic form of any disease. A review by Saha and Jaenisch recently suggested that iPSCs may not be capable of modeling sporadic forms of disease (29). Additional limitations to the field include unexplained variability between patients within a disease, between cell lines within a patient, and between replicates within a cell line.

In this chapter I test the hypotheses that sAD and fAD patient samples can be reprogrammed into iPSCs, and that the resultant iPSCs are of equal quality to non-demented control samples. Subsequent chapters explore the differentiation of iPSCs into neurons and the analysis of AD phenotypes in the iPSC-derived neurons. Additionally, I test if parental fibroblasts harboring *APP* duplications successfully maintain the genotype and secreted Aß phenotype of their respective individuals.

RESULTS

Patient details

This dissertation focuses on six individuals: two non-demented control individuals (herein referred to as NDC1 and NDC2), two sporadic AD patients (sAD1 and sAD2), and two familial AD patients who both have a single duplication of the *APP* locus ($APP^{Dp}1$ and $APP^{Dp}2$). Their details are discussed below, and summarized in **Table 1.1**. At the time of this study all six individuals were alive and enrolled in longitudinal studies, either at UCSD or at the University of Oulu.

Table 1.1. Patient details

Patient code	Original code	Diagnosis	Sex	Age at onset	Age at biopsy	MMSE	ApoE
NDC1	27	Non-demented control	M	N/A	86	30	2-3
NDC2	8011	Non-demented control	M	N/A	86	30	3-3
sAD1	8149	Sporadic AD	F	78	83	4	3-3
sAD2	3093	Sporadic AD	M	78	83	18	3-3
$APP^{Dp}1$	KOK	APP duplication	M	46	51	21	3-3
$APP^{Dp}2$	SMU	APP duplication	F	53	60	17	3-3

MMSE, Mini-mental state examination (perfect score = 30)

Since the risk of developing AD continues to increase with age, the best possible non-demented controls are as old as possible and are regularly evaluated by

neurologists. NDC1 and NDC2 were selected as the negative controls for this study because they were among the oldest individuals enrolled in the UCSD ADRC longitudinal study with no obvious signs of dementia and available for biopsy. At the ADRC, NDC1 is known as patient number 27 and NDC2 is number 8011. NDC1 and NDC2 are both non-demented males aged 86 years at the time of biopsy. Within a year of their biopsy, both NDC individuals scored a perfect 30 on the mini-mental state examination (MMSE), meaning they both were not displaying any obvious signs of dementia when biopsied. The *ApoE* genotype was 2/3 for NDC1 and 3/3 for NDC2, meaning that no copies of the ApoE4 allele were present in either individual. Both individuals have no obvious family history of dementia. Overall, NDC1 and NDC2 are ideal control individuals for an AD study.

SAD1 and sAD2 were selected for this study because they were among the most highly demented individuals enrolled in the UCSD ADRC longitudinal study available for biopsy. At the ADRC sAD1 is known as patient number 8149 and sAD2 is number 3093. For both individuals, the disease onset occurred at the age of 78 and biopsy occurred at the age of 83. This is consistent with late-onset AD (> 65 years old). At the year of biopsy, sAD1 scored a 4 out of 30 on the MMSE and sAD2 scored an 18 out of 30, indicating that at the age of 83, sAD1 was severely demented and sAD2 was moderately demented. The genotype of both individuals was ApoE 3/3.

$APP^{Dp}1$ and $APP^{Dp}2$ were selected as the positive controls for this study because they both possess a monogenic form of AD. Thus, the driving genetic aberration of their disease should be present in any somatic biopsy. Monogenic AD patients are rare (16, 37) and were not available to us through the UCSD ADRC. Fortunately, we were able to obtain $APP^{Dp}1$ and $APP^{Dp}2$ samples through our

collaborator, Dr. Anne Remes at the University of Oulu. $APP^{Dp}1$ and $APP^{Dp}2$ are half-siblings belonging to a large family in Finland with a history of dominantly inherited AD, originally described by Remes, *et al.* (18). In the pedigree published by Remes, *et al.*, $APP^{Dp}1$ known as III-16 and $APP^{Dp}2$ is III-13. Rovelet-Lecrux, *et al.* (19) reported that affected members of this family have a ~0.55 Mb genomic duplication that includes the *APP* locus and 3 other genes. It was previously known that a single duplication of *APP* is sufficient to cause AD (38, 39). The age of disease onset for $APP^{Dp}1$ and $APP^{Dp}2$ was 46 and 53, respectively, which is consistent with early onset AD (< 65 years old). $APP^{Dp}1$ and $APP^{Dp}2$ were biopsied at the ages of 51 and 60, respectively. Around the time of biopsy, $APP^{Dp}1$ scored a 21 out of 30 on the MMSE (mild dementia), and $APP^{Dp}2$ scored a 17 out of 30 (moderate dementia). The ApoE genotype for both APP^{Dp} individuals was determined to be 3/3, meaning that the ApoE4 allele was not present in any of the six individuals.

Properties of patient-specific somatic cell lines

Fibroblasts are one of the most common types of primary somatic cells used in laboratories. They derive from small, minimally invasive skin biopsies, and are capable of undergoing a large number of population doublings (> 50) before senescence and while maintaining a euploid karyotype. The AD field has been using fibroblasts to study APP expression and Aß secretion for over fifteen years (22, 40). Fibroblasts are currently the most commonly used cell type for reprogramming into iPSCs. For all of these reasons we chose to establish primary fibroblast cell lines for each of the six individuals.

After obtaining IRB approval and informed consent, a physician or nurse practitioner took one small (4 mm^3) biopsy from each individual. Primary fibroblast cell lines were established from the biopsies (see methods). Representative images of fibroblast lines are shown in **Figure 1.1**. It took 7-10 days for one 4 mm biopsy to grow into a confluent well of a 48-well plate. It took approximately 28 days to expand a confluent 48-well into a sufficient number of fibroblasts for reprogramming. I did not observe any qualitative difference in morphology or growth rate between the six cell lines.

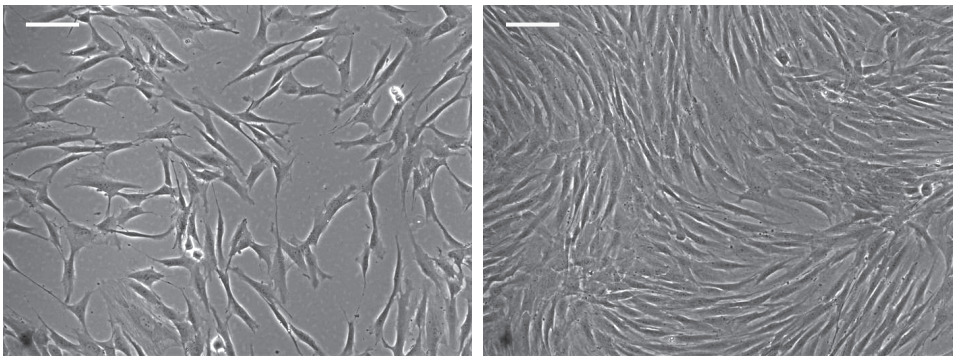

Figure 1.1. Representative brightfield images of fibroblast lines. Line NDC1 shown. Scale bar = 50 µm. Left image shows culture at low confluency. Note dividing cells. Right image shows culture at high confluency. Note swirling morphology.

To be useful, fibroblasts must be capable of maintaining the genotype of their respective patient. I confirmed the presence of the *APP* duplication in both APP^{Dp} fibroblast lines. Quantitative PCR (QPCR) was performed on genomic DNA preparations to determine the number of genomic *APP* copies relative to genes not in the duplicated region. Results are presented in **Figure 1.2 A**. All NDC and sAD

individuals maintained two copies of *APP*. Both APP^{Dp} individuals, and a sample from an individual with Down's syndrome maintained three copies of *APP*.

An extra copy of *APP* has been hypothesized to cause AD by causing increased expression of APP and Aß. Kusuga, *et al.* observed significantly increased APP mRNA levels in peripheral blood samples from their *APP* duplication patients relative to a control sample (41). It is unknown whether fibroblasts from APP duplication fAD patients recapitulate this aspect of AD pathogenesis. To address this question I prepared cDNA from the six fibroblast lines and quantified APP expression levels by QPCR. I observed an increase in APP mRNA levels in both APP^{Dp} fibroblast samples relative to NDC and sAD samples (**Figure 1.2 B**). Although Kasuga, *et al*. observed a 1.5-increase and I observed a 3-fold increase, this small difference is likely due to technical differences between the two experiments, such as control samples used or differences in the housekeeping gene used to normalize APP levels, and does not affect my interpretation of the data.

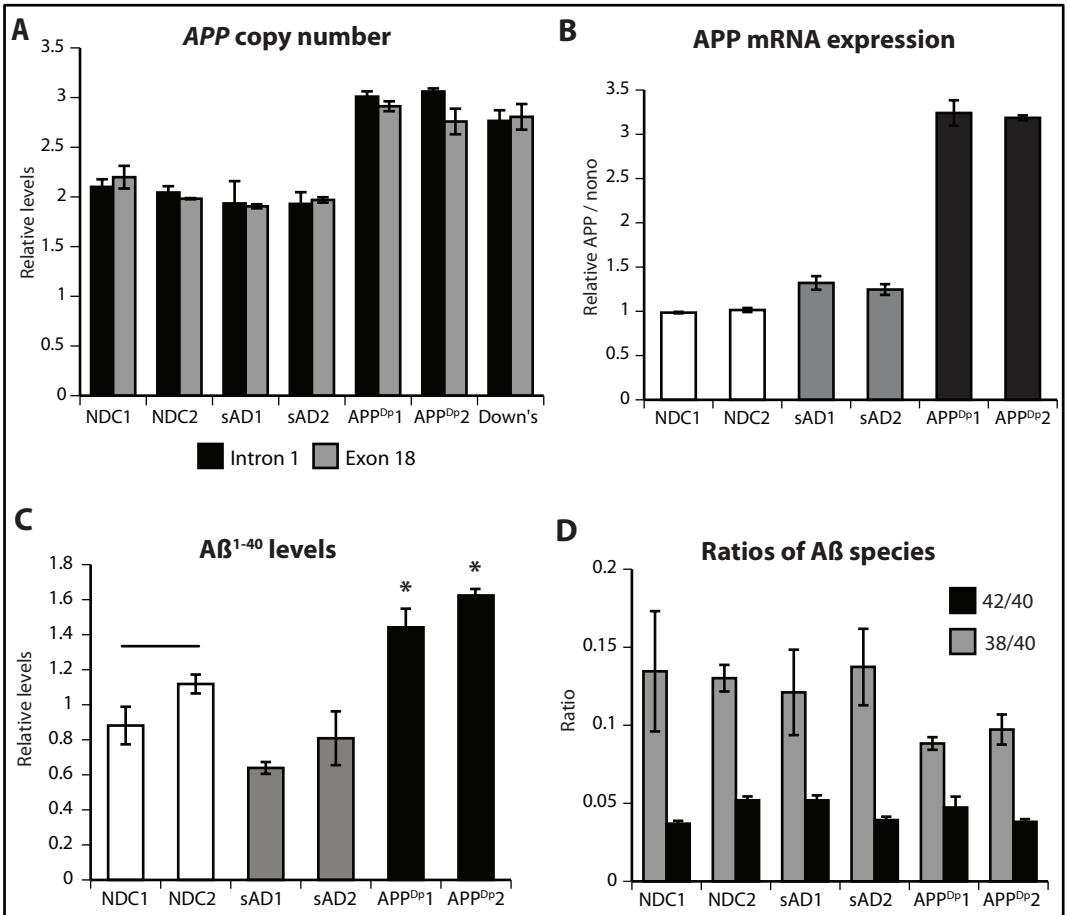

Figure 1.2. APP and Aß expression are elevated in APP^{Dp} fibroblasts relative to NDC and sAD fibroblasts. (A) QPCR was used to determine *APP* copy number in genomic DNA samples. (B) QPCR was used to quantify APP mRNA expression levels in cDNA samples. (C) ELISA was used to quantify Aß$^{1\text{-}40}$ levels in culture media conditioned for 48 hours. Aß$^{1\text{-}40}$ was increased in APP^{Dp}1 and APP^{Dp}2 samples compared to NDC cells (P= 0.01 and 0.0008, respectively, n=3). sAD samples were not elevated. (D) No significant difference in Aß 1-42/1-40 or 1-38/1-40 between patients.

Autopsies from *APP* duplication patients have increased numbers of amyloid plaques and cerebral vascular amyloid deposits (both are extracellular structures), relative to non-demented samples. Thus, the *APP* duplication is thought to cause increased secretion of Aß peptides. However, it is unknown if primary cells from *APP* duplication patients have increased Aß secretion. To determine if secreted Aß levels

are increased in APP^{Dp} fibroblasts relative to NDC samples, I plated equal numbers of passage 10 fibroblasts from all individuals, and collected the culture media after it had been conditioned by the fibroblasts for 48 hours. Aß levels in the conditioned media were measured by MSD ELISA and normalized to total protein levels of the corresponding cell lysate (**Figure 1.2 C**). The experiment was performed in biological triplicate. I observed that, relative to NDC and sAD cells, APP^{Dp} fibroblasts secreted 1.5- to 2-fold higher amounts of $Aß^{1-40}$ peptides into the conditioned media compared to NDC cells. This difference was statistically significant for both $APP^{Dp}1$ and $APP^{Dp}2$, when compared to the pool of NDC samples ($p = 0.01$ and 0.0008, respectively, Tukey HSD test, n = 3 biological replicates for each). These data demonstrate that in our APP^{Dp} fibroblast samples we have captured genomes that cause monogenic AD and that AD-relevant phenotypes can be measured in these patient samples. In addition, since this is the first report, to my knowledge, of Aß expression in *APP* duplication fibroblasts, these data are an important addition to the body of evidence that all fibroblasts from familial AD patients have Aß phenotypes relative to controls. Most importantly, we can determine if the Aß secretion phenotype seen in the APP^{Dp} fibroblasts is maintained in iPSC-derived neurons from the same patients, thus validating our positive control samples before performing other experiments in neurons that are not possible in fibroblast samples.

In contrast to APP^{Dp} samples, neither sAD1 nor sAD2 fibroblast line secreted elevated Aß relative to controls. These data in combination with the other data presented in Figure 2.2 suggest that the AD of sAD1 and sAD2 is different than the AD of the APP^{Dp} patients.

The ratio of Aß$^{1-42}$ expression levels relative to Aß$^{1-40}$ has been observed to be aberrant in fibroblasts harboring certain familial AD mutations, such as Presenilin1 mutations and the APP^{SWE} mutation (22, 42). It is not known whether APP duplication patients and their fibroblasts have altered ratios, or if the levels of all Aß species are equally increased. It is also unclear if fibroblasts from patients sAD1 and sAD2 have altered ratios. To determine if APP^{Dp} and/or sAD fibroblasts also have aberrant 42/40 ratios, I measured the 42/40 as well as the 38/40 in the experiment previously described. I did not detect any significant differences in the 42/40 nor the 38/40 between any of the patients (**Figure 1.2 D**). These data suggest that the APP^{Dp} mutation causes increased expression of all Aß species. Additionally, these data argue against either sAD patient having genetic aberrations that result in altered 42/40 in all APP expressing cells, unlike what has been observed in familial AD patients harboring Presenilin mutations or specific APP mutations.

Taken together, the patient information and fibroblast data sets suggest that I obtained a collection of biopsies that includes ideal positive and negative controls. Fibroblast lines are capable of maintaining genotype as well as APP expression and Aß secretion phenotypes thought to play initiating roles in AD pathogenesis. These data suggest that this collection of fibroblasts is ideal material for cellular reprogramming.

Reprogramming patient fibroblasts into iPSCs

Fibroblasts were reprogrammed into clonal iPSC lines using Yamanaka's original human protocol, with a few minor modifications (see methods). Retroviruses were prepared that encode cDNAs for the transcription factors OCT4, SOX2, KLF4,

cMYC and EGFP. EGFP was used in 1 out of 3 transduction wells as a live-cell marker for transgene expression and silencing (43). In order to ensure that iPSC lines from a given patient did not all share the same retroviral integration sites, fibroblasts from each patient were split into three different culture wells and three independent transductions were performed. In wells transduced with EGFP retrovirus, cultures averaged 90-95% EGFP+ by FACS, suggesting a high efficiency of infection. All six fibroblast lines were transduced at passage 5. Having all patient samples reprogrammed at the same, very early passage number is rare or non-existent in the current iPSC literature.

After retroviral transduction and 2 weeks in hESC culture conditions, patient samples were a heterogeneous mix of cell morphologies, with highly proliferative colonies beginning to dominate growth area (**Figure 1.3 A-D**). By 4 weeks post-transduction, cultures had proliferated into a lawn of cells. Potential iPSC colonies were manually picked during this two-week window. Colonies were chosen based on morphological resemblance to hESC colonies (**Figure 1.3 E**). Important hESC-like features included dense, flat colonies with defined borders and prominent nucleoli. For cultures that had also been transduced with EGFP retrovirus, selection was also based on robust silencing of EGFP. Colonies averaged 100 cells in size when picked. The efficiency of potential iPSC colony formation was roughly 100 colonies per $1x10^5$ fibroblasts at 3 weeks. Approximately 50 colonies were picked per individual.

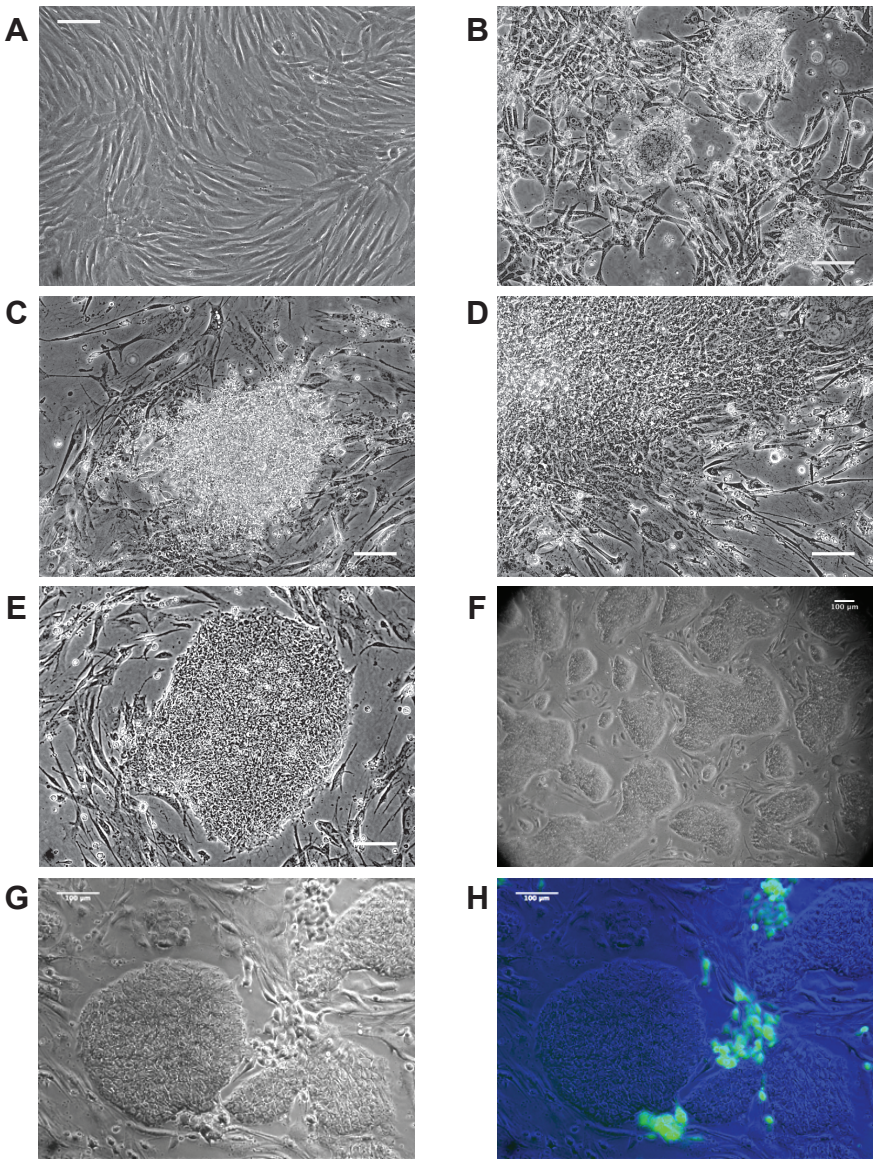

Figure 1.3. Morphologies encountered during the reprogramming process. (A) Typical fibroblast culture before transduction. (B-D) Examples of highly proliferative, non-hESC-like colonies commonly encountered during reprogramming. Images taken 3 weeks post-transduction. (E) An example of a hESC-like colony selected to be picked out of the heterogenous mix. This colony became line NDC1.3. (F) An established iPSC line (NDC1.3 passage 10). (G-H) Transgene reactivation in an established iPSC line. By comparing G and H, note how cells expressing the EGFP transgene can generally be identified by morphology.

Each selected colony was gently transferred to its own well of a 96-well plate containing irradiated MEFs. At this point I attempted to expand single colonies into stable iPSC lines (**Figure 1.3 F**). My strategy for expansion was to pick a large number of colonies, immediately begin chemical dissociation of lines, and select the lines that morphologically resembled hESC lines after 10 passages. The majority of initial colonies did not successfully generate stable iPSC lines. The efficiency of successful establishment of a stable iPSC line from an initial colony was roughly 10%. In the other 90%, cultures had excessive spontaneous differentiation and/or transgene reactivation (**Figure 1.3 G-H**). These lines were excluded from subsequent experiments. In my hands, when an iPSC line is stable at passage 10 it generally remains stable for as many passages as needed.

The time required to expand an initial colony into an iPSC line (passage 10) was variable. Initially some lines required passaging every 3 days while other required 7 or more. The average time to reach passage 10 was approximately 50 days. This, combined with the average time required to generate an initial colony from fibroblasts, sums to an average of 71 days required to reprogram fibroblasts into established iPSC lines and ~106 days to turn a biopsy into an iPSC line. In total, at least three iPSC lines were established per individual and frozen stocks were established. I selected 3-4 of the most robust iPSC lines for in depth characterization of pluripotency and differentiation properties. Clonal lines were named by adding the line number after the patient code (*e.g*. NDC1.2 is iPSC line number two from individual NDC1). The origin of each line is summarized in **Table 1.2**.

Table 1.2. Origin of each iPSC line

Cell line	Patient code	Original code	Vectors used *	Fibroblast passage # at transduction	Transduction well #
NDC1.1	NDC1	27	OSKM	5	1
NDC1.2	NDC1	27	OSKMG	5	2
NDC1.3	NDC1	27	OSKM	5	3
NDC2.1	NDC2	8011	OSKMG	5	1
NDC2.2	NDC2	8011	OSKM	5	2
NDC2.3	NDC2	8011	OSKMG	5	1
sAD1.1	sAD1	8149	OSKM	5	1
sAD1.2	sAD1	8149	OSKM	5	2
sAD1.3	sAD1	8149	OSKMG	5	3
sAD2.1	sAD2	3093	OSKM	5	1
sAD2.2	sAD2	3093	OSKM	5	2
sAD2.3	sAD2	3093	OSKMG	5	3
APP^{Dp}1.1	APP^{Dp}1	KOK	OSKM	5	1
APP^{Dp}1.2	APP^{Dp}1	KOK	OSKMG	5	2
APP^{Dp}1.3	APP^{Dp}1	KOK	OSKM	5	3
APP^{Dp}2.1	APP^{Dp}2	SMU	OSKM	5	1
APP^{Dp}2.2	APP^{Dp}2	SMU	OSKMG	5	2
APP^{Dp}2.3	APP^{Dp}2	SMU	OSKM	5	3

* OSKM (OCT4, SOX2, KLF4, c-MYC) OSKMG (OSKM + EGFP)

Expression of pluripotency-associated markers

The essential features of a pluripotent stem cell line are self-renewal, genome maintenance and pluripotency. In practice, these features are generally determined by the following assays: possession of hESC-like morphology after multiple passages, expression of pluripotency markers, maintenance of euploidy after multiple passages, silencing of retroviral transgenes concomitantly with expression of the endogenous counterparts, and ability to differentiate into all three embryonic germ layers.

To determine if the AD-iPSC lines resembled hESCs in terms of morphology and pluripotency marker expression, iPSC lines were analyzed by immunofluorescence microscopy. All 18 iPSC lines after at least 10 passages closely resembled healthy hESC lines passaged using the same methods, such as HUES9 (44). Colonies were flat with tight borders, densely arranged cells, prominent nucleoli, and little or no spontaneous differentiation (**Figure 1.4 A**). In addition, all lines robustly expressed nanog, a transcription factor required for the maintenance of pluripotency (45), and TRA1-81, a cell surface protein expressed by hESCs and inner cell mass cells (46, 47) (**Figure 1.4 B, C**). Lines expressed SOX2 and OCT4, which are also required for pluripotency (45), although these markers were used as retroviral vectors (data not shown). These data suggest that all AD-iPSC lines express critical pluripotency-associated proteins while closely resembling hESCs morphologically.

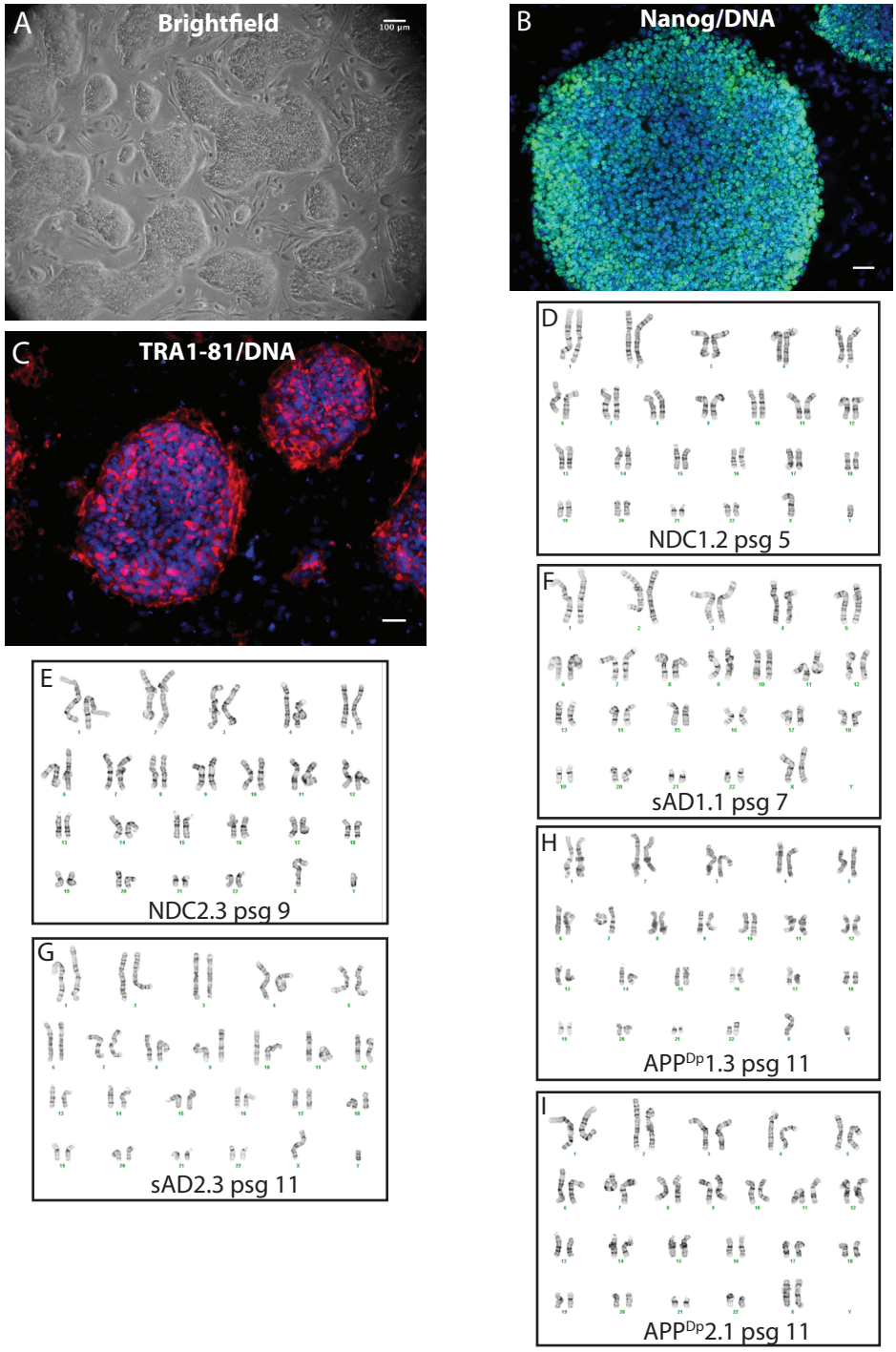

Figure 1.4. Expression of pluripotency markers and maintenance of euploidy in iPSCs. (A) Representative brightfield image showing hESC-like morphology of an iPSC line. (B, C) Representative immunofluorescence images showing expression of nanog and TRA1-81. (D-I) Euploid karyotypes of iPSC lines. One line for each patient shown. Scale bars = 100 µm.

Variability between hESC lines has been observed (48). The extent of variability in pluripotency marker expression between iPSC lines from the same individual and from different individuals is unclear, and likely varies between laboratories. To determine if the AD-iPSC lines possessed similar percentages of TRA1-81^{+} cells in culture, I stained all lines with anti-TRA1-81 antibody and analyzed samples by FACS (**Figure 1.5, Table 1.3**). IPSC lines co-cultured with MEFs were harvested with Accutase, which, in contrast to trypsin, is a dissociation enzyme designed not to degrade cell surface proteins. Percentage of TRA1-81^{+} cells in culture ranged from approximately 80-95%, mirroring hESC-MEF co-cultures. TRA1-81 negative cells were MEFs, spontaneously differentiating cells and/or false negatives. Although variability in TRA1-81 expression between iPSC lines was present, when lines were grouped together by patient no significant difference existed between patients (ANOVA $p > 0.49$). These data suggest a low degree of variability in pluripotency marker expression in the AD-iPSCs.

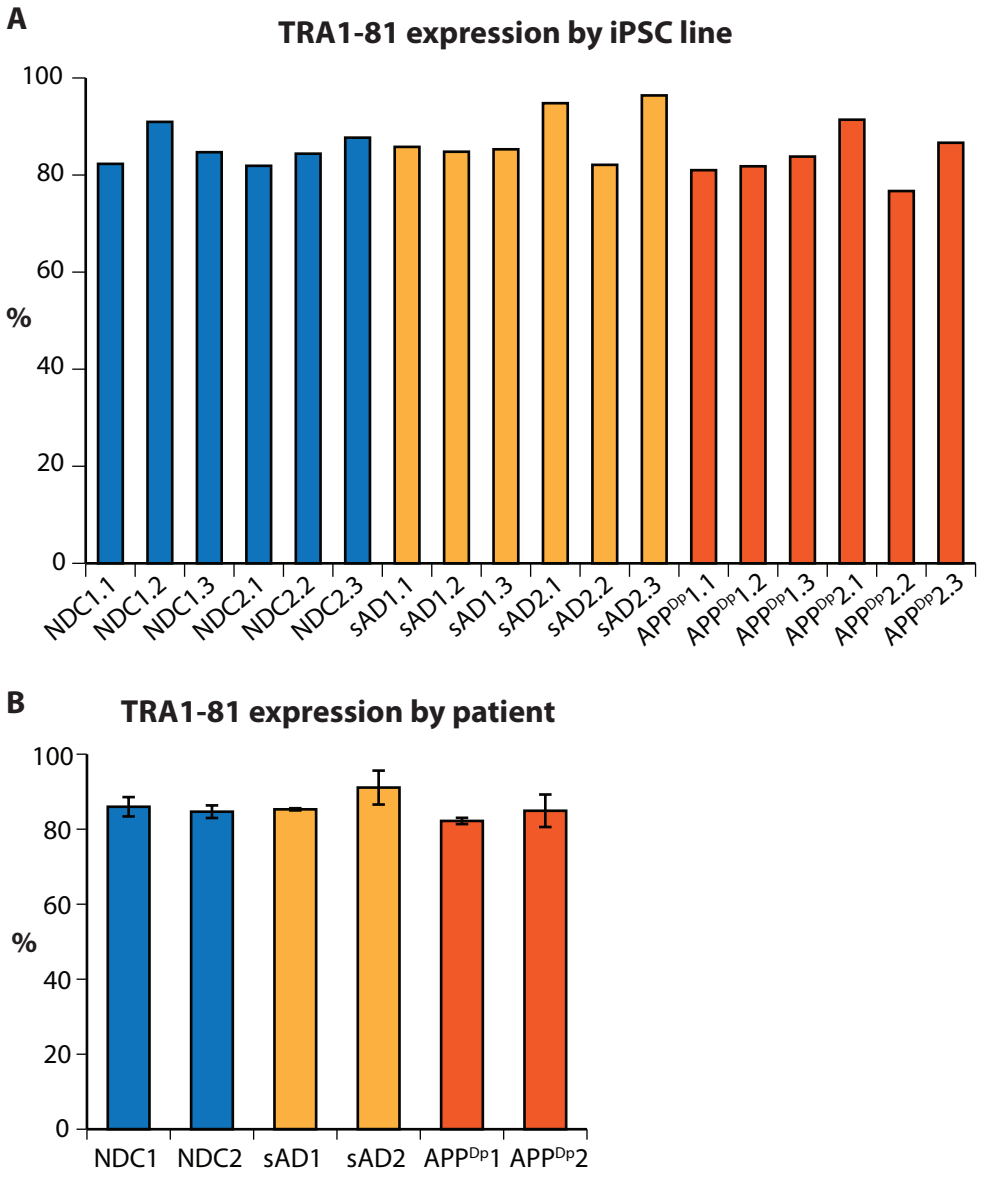

Figure 1.5. TRA1-81 expression in undifferentiated iPSC lines co-cultured with MEFs. Although a small amount of variability in expression levels existed between lines, no significant difference was observed between patients. **A**, Percentage of cells in culture expressing the pluripotency cell surface marker TRA1-81 in all 18 iPSC lines, measured by FACS. n > 100,000. **B**, Results grouped by patient.

Genetic fidelity of iPSCs

Patient-specific stem cells, by definition, maintain the genome of their respective patient. To determine if the AD-iPSC lines are chromosomally stable, I had cytogenetic analysis performed on all lines (see methods). We found that all lines maintained euploid karyotypes with the correct sex chromosomes, even after multiple passages (**Figure 1.4 D-I, Table 1.3**). Not all iPSC lines that I generated were euploid, however. Out of 25 karyotyped iPSC lines from the six individuals, 5 were found to be aneuploid. Our laboratory and many others have observed that aneuploidies are common in both hESCs (49) and hiPSCs (50), and the rate of aneuploidy in the AD-iPSC lines is not inconsistent with published reports. Nonetheless, aneuploid lines were excluded from further analysis.

Table 1.3. Details of TRA1-81 expression, transgene expression and karyotyping experiments

Cell line	Patient code	Original code	Mean % TRA1-81+ †	Passage number when karyotyped	Transgene expression*
NDC1.1	NDC1	27	82.3	8	< 0.001
NDC1.2	NDC1	27	91.0	8	< 0.001
NDC1.3	NDC1	27	84.7	10	< 0.001
NDC2.1	NDC2	8011	81.9	9	< 0.001
NDC2.2	NDC2	8011	87.7	10	7.1
NDC2.3	NDC2	8011	84.4	12	17.4
sAD1.1	sAD1	8149	85.3	7	21.0
sAD1.2	sAD1	8149	84.8	7	< 0.001
sAD1.3	sAD1	8149	85.8	7	< 0.001
sAD2.1	sAD2	3093	94.8	14	17.2
sAD2.2	sAD2	3093	82.1	15	19.7
sAD2.3	sAD2	3093	96.4	11	< 0.001
APP^{Dp}1.1	APP^{Dp}1	KOK	81.0	9	< 0.001
APP^{Dp}1.2	APP^{Dp}1	KOK	81.8	11	< 0.001
APP^{Dp}1.3	APP^{Dp}1	KOK	83.8	9	0.3
APP^{Dp}2.1	APP^{Dp}2	SMU	91.4	11	0.2
APP^{Dp}2.2	APP^{Dp}2	SMU	76.7	7	< 0.001
APP^{Dp}2.3	APP^{Dp}2	SMU	86.7	6	< 0.001

† Co-cultured with MEFs, n > 20,000

* Percent EGFP^{+} by FACS

Although karyotyping is currently the standard assay for genetic fidelity in stem cells, little is known about the extent of genetic aberrations occurring below g-band resolution. As sporadic AD is a complex genetic disease, we thought this issue was of particular importance. To address this issue, our laboratory collaborated with Dr. Kun Zhang in the UCSD Bioengineering department. The Zhang lab sequenced the exomes of two iPSC lines that we made, although these lines were not part of the AD-iPSC lines. The two sequenced iPSC lines were made by two rotation students

under my direction, using exactly the same methods I used for the AD-iPSC lines. Both iPSC lines were made from a biopsy of J. Craig Venter, so the sequences could be compared to his published sequence. In addition, multiple iPSC lines from other laboratories were sequenced and compared to their respective parental fibroblasts. The results are published in Gore, *et al.* (51). Importantly, all iPSC lines analyzed, whether they derived from our laboratory or others, had approximately 5-10 mutations per exome. This small number of mutations means that it is unlikely that a mutation will interfere with a given gene of interest and it is certainly unlikely that 3 independently derived lines will share the same mutations. Although none of the AD-iPSC lines were sequenced, I assume these results are applicable.

Transgene silencing and endogenous expression

A true iPSC line robustly silences retrovirus-derived transgenes and upregulates expression of the endogenous counterparts (*e.g.* SOX2). Transgene silencing permits differentiation of iPSCs, and endogenous expression provides evidence that the core transcriptional machinery of pluripotent cells is active.

Two sets of experiments were performed to determine if AD-iPSC lines were silencing transgenes. First, primers were designed to detect the presence of transgene-derived messages in cDNA preparations (**Figure 1.6 A**). The primers amplified a region common to all transgenes (*e.g.* OCT4, cMYC), and results were normalized to expression of the housekeeping gene *TBP*. As a positive control, a cDNA preparation was made from fibroblasts 3 days post-transduction. Similar to what has been seen by other laboratories, all 18 AD-iPSC lines expressed reduced or undetectable levels of transgenes relative to transduced fibroblasts. Silencing ranged

from 80 - 100%. While apparently low levels of transgene-derived messages were present in a subset of lines, other laboratories have not reported problems differentiating lines that are similarly affected.

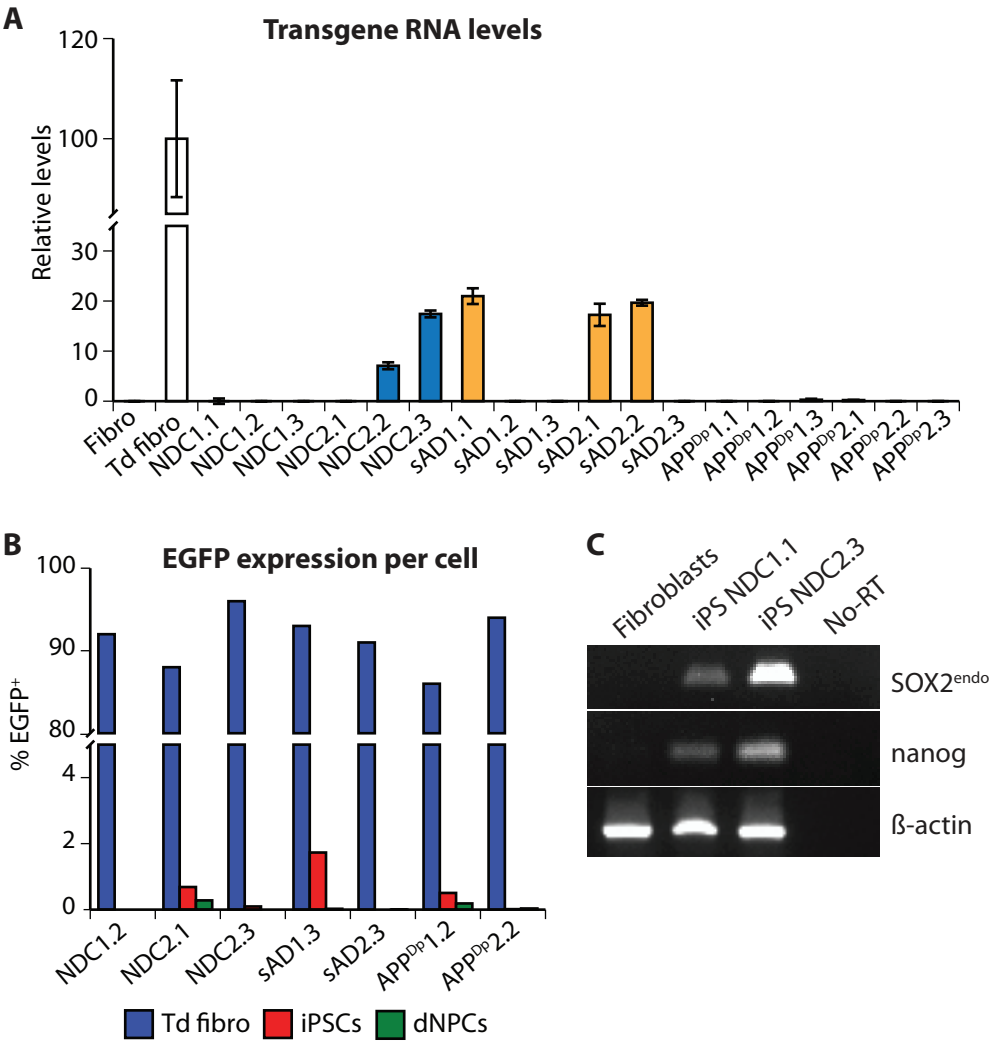

Figure 1.6. Transgene silencing and endogenous expression in iPSCs. (A) QPCR data comparing transgene expression in iPSC cultures versus fibroblast cultures 3 days post-transduction (Td-fibro). Primers amplified a region common to all transgenes. Data were normalized to expression of a housekeeping gene (*TBP*) (B) FACS data comparing percentage of iPSCs and iPSC-derived NPCs (dNPCs) expressing the EGFP retroviral vector versus Td-fibros. (C) Semi-quantitative PCR data showing expression of endogenous SOX2 in two representative iPSC lines, compared to fibroblasts. Primers detected a region in the 3' UTR not included in the

For the second silencing assay, in the subset of iPSC lines that were transduced with the EGFP retroviral vector, the percentage of $EGFP^+$ cells was measured by FACS and compared to the transduced parental fibroblasts (**Figure 1.6 B, Table 1.3**). In addition, the percentage of $EGFP^+$ cells in differentiated iPSC cultures was measured to determine if differentiation caused reactivation of transgenes. IPSC-derived neural precursor cells differentiated for 3 weeks were the specific cell type assayed (dNPCs, methods and characterization of this cell type in Chapter 2). Similar to the QPCR data set, EGFP expression was low or absent in iPSCs and dNPCs relative to transduced fibroblasts. The percentage of $EGFP^+$ cells in iPSCs and dNPCs ranged from 0-2%. These data, together with the QPCR data, suggest the AD-iPSC lines robustly silence transgenes.

To determine if the AD-iPSC lines express SOX2 derived from the endogenous locus, cDNA from each iPSC line was amplified by semi-quantitative PCR with primers that detect a region of the 3' UTR of SOX2 not included in the transgene (**Figure 1.6 C**). Expression of ß-actin and nanog were used as positive controls. Fibroblasts, which do not express SOX2, were used as a negative control. I found that all 18 iPSC lines robustly expressed endogenous SOX2 ($SOX2^{endo}$). These data, taken together with the transgene expression data, suggest that the AD-iPSC lines all have downregulated expression of transgene-derived SOX2 and have upregulated endogenous SOX2, which provides further evidence that the AD-iPSCs are *bona fide* iPSCs.

Differentiation into ectoderm, mesoderm and endoderm

Pluripotent stem cell lines theoretically have the potential to differentiate into all cell types of the adult body. In mice, this has been fully proven for both ESCs and iPSCs by tetraploid complementation (52, 53). In humans, this assay is unethical. Currently, the most widely accepted tests for human stem cell pluripotency are embryoid body (EB) differentiation and teratoma formation (54). In both assays, the cell lines of interest are allowed to differentiate, almost completely spontaneously, and after a given amount of time the presence of cells types indicative of the three embryonic germ layers (*i.e.* mesoderm, endoderm and ectoderm) is determined.

To determine if the AD-iPSCs were capable of differentiating into endoderm and mesoderm *in vitro*, I induced all 18 iPSC lines to form floating EBs, and allowed these structures to differentiate spontaneously (**Figure 1.7**). Qualitatively, all lines formed EBs of similar size and at similar efficiencies to hESCs and to each other. After 7 days of differentiation as floating EBs and an additional 7 days of differentiation attached to Matrigel-coated coverslips, cultures were stained with a widely used endodermal marker, α-fetoprotein (AFP), and a widely used mesodermal marker, α-smooth muscle actin (SMA). Reflecting results from the pluripotency marker expression data sets, all 18 iPSC lines were capable of differentiating into AFP+ and SMA+ cells. For all lines, when I plated EBs into three 0.8 cm^2 Matrigel-coated coverslips, 3 out of 3 wells contained multiple AFP+ and SMA+ cells of appropriate morphology. AFP+ cells were small, round and grew in loose colonies. SMA+ cells were large, flat and fibroblastic. Additionally, if EBs were seeded densely or allowed to differentiate for more than 7 days, spontaneously beating colonies

containing hundreds of cells, presumably cardiomyocytes, could be identified (data not shown).

The ability of the AD-iPSC lines to differentiate into the third embryonic germ layer, ectoderm, is extensively discussed in Chapter 2. Briefly, all AD-iPSC lines robustly differentiate into neural precursor cells and neurons at similar efficiencies. A representative image of nestin+ neural precursor cells differentiated from AD-iPSCs is shown in **Figure 1.7**.

I also initiated studies to determine if a representative subset of the AD-iPSCs could differentiate into teratomas that contain cellular structures indicative of all three embryonic germ layers. Only a subset was tested in order to minimize animal sacrifice and cost. In collaboration with Martin Marsala's laboratory at UCSD, we injected one iPSC line from each individual into rat spinal cords. Results are pending.

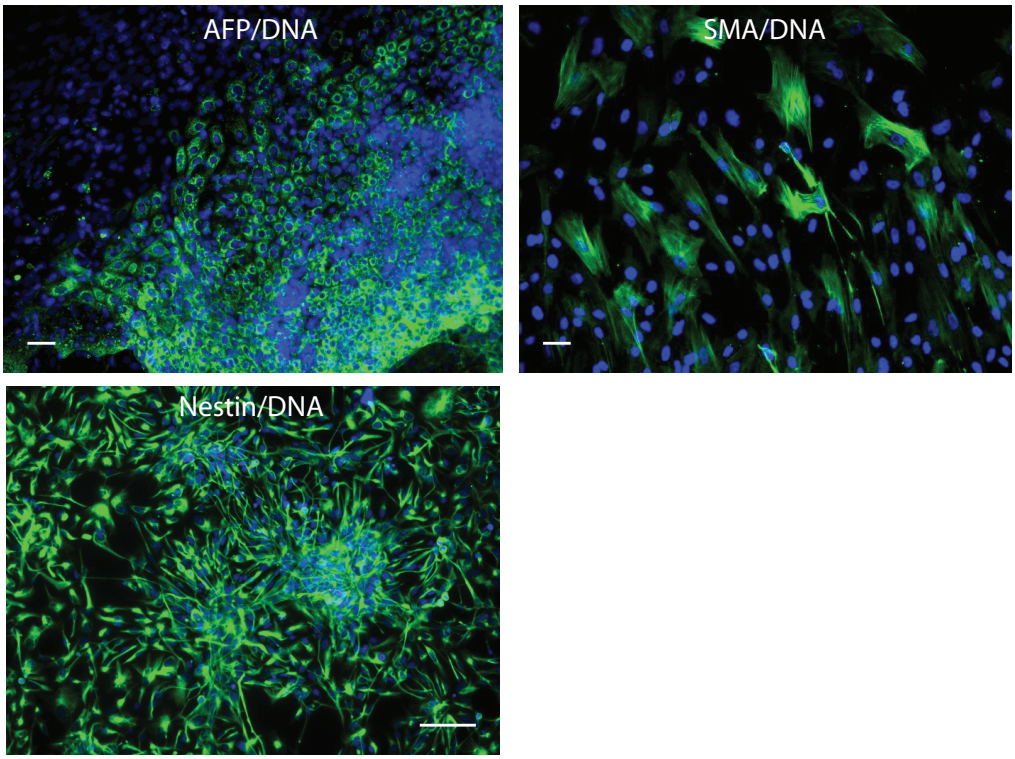

Figure 1.7. Differentiation of iPSCs into endoderm, mesoderm and ectoderm *in vitro*. Representative images of AD-iPSC lines differentiated into cells indicative of endoderm (AFP, alpha fetoprotein), mesoderm (SMA, alpha smooth muscle actin), and ectoderm (nestin). Scale bars = 50µm.

CONCLUSIONS AND DISCUSSION

Fibroblast data

We successfully biopsied and established primary fibroblast cell lines from six individuals: two non-demented controls, two patients with sporadic AD and two individuals with a duplication of *APP*. This set of individuals has three critical features: control individuals both have no signs of dementia in their late 80's, all individuals are ApoE4 negative, and all individuals are enrolled in longitudinal studies.

Fibroblasts harboring the *APP* duplication had increased expression of APP mRNA and increased secretion of Aß peptides, demonstrating that we can

recapitulate an important mechanism of AD pathogenesis in APP^{Dp} fibroblasts. It was previously unknown if APP^{Dp} fibroblasts had elevated Aß secretion. Unlike Down's syndrome fibroblasts, APP^{Dp} fibroblasts can be used to study APP processing without the complication of a large number of additional duplicated genes. Both sAD fibroblast lines closely resembled controls in terms of APP mRNA expression, Aß secretion and 42/40 ratio. These data support previous reports that fibroblasts from sporadic AD patients generally resemble controls (42). No difference was detected in Aß 42/40 or 38/40 between any of the fibroblast lines. This demonstrates that fibroblasts with a duplication of *APP* have elevated levels of all Aß species, a finding that was previously unknown.

In the future it will be important to characterize fibroblasts from additional NDC and sAD individuals. This would allow for more powerful experiments to address the important issues of sAD heterogeneity and NDC heterogeneity. In the future it will also be interesting to characterize the morphology and distribution of endosomes in the fibroblast lines (55), in order to see if APP^{Dp} fibroblasts have the same endosomal phenotypes seen in Down's syndrome fibroblasts and to compare with the endosomal morphologies of iPSC-derived neurons from these same individuals.

Overall, this set of six low-passage, patient-specific fibroblast lines provides novel starting material for iPSC studies, which have the potential to provide powerful new insight into AD pathogenesis.

IPSC data

The data of this chapter demonstrate that it is possible to generate high quality iPSCs from individuals with familial AD, sporadic AD, and age-matched, non-demented controls. These AD-iPSCs express critical, endogenous pluripotency

markers, silence retrovirus-derived transgenes, maintain karyotype and have the potential to differentiate into the three embryonic germ layers. These data strongly suggest that the AD-iPSC lines are high quality tools that have the potential to be used to model aspects of AD pathogenesis and serve as platforms for therapeutic development.

Expression of TRA1-81 and silencing of transgenes were measured quantitatively by FACS and I found a small degree of variability between iPSC lines but no significant difference between individuals. These data provide evidence that it is valid to compare lines from different individuals. The variability between iPSC lines demonstrates the importance of representing each individual with at least 3 lines.

The reprogramming efficiency of AD and NDC fibroblasts into euploid iPSCs was similar to published reports. Since four of the individuals were over 80 years old at the time of biopsy, this finding confirms other reports that old age is not a refractory factor to reprogramming into euploid iPSCs. For the study of AD, this is an important issue since disease onset can take place very late in life. These findings suggest that non-demented control individuals should be as old as possible at the time of biopsy, since neurological status can be more completely assessed without apparent sacrifice of reprogramming efficiency.

Although all lines of evidence suggest that the AD-iPSC collection consists of high quality iPSC lines, future experiments should be done to further substantiate this statement. Demonstrating ability of AD-iPSCs to form teratomas, maintain correct DNA fingerprints and closely resemble hESCs on the transcriptomic level would be interesting future experiments. Additionally, comparing the transcriptomes of all AD-iPSC lines has the potential to reveal novel, *very* early events in AD pathogenesis.

Working with collaborators, we found that iPSCs that we generated carried only a small number of coding mutations relative to parental fibroblasts or other somatic cells. This provides evidence that iPSCs maintain a very high degree of genomic fidelity and can truly be called patient-specific. I estimate that this small number of mutations is unlikely to disrupt a given biochemical pathway of interest or disrupt unidentified gene variants of sporadic patients, especially if multiple lines are studied per individual. It is even possible that this phenomenon is mirroring what occurs to somatic cells *in vivo*. Nevertheless, it is important to recognize this limitation of iPSC technology, which is likely to persist as technology improves.

I have demonstrated, to some extent, that the AD-iPSC collection is pluripotent. This suggests that these cell lines can be directed to differentiate into any desired cell type. For the study of AD, neurons are likely to be the cell type most commonly harvested, at least in the initial phases. However, astrocytes, microglia and vascular cells play clear roles in AD pathogenesis and may serve as better targets for therapeutic intervention. Improved differentiation methods for these cell types are currently required.

Since iPSCs appear to grow indefinitely, AD-iPSCs can be shared with an unlimited number of laboratories and a given laboratory need not worry about depleting their supply if the cells are managed properly. Since iPSCs are live, human cells, they have the potential to serve as an excellent complement to animal models and patient imaging studies. Since iPSCs are patient-specific, they are tools with the potential to dissect the heterogeneity of AD and help move the field towards an era of personalized medicine.

MATERIALS AND METHODS

Patient data. NDC and sAD individuals were neurologically evaluated as part of their enrollment in the longitudinal study at the UCSD Alzheimer's Disease Research Center. APP^{Dp} individuals were evaluated as part of their enrollment in studies at the Department of Clinical Medicine, Neurology, Oulu University Hospital, Oulu, Finland.

Biopsies. For all individuals, biopsies were taken following informed consent and IRB approval. A single 4 mm dermal punch biopsy was taken from the forearm of each individual by a certified dermatologist or nurse practitioner using the Sklar Punch Biopsy Tray.

Fibroblast derivation and culture. Primary fibroblast cultures were established from biopsies using the collagenase method of Takashima, *et al.* (56). Fibroblasts were cultured in DMEM containing 15% FBS, L-glutamine, and Penicillin/Streptomycin (all from Gibco). For dissociation, fibroblasts were treated with 0.25% trypsin-EDTA (Gibco) until detached. For storage, fibroblasts were slow-frozen in a solution consisting of 90% FBS, 10% DMSO (Sigma) and stored at -150° C.

***APP* copy number genotyping.** APP copy number in fibroblast samples was determined using the method of Blom, *et al.* (57), with modifications. Genomic DNA was isolated from fibroblasts using the Qiagen DNeasy Kit. Quantitative PCR (QPCR) was performed using FastStart Universal SYBR Green Master Mix (Roche) and primers that amplify *APP* intron 1, *APP* exon 18, *ß-globin*, and *albumin* (primer sequences are listed in the appendix). Reactions were performed and analyzed on an Applied Biosystems 7300 Real Time PCR System using the $\Delta\Delta$Ct method. *APP* levels were normalized to mean levels of *ß-globin* and *albumin*.

APP mRNA expression levels. To compare RNA levels between samples, RNA was purified (PARIS kit, Ambion), DNase treated (Ambion) and reverse transcribed (Superscript II, Invitrogen). QPCR was performed using the reagents described in the previous paragraph with a primer set that recognizes all APP isoforms. All fibroblast samples were measured at passage number 10.

Fibroblast Aß measurements. For each line, 80,000 fibroblasts in 2 mL of culture media were seeded into one well of a 6-well plate. All lines were at passage number 10. After 48 hours of media conditioning, media was harvested and protease inhibitors (EMD) were added at the suggested concentration. Samples were centrifuged at 4° C to remove cellular debris and stored at -80° C for approximately one week. On the day of analysis, 500uL of thawed sample was concentrated to precisely 120uL using an Amicon Ultra filter. Aß levels were quantified from these samples with MSD Human (6E10) Abeta3-Plex Kits (Meso Scale Discovery). A standard curve was generated and only samples that were in the linear range were analyzed. Fibroblast Aß levels were measured in biological triplicate and normalized to total protein levels determined by Bradford assay.

iPSC generation. iPSC were generated as described (58), with the following modifications. The cDNAs for *OCT4*, *SOX2*, *KLF4*, *c-MYC* and *EGFP* were cloned into pCX4 vectors (59) and vectors were packaged into VSVG-pseudotyped retroviruses. cDNAs were a generous gift from Steve Dowdy and Naohisa Yoshioka (UCSD). Viral preps were concentrated approximately 80-fold by centrifugation. For each patient, 3 independent viral transductions were performed. Three wells each containing ~$1x10^5$ fibroblasts were transduced with retroviruses. On days 2-8, 2 mM valproic acid was added to cultures. Potential iPSC colonies were picked at ~3 weeks

and transferred to 96-well plates containing irradiated mouse embryonic fibroblasts (MEFs).

iPSC culture conditions. Undifferentiated iPSCs were routinely cultured using the HUES protocol (44), with the following modifications. The final concentration of bFGF was 30ng/mL. Culture media are detailed in Appendix I. Cells were dissociated by briefly treating with TrypLE (Invitrogen) followed by gentle tituration. 10 μM of ROCK inhibitor Y-27632 (Calbiochem) was added to the culture media for two days following sub-culturing.

Immunocytochemistry and FACS. Cells were fixed in 4% paraformaldehyde, permeabilized with buffer containing TritonX-100, and stained with primary and secondary antibodies (see Appendix III). Samples were imaged on a Nikon TE2000-U inverted microscope and acquired using Metamorph software (Molecular Devices). ImageJ software (NIH) was used to pseudo-color images, adjust contrast, and add scale bars. FACS experiments were carried out on a FACSAria II cytometer (BD Biosciences) and analyzed using FloJo software (Tree Star).

mRNA expression levels. To detect endogenous SOX2 expression in iPSC lines, RNA was purified (PARIS kit, Ambion), DNase treated (Ambion) and reverse transcribed (Superscript II, Invitrogen). Semi-quantitative PCR was performed using HotStarTaq (Qiagen) and primers that detect a segment of the SOX2 3' UTR not included in the retroviral vectors (primer sequences are listed in Appendix II).

Karyotype analysis. Cytogenetic analysis was performed by Cell Line Genetics (Madison, WI) on live, undifferentiated iPSCs. 19-20 cells were karyotyped per cell line.

Differentiation to mesoderm and endoderm. To determine if iPSC lines could generate endoderm and mesoderm, iPSC cultures were dissociated with dispase, and embryoid bodies were generated by plating cultures in low-attachment culture plates in media containing 15% fetal bovine serum (FBS). After 7 days with media changes on alternate days, cultures were plated into three 0.8 cm^2 Matrigel (BD Biosciences)–coated well and cultured for an additional 7 days. At this point cultures were harvested for immunocytochemistry. A cell line was deemed capable of differentiating into endoderm if $\geq$ 10 AFP^+ were present in 3 out of 3 wells. A cell line was deemed capable of differentiating into mesoderm if $\geq$ 10 SMA^+ were present in 3 out of 3 wells.

Statistics. Data were analyzed using JMP software (SAS Institute). Cell lines were compared by performing ANOVA followed by Tukey's HSD posthoc test. $P<0.05$ was considered statistically significant.

Antibodies: See Appendix III.

ACKNOWLEDGEMENTS

Chapters 1 contains work submitted for publication by authors: Mason A. Israel, Shauna H. Yuan, Sol M. Reyna, Yangling Mu, Christian T. Carson, Fred H. Gage, Anne M. Remes, Edward H. Koo, Lawrence S. B. Goldstein. The dissertation author was the primary investigator and author of this material.

REFERENCES

1. Querfurth HW & LaFerla FM (2010) Alzheimer's Disease. *New England Journal of Medicine* 362(4):329-344.

2. Tanzi RE & Bertram L (2005) Twenty Years of the Alzheimer s Disease Amyloid Hypothesis: A Genetic Perspective. *Cell* 120(4):545-555.

3. Citron M (2010) Alzheimer's disease: strategies for disease modification. *Nat Rev Drug Discov* 9(5):387-398.

4. Alzheimer A (1907) About a peculiar disease of the cortex (German). *Allg. Z. Psychiat. Med.* 64:146-148.

5. Arriagada PV, Growdon JH, Hedley-Whyte ET, & Hyman BT (1992) Neurofibrillary tangles but not senile plaques parallel duration and severity of Alzheimer's disease. *Neurology.* 42(3 Pt 1):631-639.

6. Buerger K, Teipel SJ, Zinkowski R, Blennow K, Arai H, Engel R, Hofmann-Kiefer K, McCulloch C, Ptok U, Heun R, Andreasen N, DeBernardis J, Kerkman D, Moeller H-J, Davies P, & Hampel H (2002) CSF tau protein phosphorylated at threonine 231 correlates with cognitive decline in MCI subjects. *Neurology* 59(4):627-629.

7. Cleveland DW, Hwo S-Y, & Kirschner MW (1977) Purification of tau, a microtubule-associated protein that induces assembly of microtubules from purified tubulin. *Journal of Molecular Biology* 116(2):207-225.

8. Ballatore C, Lee VMY, & Trojanowski JQ (2007) Tau-mediated neurodegeneration in Alzheimer's disease and related disorders. *Nat Rev Neurosci* 8(9):663-672.

9. Cho J & Johnson G (2003) Glycogen Synthase Kinase 3ß Phosphorylates Tau at Both Primed and Unprimed Sites. *J. Biol. Chem.* 278(1):187-193.

10. Cho J-H & Johnson GVW (2004) Primed phosphorylation of tau at Thr231 by glycogen synthase kinase 3ß (GSK3ß) plays a critical role in regulating tau's ability to bind and stabilize microtubules. *J. Neurochem.* 88(2):349-358.

11. Hoover BR, Reed MN, Su J, Penrod RD, Kotilinek LA, Grant MK, Pitstick R, Carlson GA, Lanier LM, Yuan L-L, Ashe KH, & Liao D (2010) Tau Mislocalization to Dendritic Spines Mediates Synaptic Dysfunction Independently of Neurodegeneration. *Neuron* 68(6):1067-1081.

12. Gunawardena S & Goldstein LSB (2001) Disruption of Axonal Transport and Neuronal Viability by Amyloid Precursor Protein Mutations in Drosophila. *Cell* 32(3):389-401.

13. Salehi A, Delcroix J-D, Belichenko PV, Zhan K, Wu C, Valletta JS, Takimoto-Kimura R, Kleschevnikov AM, Sambamurti K, Chung PP, Xia W, Villar A, Campbell WA, Kulnane LS, Nixon RA, Lamb BT, Epstein CJ, Stokin GB, Goldstein LSB, & Mobley WC (2006) Increased App Expression in a Mouse Model of Down's Syndrome Disrupts NGF Transport and Causes Cholinergic Neuron Degeneration. 51(1):29-42.

14. Nikolaev A, McLaughlin T, O/'Leary DDM, & Tessier-Lavigne M (2009) APP binds DR6 to trigger axon pruning and neuron death via distinct caspases. *Nature* 457(7232):981-989.

15. Jiang Y, Mullaney KA, Peterhoff CM, Che S, Schmidt SD, Boyer-Boiteau A, Ginsberg SD, Cataldo AM, Mathews PM, & Nixon RA (2010) Alzheimer's-related endosome dysfunction in Down syndrome is Aß-independent but requires APP and is reversed by BACE-1 inhibition. *Proceedings of the National Academy of Sciences* 107(4):1630-1635.

16. Campion D, Dumanchin C, Hannequin D, Dubois B, Belliard S, Puel M, Thomas-Anterion C, Michon A, Martin C, Charbonnier F, Raux G, Camuzat A, Penet C, Mesnage V, Martinez M, Clerget-Darpoux F, Brice A, & Frebourg T (1999) Early-Onset Autosomal Dominant Alzheimer Disease: Prevalence, Genetic Heterogeneity, and Mutation Spectrum. *American journal of human genetics* 65(3):664-670.

17. Gatz M, Reynolds CA, Fratiglioni L, Johansson B, Mortimer JA, Berg S, Fiske A, & Pedersen NL (2006) Role of Genes and Environments for Explaining Alzheimer Disease. *Arch. Gen. Psychiatry* 63(2):168-174.

18. Remes AM, Finnila S, Mononen H, Tuominen H, Takalo R, Herva R, & Majamaa K (2004) Hereditary dementia with intracerebral hemorrhages and cerebral amyloid angiopathy. *Neurology* 63(2):234-240.

19. Rovelet-Lecrux A, Frebourg T, Tuominen H, Majamaa K, Campion D, & Remes AM (2007) APP locus duplication in a Finnish family with dementia and intracerebral haemorrhage. *J. Neurol. Neurosurg. Psychiatry* 78(10):1158-1159.

20. Duyckaerts C, Potier M-C, & Delatour B (2008) Alzheimer disease models and human neuropathology: similarities and differences. *Acta Neuropathologica* 115(1):5-38.

21. Guela C, Wu C-K, Saroff D, Lorenzo A, Yuan M, & Yankner BA (1998) Aging renders the brain vulnerable to amyloid ß-protein neurotoxicity. *Nat. Med.* 4(7):827-831.

22. Citron M, Vigo-Pelfrey C, Teplow DB, Miller C, Schenk D, Johnston J, Winblad B, Venizelos N, Lannfelt L, & Selkoe DJ (1994) Excessive production of amyloid ß-protein by peripheral cells of symptomatic and presymptomatic patients carrying the

Swedish familial Alzheimer disease mutation. *Proc. Natl. Acad. Sci. U.S.A.* 91(25):11993-11997.

23. Cataldo AM, Peterhoff CM, Troncoso JC, Gomez-Isla T, Hyman BT, & Nixon RA (2000) Endocytic pathway abnormalities precede amyloid beta deposition in sporadic Alzheimer's disease and Down syndrome: differential effects of APOE genotype and presenilin mutations. *Am J Pathol.* 157(1):277-286.

24. Stokin GB, Lillo C, Falzone TL, Brusch RG, Rockenstein E, Mount SL, Raman R, Davies P, Masliah E, Williams DS, & Goldstein LSB (2005) Axonopathy and Transport Deficits Early in the Pathogenesis of Alzheimer's Disease. *Science* 307(5713):1282-1288.

25. Takahashi K & Yamanaka S (2006) Induction of Pluripotent Stem Cells from Mouse Embryonic and Adult Fibroblast Cultures by Defined Factors. *Cell* 126(4):663-676.

26. Takahashi K, Tanabe K, Ohnuki M, Narita M, Ichisaka T, Tomoda K, & Yamanaka S (2007) Induction of Pluripotent Stem Cells from Adult Human Fibroblasts by Defined Factors. *Cell* 131(5):861-872.

27. Yu J, Vodyanik MA, Smuga-Otto K, Antosiewicz-Bourget J, Frane JL, Tian S, Nie J, Jonsdottir GA, Ruotti V, Stewart R, Slukvin II, & Thomson JA (2007) Induced Pluripotent Stem Cell Lines Derived from Human Somatic Cells. *Science* 318(5858):1917-1920.

28. Ebert AD, Yu J, Rose FF, Mattis VB, Lorson CL, Thomson JA, & Svendsen CN (2009) Induced pluripotent stem cells from a spinal muscular atrophy patient. *Nature* 457(7227):277-280.

29. Saha K & Jaenisch R (2009) Technical Challenges in Using Human Induced Pluripotent Stem Cells to Model Disease. *Cell stem cell* 5(6):584-595.

30. Marchetto MCN, Winner B, & Gage FH (2010) Pluripotent stem cells in neurodegenerative and neurodevelopmental diseases. *Human Molecular Genetics* 19(R1):R71-R76.

31. Lee G, Papapetrou EP, Kim H, Chambers SM, Tomishima MJ, Fasano CA, Ganat YM, Menon J, Shimizu F, Viale A, Tabar V, Sadelain M, & Studer L (2009) Modelling pathogenesis and treatment of familial dysautonomia using patient-specific iPSCs. *Nature* 461(7262):402-406.

32. Dimos JT, Rodolfa KT, Niakan KK, Weisenthal LM, Mitsumoto H, Chung W, Croft GF, Saphier G, Leibel R, Goland R, Wichterle H, Henderson CE, & Eggan K (2008) Induced Pluripotent Stem Cells Generated from Patients with ALS Can Be Differentiated into Motor Neurons. *Science* 321(5893):1218-1221.

33. Soldner F, Hockemeyer D, Beard C, Gao Q, Bell GW, Cook EG, Hargus G, Blak A, Cooper O, Mitalipova M, Isacson O, & Jaenisch R (2009) Parkinson's Disease Patient-Derived Induced Pluripotent Stem Cells Free of Viral Reprogramming Factors. *Cell* 136(5):964-977.

34. Zhang N, An MC, Montoro D, & Ellerby LM (2010) Characterization of Human Huntington's Disease Cell Model from Induced Pluripotent Stem Cells. *PLoS Curr.* 2:RRN1193.

35. Park I-H, Arora N, Huo H, Maherali N, Ahfeldt T, Shimamura A, Lensch MW, Cowan C, Hochedlinger K, & Daley GQ (2008) Disease-Specific Induced Pluripotent Stem Cells. *Cell* 134(5):877-886.

36. Urbach A, Bar-Nur O, Daley GQ, & Benvenisty N (2010) Differential Modeling of Fragile X Syndrome by Human Embryonic Stem Cells and Induced Pluripotent Stem Cells. *Cell Stem Cell* 6(5):407-411.

37. Anonymous (2010) 2010 Alzheimer's disease facts and figures. *Alzheimer's and Dementia* 6(2):158-194.

38. Rovelet-Lecrux A, Hannequin D, Raux G, Meur NL, Laquerriere A, Vital A, Dumanchin C, Feuillette S, Brice A, Vercelletto M, Dubas F, Frebourg T, & Campion D (2006) APP locus duplication causes autosomal dominant early-onset Alzheimer disease with cerebral amyloid angiopathy. *Nat. Genet.* 38(1):24-26.

39. Sleegers K, Brouwers N, Gijselinck I, Theuns J, Goossens D, Wauters J, Del-Favero J, Cruts M, Duijn CMv, & Broeckhoven CV (2006) APP duplication is sufficient to cause early onset Alzheimer's dementia with cerebral amyloid angiopathy. *Brain* 129(11):2977-2983.

40. Querfurth HW, Wijsman EM, George-Hyslop PHS, & Selkoe DJ (1995) ß-APP mRNA transcription is increased in cultured fibroblasts from the familial Alzheimer's disease-1 family. *Molecular Brain Research* 28(2):319-337.

41. Kasuga K, Shimohata T, Nishimura A, Shiga A, Mizuguchi T, Tokunaga J, Ohno T, Miyashita A, Kuwano R, Matsumoto N, Onodera O, Nishizawa M, & Ikeuchi T (2009) Identification of independent APP locus duplication in Japanese patients with early-

onset Alzheimer disease. *Journal of Neurology, Neurosurgery & Psychiatry* 80(9):1050-1052.

42. Scheuner D, Eckman C, Jensen M, Song X, Citron M, Suzuki N, Bird TD, Hardy J, Hutton M, Kukull W, Larson E, Levy-Lahad L, Viitanen M, Peskind E, Poorkaj P, Schellenberg G, Tanzi R, Wasco W, Lannfelt L, Selkoe D, & Younkin S (1996) Secreted amyloid ß-protein similar to that in the senile plaques of Alzheimer's disease is increased in vivo by the presenilin 1 and 2 and APP mutations linked to familial Alzheimer's disease. *Nat. Med.* 2(8):864-870.

43. Chan EM, Ratanasirintrawoot S, Park I-H, Manos PD, Loh Y-H, Huo H, Miller JD, Hartung O, Rho J, Ince TA, Daley GQ, & Schlaeger TM (2009) Live cell imaging distinguishes bona fide human iPS cells from partially reprogrammed cells. *Nat Biotech* 27(11):1033-1037.

44. Cowan CA, Klimanskaya I, McMahon J, Atienza J, Witmyer J, Zucker JP, Wang S, Morton CC, McMahon AP, Powers D, & Melton DA (2004) Derivation of Embryonic Stem-Cell Lines from Human Blastocysts. *New England Journal of Medicine* 350(13):1353-1356.

45. Boyer LA, Lee TI, Cole MF, Johnstone SE, Levine SS, Zucker JP, Guenther MG, Kumar RM, Murray HL, Jenner RG, Gifford DK, Melton DA, Jaenisch R, & Young RA (2005) Core Transcriptional Regulatory Circuitry in Human Embryonic Stem Cells. *Cell* 122(6):947-956.

46. Thomson JA, Itskovitz-Eldor J, Shapiro SS, Waknitz MA, Swiergiel JJ, Marshall VS, & Jones JM (1998) Embryonic Stem Cell Lines Derived from Human Blastocysts. *Science* 282(5391):1145-1147.

47. Henderson JK, Draper JS, Baillie HS, Fishel S, Thomson JA, Moore H, & Andrews PW (2002) Preimplantation Human Embryos and Embryonic Stem Cells Show Comparable Expression of Stage-Specific Embryonic Antigens. *Stem Cells* 20(4):329-337.

48. Osafune K, Caron L, Borowiak M, Martinez RJ, Fitz-Gerald CS, Sato Y, Cowan CA, Chien KR, & Melton DA (2008) Marked differences in differentiation propensity among human embryonic stem cell lines. *Nat. Biotechnol.* 26(3):313-315.

49. Draper JS, Smith K, Gokhale P, Moore HD, Maltby E, Johnson J, Meisner L, Zwaka TP, Thomson JA, & Andrews PW (2004) Recurrent gain of chromosomes 17q and 12 in cultured human embryonic stem cells. *Nat Biotech* 22(1):53-54.

50. Mayshar Y, Ben-David U, Lavon N, Biancotti J-C, Yakir B, Clark AT, Plath K, Lowry WE, & Benvenisty N (2010) Identification and Classification of Chromosomal Aberrations in Human Induced Pluripotent Stem Cells. *Cell stem cell* 7(4):521-531.

51. Gore A, Li Z, Fung H, Young J, Agarwal S, Antosiewicz-Bourget J, Canto I, Giorgetti A, Israel M, Kiskinis E, Lee J, Loh Y, Manos P, Montserrat N, Panopoulos A, Ruiz S, Wilbert M, Yu J, Kirkness E, Belmonte J, Rossi D, Thomson J, Eggan K, Daley G, Goldstein L, & Zhang K (2011) Somatic coding mutations in human induced pluripotent stem cells. *In press at Nature*.

52. Nagy A, Gocza E, Diaz EM, Prideaux VR, Ivanyi E, Markkula M, & Rossant J (1990) Embryonic stem cells alone are able to support fetal development in the mouse. *Development* 110(3):815-821.

53. Boland MJ, Hazen JL, Nazor KL, Rodriguez AR, Gifford W, Martin G, Kupriyanov S, & Baldwin KK (2009) Adult mice generated from induced pluripotent stem cells. *Nature* 461(7260):91-94.

54. Daley GQ, Lensch MW, Jaenisch R, Meissner A, Plath K, & Yamanaka S (2009) Broader Implications of Defining Standards for the Pluripotency of iPSCs. *Cell stem cell* 4(3):200-201.

55. Cataldo AM, Mathews PM, Boiteau AB, Hassinger LC, Peterhoff CM, Jiang Y, Mullaney K, Neve RL, Gruenberg J, & Nixon RA (2008) Down syndrome fibroblast model of Alzheimer-related endosome pathology: accelerated endocytosis promotes late endocytic defects. *Am J Pathol.* 173(2):370-384. Epub 2008 Jun 2005.

56. Takashima A (2001) Establishment of Fibroblast Cultures. *Current Protocols in Cell Biology*, (John Wiley & Sons, New Jersey), p 12.

57. Blom ES, Viswanathan J, Kilander L, Helisalmi S, Soininen H, Lannfelt L, Ingelsson M, Glaser A, & Hiltunen M (2007) Low prevalence of APP duplications in Swedish and Finnish patients with early-onset Alzheimer's disease. *Eur J Hum Genet* 16(2):171-175.

58. Park I-H, Lerou PH, Zhao R, Huo H, & Daley GQ (2008) Generation of human-induced pluripotent stem cells. *Nat. Protoc.* 3(7):1180-1186.

59. Akagi T, Sasai K, & Hanafusa H (2003) Refractory nature of normal human diploid fibroblasts with respect to oncogene-mediated transformation. *Proc. Natl. Acad. Sci. U.S.A.* 100(23):13567-13572.

CHAPTER 2.

Comparative differentiation and purification of neural precursor cells and neurons derived from induced pluripotent stem cells

ABSTRACT

A critical limitation in our understanding of Alzheimer's disease (AD) is the inability to test hypotheses on live, patient-specific neurons. Animal models harboring familial AD mutations lack important pathologies and have not been useful in modeling the sporadic form of AD. Here I report the robust differentiation and purification of patient-specific neural precursor cells (NPCs) and neurons from induced pluripotent stem cells (iPSCs). No significant differences were found between AD patients and controls in the ability to differentiate into NPCs or neurons. Purified neuronal cultures contained greater than 90% neurons and were electrophysiologically active. These data suggest that it is possible to generate human patient-specific neurons for the study of familial and sporadic AD, and these tools have the potential to elucidate mechanisms of AD pathogenesis and serve as platforms for therapeutic development.

BACKGROUND AND SIGNIFICANCE

Human pluripotent stem cells, such as human embryonic stem cells (hESCs) and iPSCs, can theoretically differentiate into any cell type of the adult body. A wide variety of differentiated cell types, representing all three embryonic germ layers, have been generated from these types of stem cells (1, 2). The most successful directed differentiation protocols apply knowledge gained by the developmental biology field to these *in vitro* cultures (3). High quality differentiation protocols in concert with iPSC technology have the potential to provide unlimited supplies of live, patient-specific neurons, which can be used to ask scientific questions recently considered to be infeasible.

Important for the study of AD, several neural induction protocols have been described. Pluripotent stem cells have been successfully differentiated into NSCs, a more restricted type of stem cell that can subsequently be differentiated into the three major cell types of the central nervous system (*i.e.* neurons, astrocytes and oligodendrocytes) (4, 5). Much research energy has focused on neuronal differentiation methods, and pluripotent stem cells have been made into several neuronal subtypes, including dopaminergic, GABAergic and motor neurons (3, 6-8). Unfortunately, efforts to generate forebrain cholinergic neurons, a subtype preferentially destroyed in AD, are in a relatively primitive stage.

In the brief window of their collective existence, stem-cell-derived neurons have passed a wide variety of functional tests, have successfully been used to model diseases *in vitro*, and have served in assays used to validate the effect of drugs. Differentiated NSCs and neurons have been transplanted into the brains of animal models, and transplanted cells were capable of participating in brain development, myelinating endogenous neurons and even ameliorating disease symptoms (5, 9-12). In a dish, differentiated neurons are capable of forming synapses with other neurons, generating action potentials, and have been used to test drugs (13).

Despite this rapid progress, multiple issues regarding the utility of iPSC-derived neurons remain unresolved. One major issue is variability in differentiation propensity between lines. Marked differences in differentation propensity between pluripotent stem cell lines have been reported (14), and as many research groups have recently begun to compare the differentiated progeny of multiple iPSC lines, differentiation variability has become an issue of paramount importance. This issue becomes more complex if one seeks to use iPSC technology to investigate a disease

with unknown or unclear developmental alterations. In the brains of AD patients and AD animal models, for example, altered neurogenesis has been observed, but these findings remain controversial (15). Thus, it is unclear if iPSC-derived NPCs from AD patients should generate neurons differently than control NPCs. Improved methods of quantitatively monitoring differentiation will be important contributions to the stem cell field.

A second critical issue in stem cell differentiation is cell type heterogeneity in differentiated cultures. HESCs, iPSCs and iPSC-derived NPCs all preferentially differentiate into cultures containing a multiple cell types, a property that reflects the function of stem cells *in vivo*. The vast majority of stem cell “disease in a dish” publications to date study heterogeneous cultures. Often, heterogeneity is minimized to a large extent by subculturing or growth factor treatment, but accompanying cell types remain present. Depending on the scientific question and the identity of the accompanying cell types, heterogeneity can be unimportant, desirable or problematic. As an example of how heterogeneity can be problematic, one can turn to the study of Aß secretion by differentiated neurons. Aß, commonly thought to be the initiating factor of AD, is highly secreted by neurons. It is not known, however, if neurons from AD patients secrete higher levels of Aß than controls. This measurement has proven to be difficult, and a major reason for this is because astrocytes and microglia both are capable of internalizing secreted Aß, thus complicating results (16, 17). Since current protocols to differentiate iPSCs into neurons generally produce glia and unknown cell types alongside the neurons, the variable of Aß clearance cannot be excluded. A robust method to *purify* human neurons from differentiated cultures

would be a novel and potentially powerful approach to address this and many similar scientific questions.

Here I test the hypotheses that iPSCs made from AD patients can robustly differentiate into NSCs and neurons, and that no significant differences in neural differentiation exist between AD patients and controls. Using a novel flow cytometry based method of differentiation and purification developed in our laboratory, I report the purification of neurons from multiple iPSC lines and several properties of the resultant cultures.

RESULTS

Variability in differentiation efficiency exists between pluripotent cell lines (14). To determine the degree of variability in the AD-iPSC lines, I employed a FACS-based method of neuronal differentiation and purification developed in our laboratory. The detailed protocol is reported in Yuan, *et al.* (18). This novel differentiation strategy allows comparison of differentiation efficiencies between patients and between clonal iPSC lines from the same patient, while simultaneously purifying NPCs or neurons from heterogeneous cultures. For the study of neurodegenerative diseases, an additional advantage of this differentiation method is that neurons are purified to near complete homogeneity, allowing the study of live human neurons without the additional complexity of the presence of glia or other cell types.

The differentiation method is summarized in **Figure 2.1** and detailed in *Materials and Methods*. Briefly, for each of the six individuals, 3 clonal iPSC lines were differentiated and analyzed. First, NPCs were differentiated and purified from iPSCs. Second, neurons were differentiated and purified from NPCs. In the end,

cultures greater than 90% neurons were cultured for an additional 5 days and analyzed.

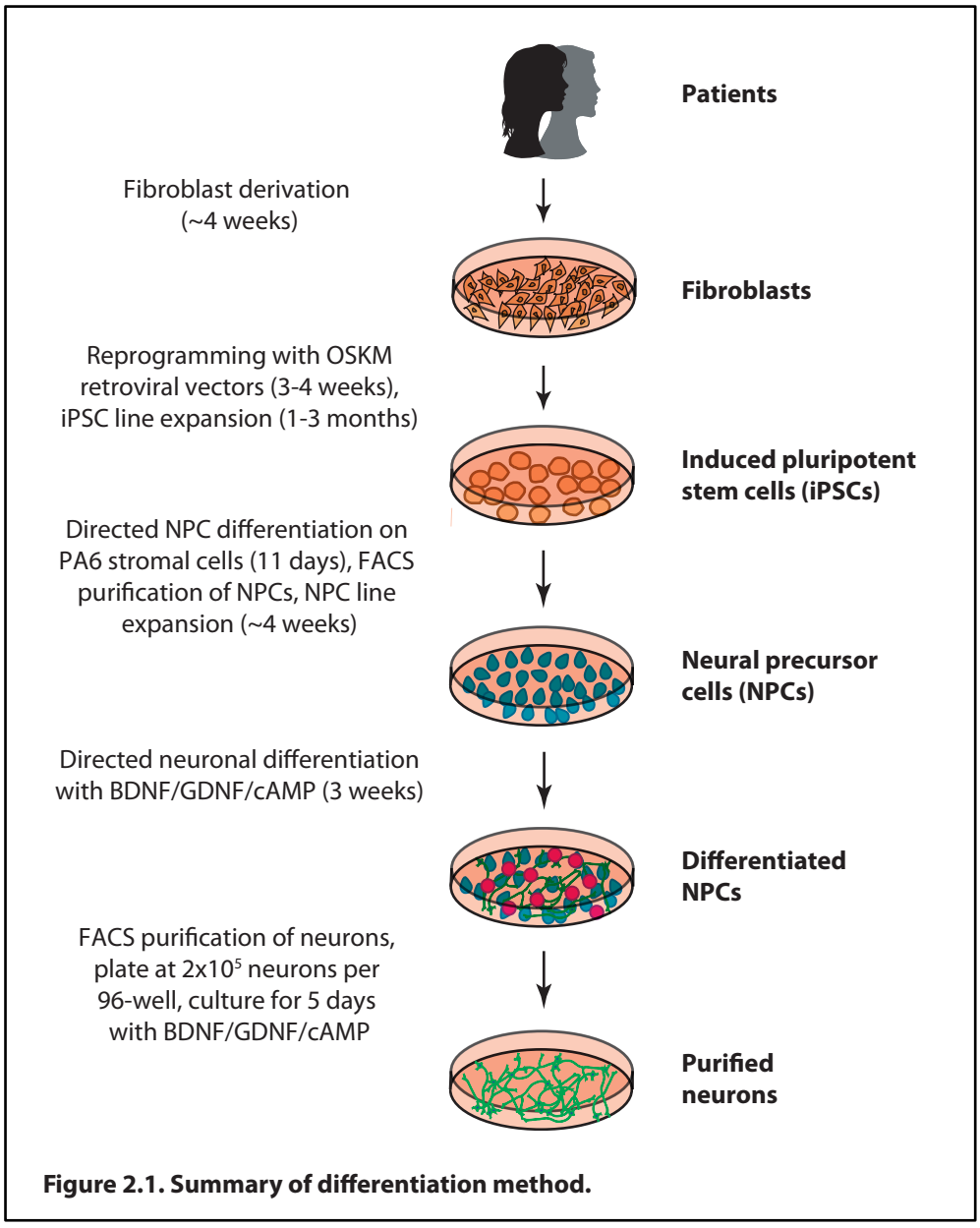

Figure 2.1. Summary of differentiation method.

To generate NPC lines from iPSCs, healthy, undifferentiated iPSC cultures were first differentiated into cultures containing neural rosettes (**Figure 2.2 A**). Rosette-containing cultures were generated by co-culturing 100,000 TRA1-81^{+} iPSCs with 500,000 mouse PA6 stromal cells, a primary cell line known to direct differentiation down the neural lineage (6, 19). From these cultures, NPCs were purified and the efficiency of NPC formation was assessed by CD184^{+}CD15^{+}CD44^{-} CD271^{-} immunoreactivity. These FACS-purified NPCs maintained expression of NPC markers over multiple passages, such as SOX2 and nestin (**Figure 2.2 B, C**). NPC lines could generally be expanded for more than 10 passages and were amenable to cryopreservation.

To generate neurons from NPCs, NPC lines were expanded for 7 passages in the presence of bFGF and were subsequently differentiated for 3 weeks in the presence of BDNF, GDNF and cAMP. Differentiated NPC cultures (dNPCs) contained many neurons with projections that could be greater than 2 cm in length (**Figure 2.2 D**). Additionally, dNPC cultures expressed neuronal proteins, such as MAP2, α-synuclein, tau, and phosphorylated tau (at Ser396, Ser404 and Thr231) (**Figure 2.3 A**). In contrast, the parental fibroblast cultures did not express tau or other neuronal markers, illustrating an important advantage of iPSC-derived cultures over primary cells. dNPCs were also found to successfully maintain correct *APP* copy number, with only APP^{Dp} samples possessing 3 copies of the *APP* locus (**Figure 2.3 B**). dNPCs, however, were far from homogeneous, containing multiple types of non-neuronal, unidentified cell types. From dNPCs, neurons were FACS-purified to near homogeneity and the efficiency of neuron generation was determined by measuring CD24^{+}CD184^{-}CD44^{-} immunoreactivity. Purified neurons were gently plated at a

density of $2x10^5$ cells per well of a 96-well plate. Within 2 hours of plating, cells could be seen that had already attached and had began growing projections from their cell bodies. Within 24 hours of plating, the projections resembled connected networks and the occasional projection would be longer than the diameter of the entire well. Purified neuronal cultures were always harvested after 5 days of culture. For future studies, it would be possible to continue aging these cultures. After 5 days in culture, more than 90% of the cells were neurons, as judged by the presence of cells possessing ßIII-tubulin$^+$MAP2$^+$ projections (**Figure 2.2 E-H**). No clear signal was detected when cultures were stained with GFAP antibody, suggesting the absence of astrocytes (data not shown).

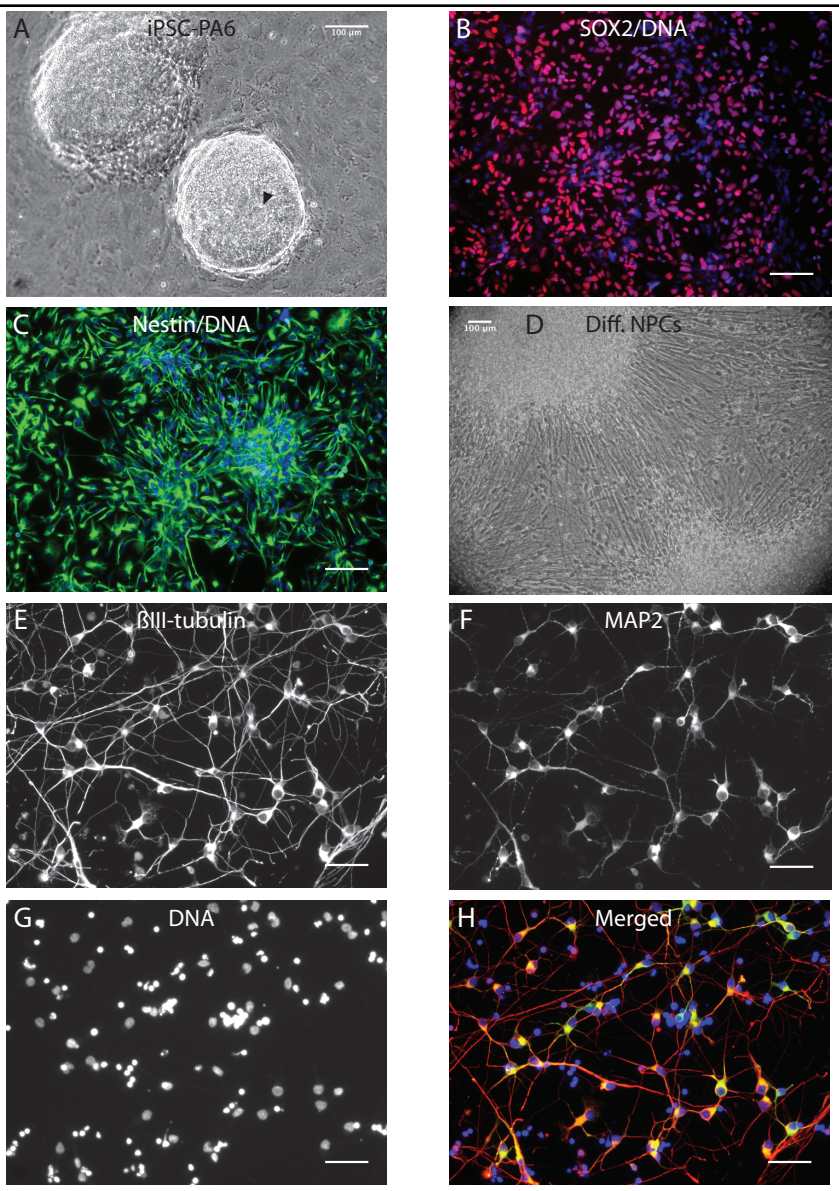

Figure 2.2. Differentiation of AD-iPSCs into neural precursor cells (NPCs) and purified neurons. A, Representative iPSC-PA6 co-culture matured for 11 days. Arrowhead indicates rosette-like structure. Cultures were harvested at this timepoint and NPCs were FACS-purified by collecting $CD15^{+}CD184^{+}CD44^{-}CD271^{-}$ cells. B-C, Immunofluorescent images showing SOX2 and nestin expression in FACS-purified NPCs. NPCs were expanded for 7 passages in the presence of bFGF and subsequently differentiated for 3 weeks in the presence of BDNF, GDNF and cAMP. D, Typical culture of NPCs differentiated for 3 weeks. Note the presence of large clusters of cells connected by long cellular projections. Cultures were harvested at this timepoint and neurons were FACS-purified by collecting $CD24^{+}CD184^{-}CD44^{-}$ cells. E-H, Immunofluorescent images showing MAP2 and ßIII-tubulin expression in FACS-purified neurons cultured for an additional 5 days. Note the high degree of homogeneity of neuronal marker expression and the apparent connectivity between neurons. Scale bars = 50um unless noted.

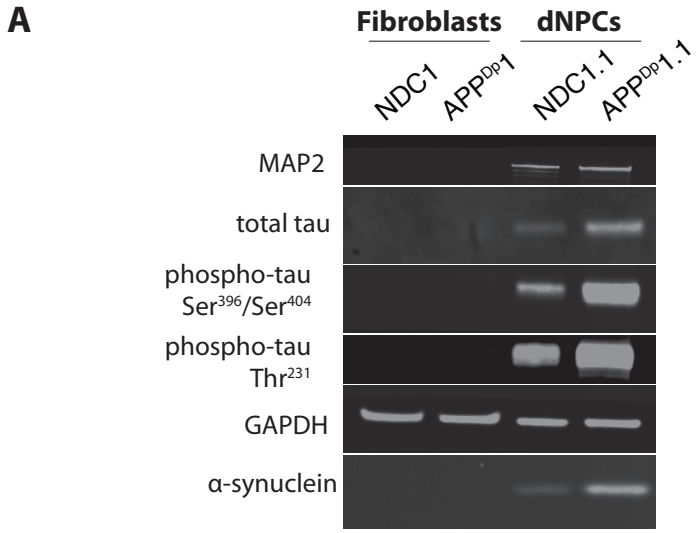

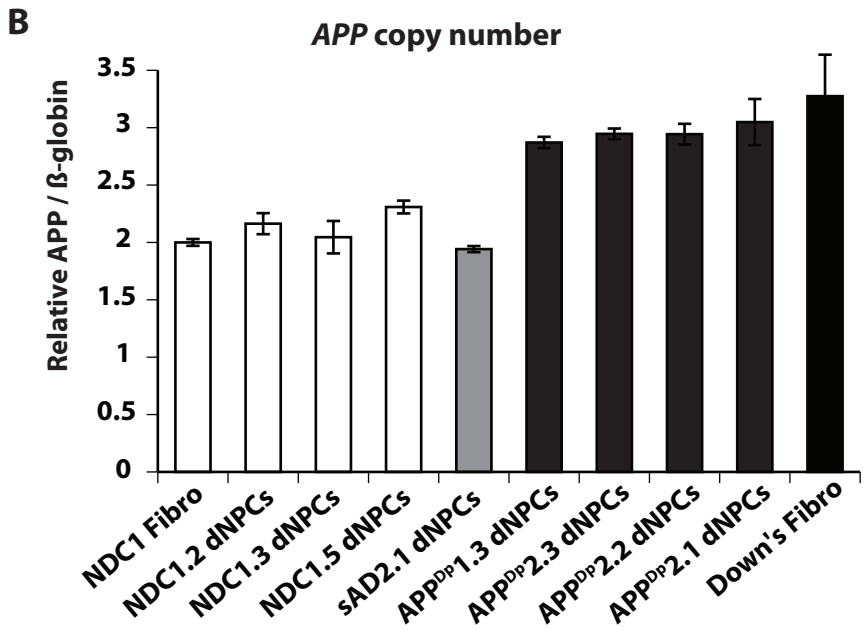

Figure 2.3. Additional properties of differentiated NPCs. A, Western blot detecting MAP2, total tau, phospho-tau, and α-synuclein expression in two representative differentiated NPC cultures (dNPCs). Note the absence of these markers in fibroblast cultures. **B**, APP copy number genotyping on dNPCs demonstrating that the APP duplication is maintained in differentiated cultures.

I found no significant differences between any of the individuals in the efficiency of NPC or neuronal differentiation (P = 0.63 and 0.17). Differentiation efficiency results are presented per individual in **Figure 2.4** and per iPSC line in **Figure 2.5**. Although variability in differentiation between lines was present, differences between lines from different individuals were not greater than between lines within individuals. These results suggest that any observed phenotypes in AD patient neurons, if present in multiple lines from the same patient, are caused by features of that patient's genotype.

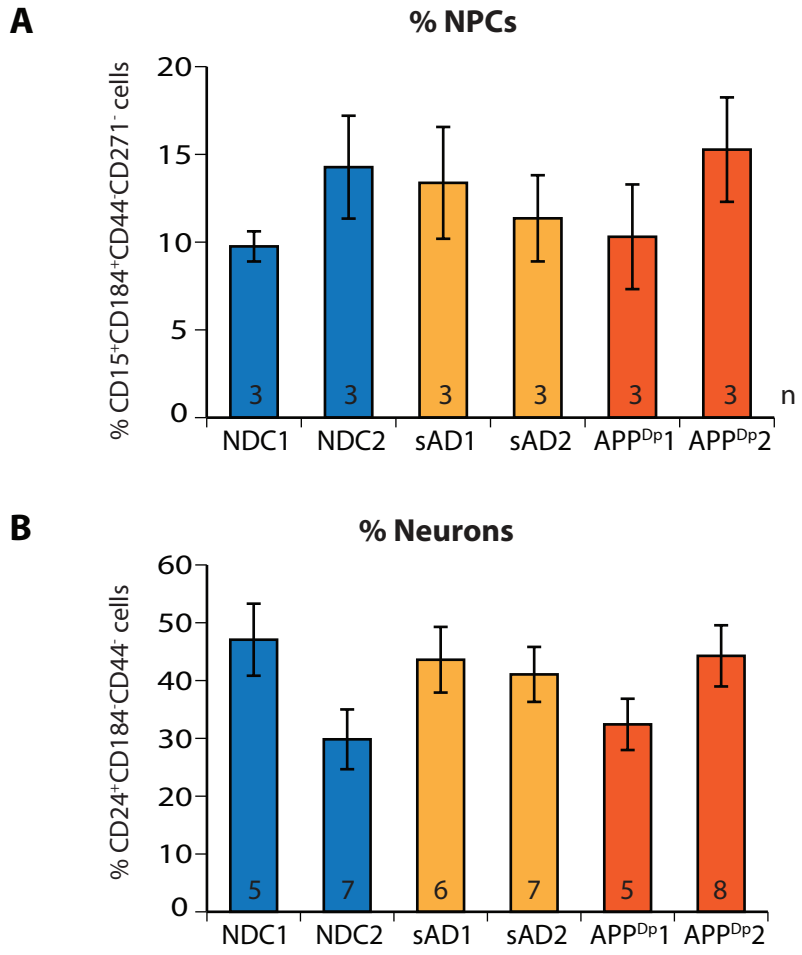

Figure 2.4. No significant difference in differentiation between patients. A, FACS data comparing the ability of iPSC lines to differentiate into $CD15^{+}CD184^{+}CD44^{-}CD271^{-}$ NPCs after 11 days of co-culture with PA6 cells. Although not all lines differentiated at the same efficiencies, when lines were grouped together by individual no significant difference was found ($p > 0.63$). **B**, FACS data comparing the ability of FACS-purified NPCs to differentiate into $CD24^{+}CD184^{-}CD44^{-}$ NPCs after 7 passages and 3 weeks of differentiation. Although not all lines differentiated at the same efficiencies, when lines were grouped together by individual no significant difference was found ($p > 0.17$).

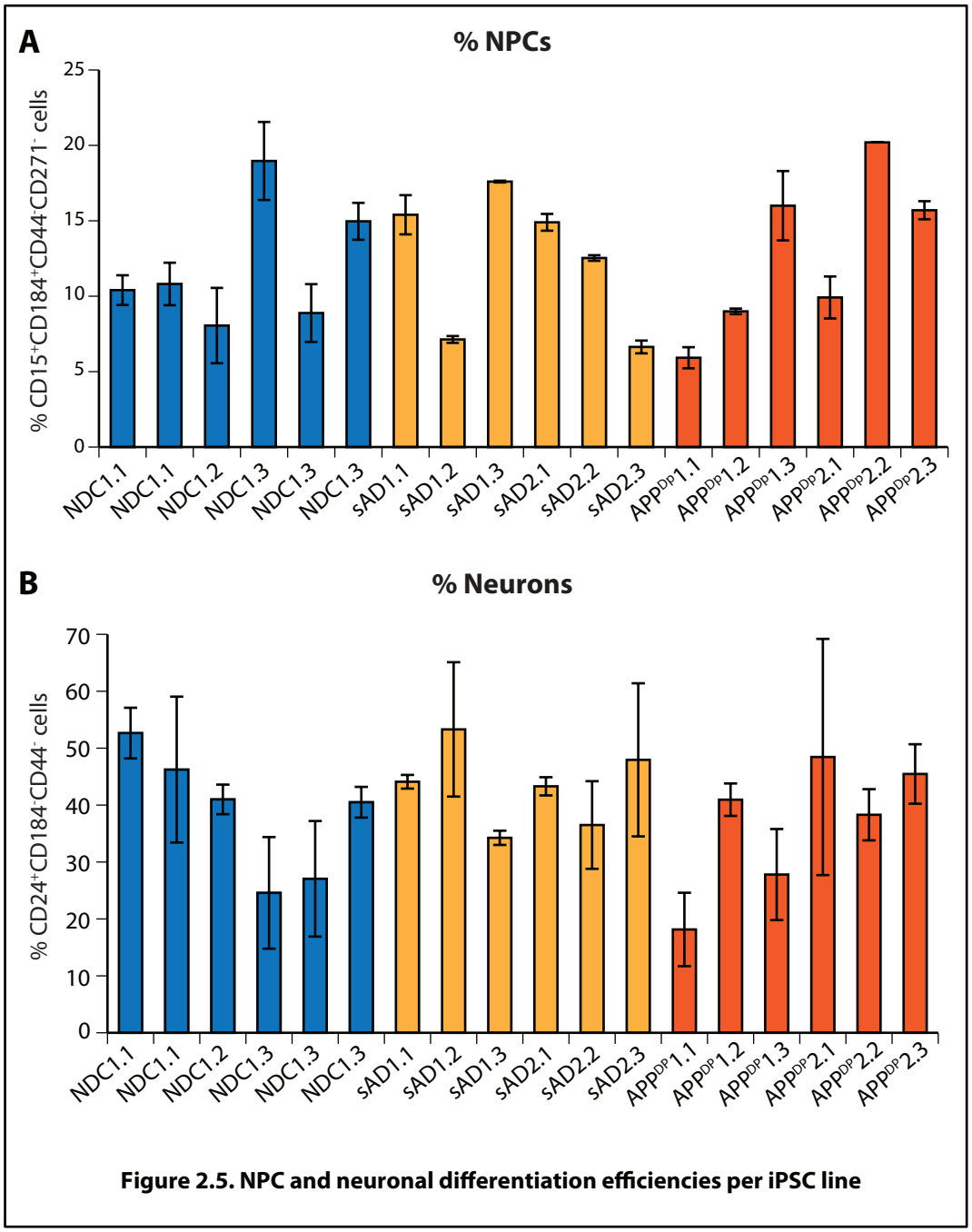

Figure 2.5. NPC and neuronal differentiation efficiencies per iPSC line

To estimate the maturity of purified neurons, we determined if individual neurons were electrophysiologically active. Current- and voltage-clamp experiments were performed on two representative cultures (**Figure 2.6**). These studies were

done in collaboration with Dr. Yangling Mu, a postdoctoral researcher in Fred Gage's lab. We found that purified neurons were capable of generating action potentials in response to somatic current injections (**Figure 2.6 A**). These action potentials are likely sodium spikes rather than calcium spikes, as evidenced by their relatively short width and high amplitude. Additionally, neurons had normal transient sodium and sustained potassium current in response to voltage step depolarizations (**Figure 2.6 B**). Since most current recordings had time courses less than 10 ms, currents generally resembled excitatory postsynaptic currents (EPSCs) more than inhibitory postsynaptic currents (IPSCs). This suggests that glutamatergic synaptic inputs were more common than GABAergic inputs. 13 of 13 neurons analyzed generated both action potentials and currents. Interestingly, 1 out of the 13 analyzed neurons was found to be spontaneously generating currents resulting from synaptic activity (**Figure 2.6 C**). This suggests a fully mature neuron. Since not all neurons were found to spontaneously generate currents, these data suggest that the neuronal cultures I used in this and subsequent experiments are a mix of mature and developing neurons.

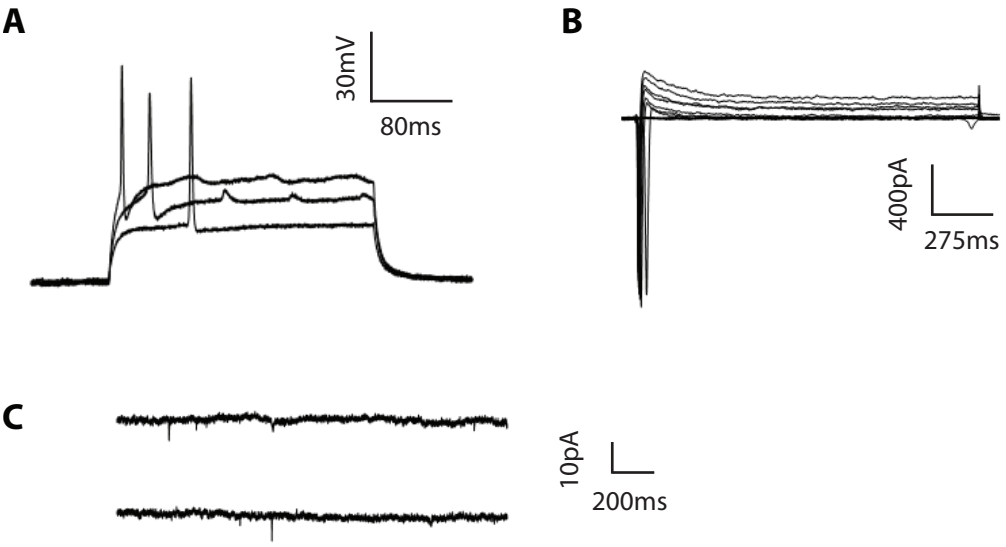

Figure 2.6. Electrophysiological properties of purified neurons A, Representative action potentials in response to somatic current injections. **B**, Normal transient sodium and sustained potassium currents in response to voltage step depolarizations. **C**, Spontaneous currents resulting from synaptic activity when voltage-clamped at -70 mV. 13 of 13 neurons analyzed exhibited currents and action potentials when current clamped and voltage clamped. 1 of 13 neurons analyzed exhibited spontaneous synaptic currents. Experiments performed by Yangling Mu, Gage lab.

To determine the subtypes of neurons in purified neuronal cultures, we analyzed the expression of neuronal subtype markers by immunofluorescence (I.F.) and by QPCR. By I.F., cultures appeared to contain a high percentage of neurons expressing the GABAergic markers GABA and GAD65/67 (**Figure 2.7**). Approximately 40% of neurons brightly expressed GABAergic markers. We also stained cultures against markers for glutamatergic, cholinergic, and dopaminergic neurons. Although we did not detect convincing levels of any of these markers, we suspect this could be due to poor antibodies. Due to the excitatory postsynaptic currents observed in the electrophysiology experiments, it is likely that a large

proportion of the GABA negative cells are glutamatergic neurons. I.F. experiments were performed by Sol Reyna during her rotation in our laboratory.

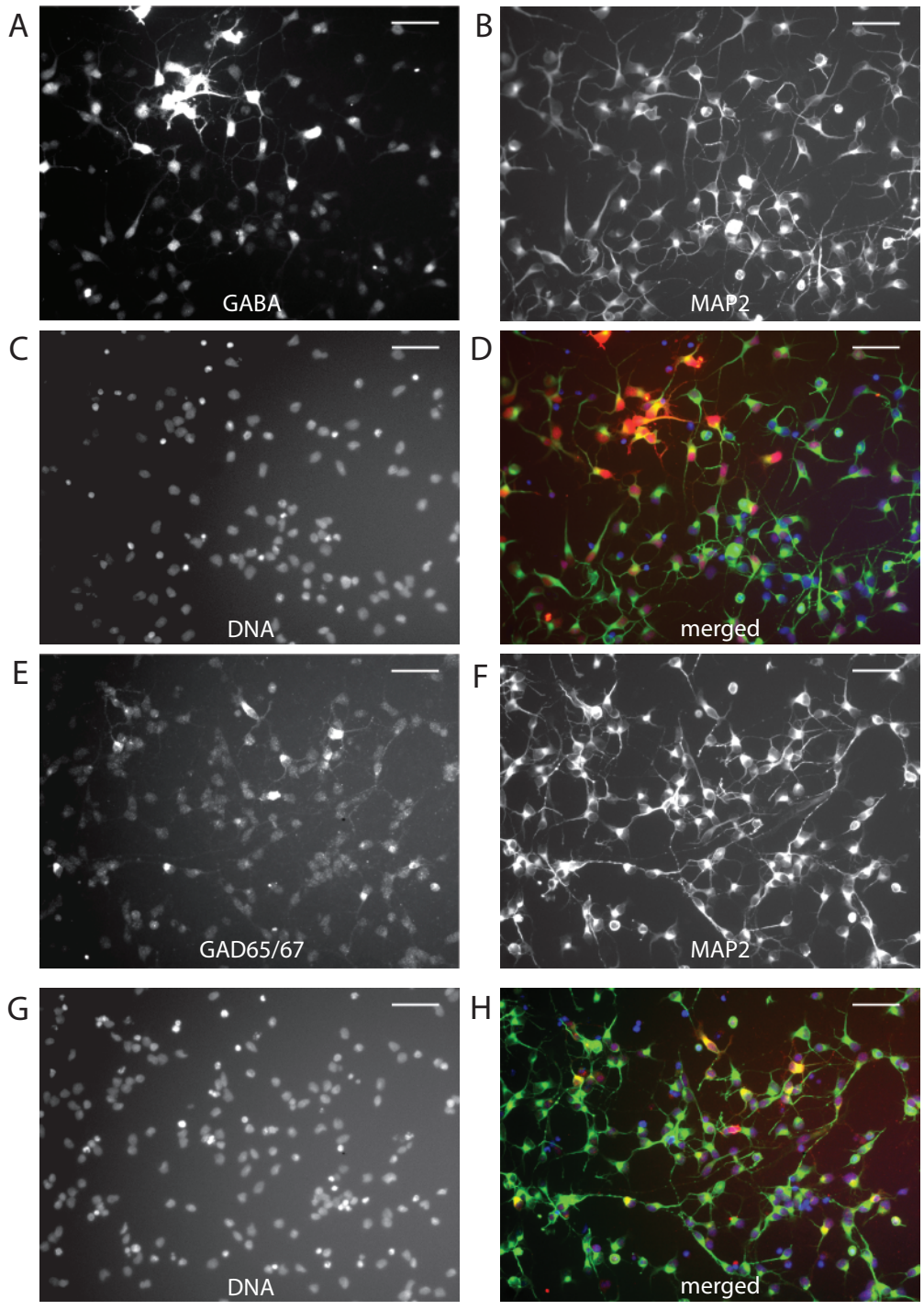

Figure 2.7. GABAergic expression in purified neuronal cultures. A-D, Representative immunofluorescent image showing GABA and MAP2 expression in purified neurons. **E-H**, GAD65/67 expression in purified neurons. Scale bars = 50μm.

In contrast to the I.F. experiments, on the RNA level most neuronal cultures expressed detectable levels of the glutamatergic, cholingeric and GABAergic markers VGLUT1, CHAT and GAD67, respectively. No significant difference in the expression of these markers was detected between individuals by quantitative PCR ($p > 0.05$ for all). Results are presented per individual in **Figure 2.8** and per iPSC line in **Figure 2.9**. Similar to the cell surface marker comparative differentiation data, although variability between iPSC lines was evident, little or none of this variability appears to be due to differences between individuals. These data further demonstrate that the six individuals of the AD-iPSCs differentiate at similar rates and efficiencies, which suggests that phenotypic comparisons between individuals are valid.

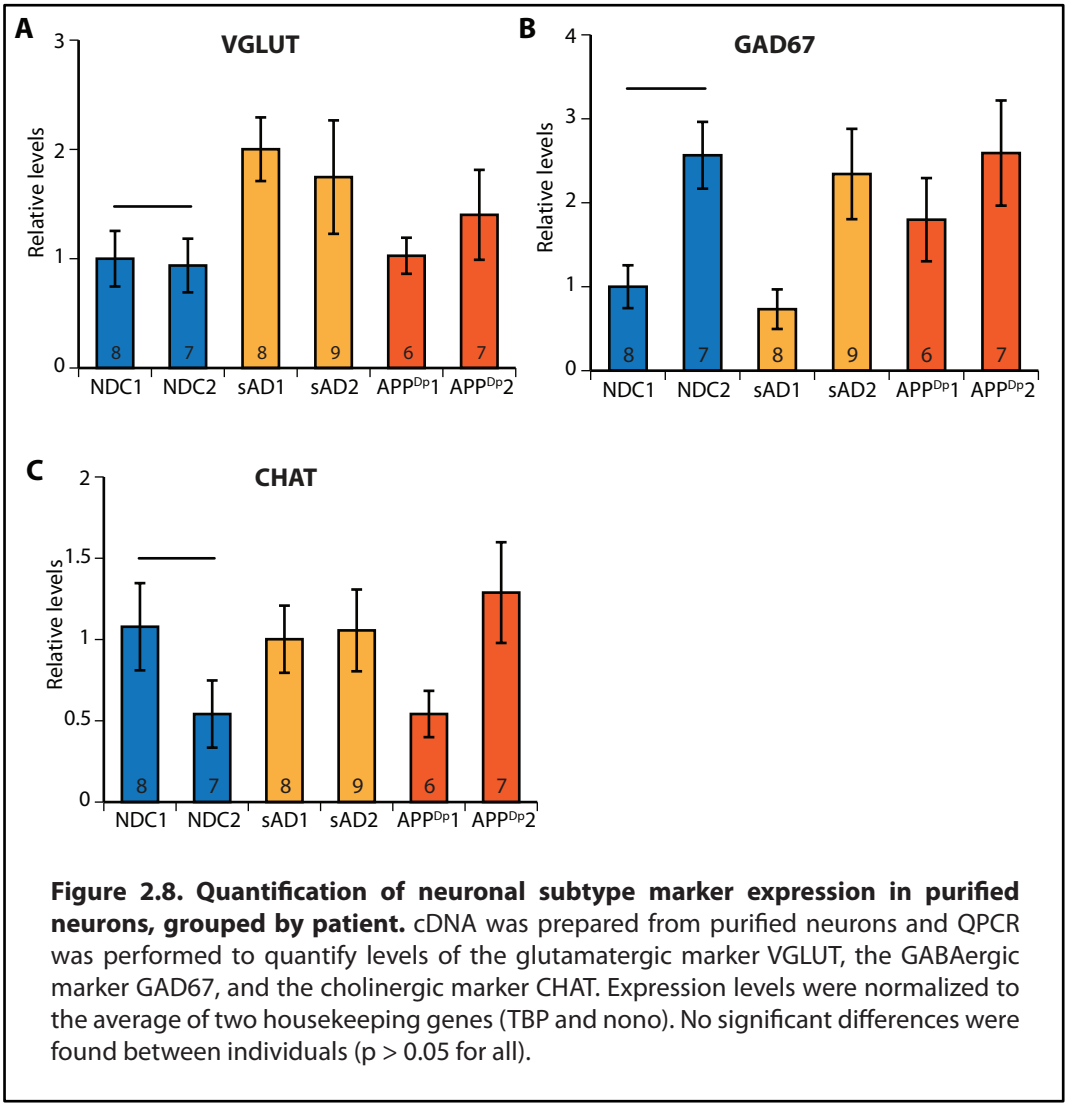

Figure 2.8. Quantification of neuronal subtype marker expression in purified neurons, grouped by patient. cDNA was prepared from purified neurons and QPCR was performed to quantify levels of the glutamatergic marker VGLUT, the GABAergic marker GAD67, and the cholinergic marker CHAT. Expression levels were normalized to the average of two housekeeping genes (TBP and nono). No significant differences were found between individuals ($p > 0.05$ for all).

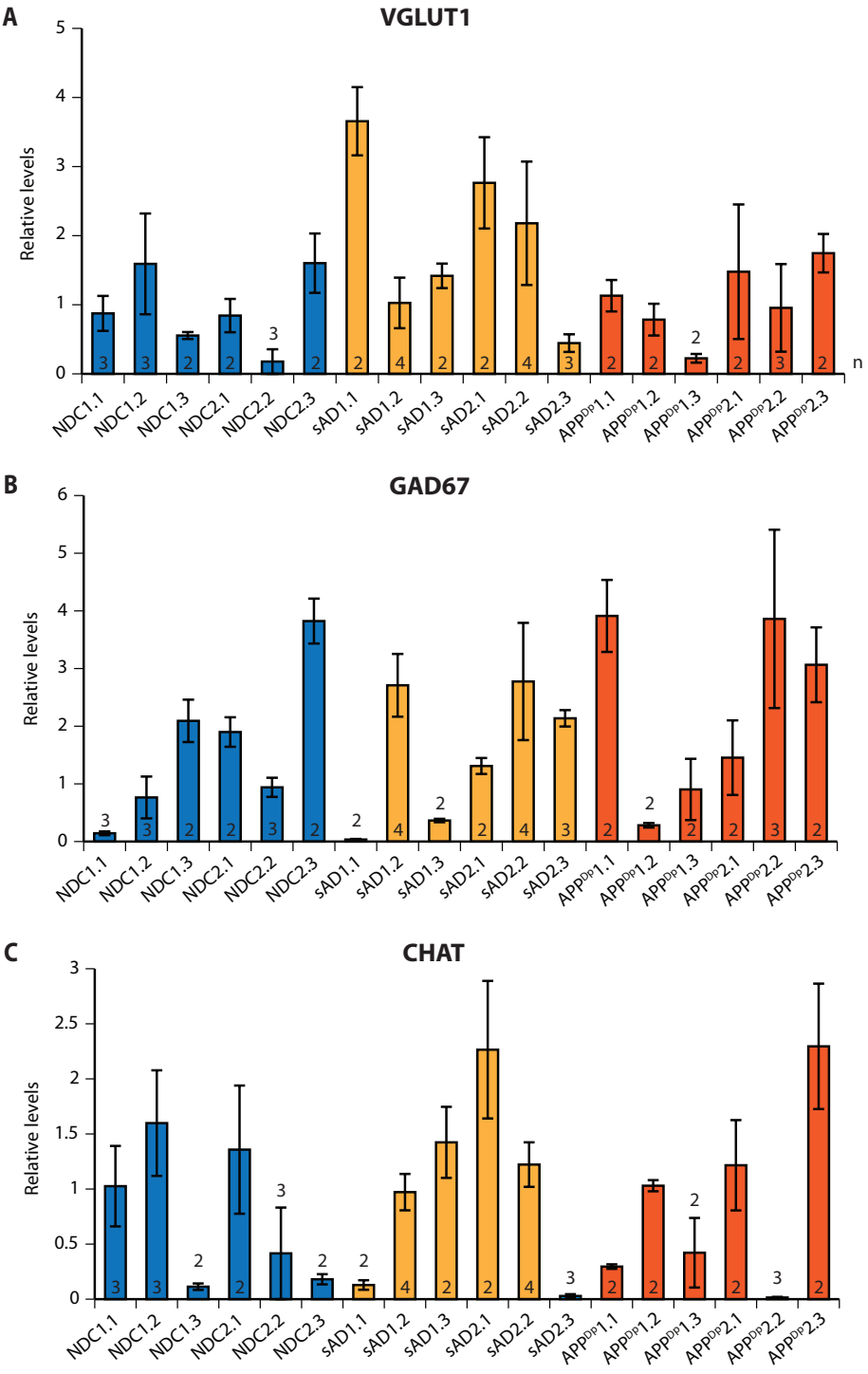

Figure 2.9. Quantification of neuronal subtype marker expression in purified neurons, grouped by iPSC line. cDNA was prepared from purified neurons and QPCR was performed to quantify levels of the glutamatergic marker VGLUT, the GABAergic marker GAD67, and the cholinergic marker CHAT. Expression levels were normalized to the average of two housekeeping genes (TBP and nono).

CONCLUSION AND DISCUSSION

Taken together, the cell surface marker comparative differentiation data and neuronal subtype RNA expression data suggest that iPSC-derived neurons from different individuals can be compared since they differentiated at equivalent rates into equivalent cell types. The electrophysiology and I.F. data suggest that these cultures contain both mature and developing neurons, with a high percentage of GABAergic subtypes. Thus, these cultures appear to consist of highly relevant cell types for the study of AD. In the future, however, the use of differentiated cholinergic neurons as well as aged neurons should be explored. The iPSC-derived NPCs described in this chapter should also be able to differentiate into glia and oligodendrocytes. In the future it will be interesting to FACS purify these cell types as well as compare their differentiation efficiencies between individuals. Although the method described in Yuan, *et al.* is still being optimized for glial differentiation, preliminary data suggests that the AD-iPSCs can be used to generate astrocytes. Importantly, the data in this chapter demonstrate how the method described in Yuan, *et al*. can be used to precisely compare the differentiation efficiencies of multiple iPSC lines, an issue that is becoming critically important as it is unclear how much variability is introduced by iPSC technology.

MATERIALS AND METHODS

NPC and neuronal differentiation method. Differentiation to NPCs and neurons followed Yuan, *et al* (18) and is summarized in **Figure 2.1**. Briefly, differentiation began with a confluent 10 cm dish of undifferentiated iPSC. Cells were

dissociated with Accutase (Innovative Cell Technologies) and for each plate, ~$5x10^5$ TRA1-81$^+$ iPSC were isolated by FACS. $3x10^5$ FACS-purified cells were seeded onto 3x10 cm plates that were seeded the previous day with $5x10^5$ PA6 cells in PA6 media. At day 11, cells were dissociated with Accutase and ~$5x10^5$ CD184$^+$CD15$^+$CD44$^-$CD271$^-$ NPCs were FACS-purified and plated onto poly-ornithine/laminin-coated plates and cultured with bFGF. On passage 7, NPCs were differentiated with BDNF, GDNF and cAMP. After 3 weeks of differentiation, cells were dissociated with Accutase and 1-2 million CD24$^+$CD184$^-$CD44$^-$ cells were collected and carefully plated at a density of $2x10^5$ per 96-well. Cells were cultured for an additional 5 days with a full-media change on day 3. At this point, cultures were harvested for analysis.

NPC and purified neuronal culture conditions. Culture media are detailed in Appendix I. NPCs were dissociated with Accutase (Innovated Cell Technologies) and split 1:3. Purified neurons were seeded at a concentration of 150,000 cells per well of a 96 well imaging plate (BD Biosciences).

Immunocytochemistry and FACS. Cells were fixed in 4% paraformaldehyde, permeabilized with buffer containing TritonX-100, and stained with primary and secondary antibodies (see Appendix III). Samples were imaged on a Nikon TE2000-U inverted microscope and acquired using Metamorph software (Molecular Devices). ImageJ software (NIH) was used to pseudo-color images, adjust contrast, and add scale bars. FACS experiments were carried out on a FACSAria II cytometer (BD Biosciences) and analyzed using FloJo software (Tree Star).

Quantitative PCR. cDNA was prepared from purified neurons cultured for 5 days using the Power SYBR Green Cells-to-Ct Kit (Life Technologies). QPCR was

performed following manufacturer's recommendations on an Applied Biosystems 7300 QPCR machine. Expression levels of neuronal subtype markers were normalized to the average of two housekeeping genes (TBP and NONO). For APP copy number genotyping methods see Chapter 2. Primer sequences are listed in Appendix II.

Western blotting. Protein was prepared from differentiated NPC and fibroblast cultures using MSD complete lysis buffer (Meso Scale Diagnostics). Western blots were performed using standard methods. Antibodies are detailed in Appendix III.

Electrophysiology methods. Whole-cell perforated patch recordings were performed on purified neurons cultured for 5 days. Methods were previously described in Marchetto, *et al* (13).

Statistics. Data were analyzed using JMP software (SAS Institute). Cell lines were compared by performing ANOVA followed by Tukey's HSD posthoc test. $P<0.05$ was considered statistically significant.

***APP* copy number genotyping.** See Chapter 2 methods.

Antibodies: See Appendix III.

ACKNOWLEDGEMENTS

Chapters 2 contains work submitted for publication by authors: Mason A. Israel, Shauna H. Yuan, Sol M. Reyna, Yangling Mu, Christian T. Carson, Fred H. Gage, Anne M. Remes, Edward H. Koo, Lawrence S. B. Goldstein. The dissertation author was the primary investigator and author of this material.

REFERENCES

1. Thomson JA, Itskovitz-Eldor J, Shapiro SS, Waknitz MA, Swiergiel JJ, Marshall VS, & Jones JM (1998) Embryonic Stem Cell Lines Derived from Human Blastocysts. *Science* 282(5391):1145-1147.

2. Takahashi K, Tanabe K, Ohnuki M, Narita M, Ichisaka T, Tomoda K, & Yamanaka S (2007) Induction of Pluripotent Stem Cells from Adult Human Fibroblasts by Defined Factors. *Cell* 131(5):861-872.

3. Keller G (2005) Embryonic stem cell differentiation: emergence of a new era in biology and medicine. *Genes & Development* 19(10):1129-1155.

4. Reubinoff BE, Itsykson P, Turetsky T, Pera MF, Reinhartz E, Itzik A, & Ben-Hur T (2001) Neural progenitors from human embryonic stem cells. *Nat Biotech* 19(12):1134-1140.

5. Zhang S-C, Wernig M, Duncan ID, Brustle O, & Thomson JA (2001) In vitro differentiation of transplantable neural precursors from human embryonic stem cells. *Nat Biotech* 19(12):1129-1133.

6. Perrier AL, Tabar V, Barberi T, Rubio ME, Bruses J, Topf N, Harrison NL, & Studer L (2004) Derivation of midbrain dopamine neurons from human embryonic stem cells. *Proceedings of the National Academy of Sciences of the United States of America* 101(34):12543-12548.

7. Zeng X, Cai J, Chen J, Luo Y, You Z-B, Fotter E, Wang Y, Harvey B, Miura T, Backman C, Chen G-J, Rao MS, & Freed WJ (2004) Dopaminergic Differentiation of Human Embryonic Stem Cells. *Stem Cells* 22(6):925-940.

8. Di Giorgio FP, Carrasco MA, Siao MC, Maniatis T, & Eggan K (2007) Non-cell autonomous effect of glia on motor neurons in an embryonic stem cell-based ALS model. *Nat Neurosci* 10(5):608-614.

9. Brustle O, Spiro AC, Karram K, Choudhary K, Okabe S, & McKay RDG (1997) In vitro-generated neural precursors participate in mammalian brain development. *Proceedings of the National Academy of Sciences of the United States of America* 94(26):14809-14814.

10. Brustle O, Jones KN, Learish RD, Karram K, Choudhary K, Wiestler OD, Duncan ID, & McKay RDG (1999) Embryonic Stem Cell-Derived Glial Precursors: A Source of Myelinating Transplants. *Science* 285(5428):754-756.

11. Wernig M, Zhao J-P, Pruszak J, Hedlund E, Fu D, Soldner F, Broccoli V, Constantine-Paton M, Isacson O, & Jaenisch R (2008) Neurons derived from reprogrammed fibroblasts functionally integrate into the fetal brain and improve symptoms of rats with Parkinson's disease. *Proceedings of the National Academy of Sciences* 105(15):5856-5861.

12. Ben-Hur T, Idelson M, Khaner H, Pera M, Reinhartz E, Itzik A, & Reubinoff BE (2004) Transplantation of Human Embryonic Stem Cell–Derived Neural Progenitors Improves Behavioral Deficit in Parkinsonian Rats. *Stem Cells* 22(7):1246-1255.

13. Marchetto MCN, Carromeu C, Acab A, Yu D, Yeo GW, Mu Y, Chen G, Gage FH, & Muotri AR (2010) A Model for Neural Development and Treatment of Rett Syndrome Using Human Induced Pluripotent Stem Cells. *Cell* 143(4):527-539.

14. Osafune K, Caron L, Borowiak M, Martinez RJ, Fitz-Gerald CS, Sato Y, Cowan CA, Chien KR, & Melton DA (2008) Marked differences in differentiation propensity among human embryonic stem cell lines. *Nat. Biotechnol.* 26(3):313-315.

15. Crews L & Masliah E (2010) Molecular mechanisms of neurodegeneration in Alzheimer's disease. *Human Molecular Genetics* 19(R1):R12-R20.

16. Funato H, Yoshimura M, Yamazaki T, Saido TC, Ito Y, Yokofujita J, Okeda R, & Ihara Y (1998) Astrocytes containing amyloid beta-protein (Abeta)-positive granules are associated with Abeta40-positive diffuse plaques in the aged human brain. (Translated from eng) *Am J Pathol* 152(4):983-992 (in eng).

17. Mitrasinovic OM & Murphy GM (2002) Accelerated Phagocytosis of Amyloid-ß by Mouse and Human Microglia Overexpressing the Macrophage Colony-stimulating Factor Receptor. *Journal of Biological Chemistry* 277(33):29889-29896.

18. Yuan S, Martin J, Elia J, Flippin J, Rosanto I, Paramban R, Hefferan M, Vidal J, Mu Y, Killian R, Israel MA, Emre N, Marsala S, Marsala M, Gage F, Goldstein LSB, & Carson C (2011) Cell-surface marker signatures for the isolation of neural stem cells, glia and neurons derived from human pluripotent stem cells. *In press at PLoS One*.

19. Kawasaki H, Mizuseki K, Nishikawa S, Kaneko S, Kuwana Y, Nakanishi S, Nishikawa S-I, & Sasai Y (2000) Induction of Midbrain Dopaminergic Neurons from ES Cells by Stromal Cell Derived Inducing Activity. *Neuron* 28(1):31-40.

CHAPTER 3.

Recapitulation of Alzheimer's disease pathogenesis in neurons derived from induced pluripotent stem cells

ABSTRACT

Our understanding of Alzheimer's disease (AD) pathogenesis is currently limited by difficulties in obtaining live neurons from patients and the inability to model the sporadic form of AD. It may be possible to overcome these challenges by reprogramming primary cells from patients into induced pluripotent stem cells (iPSCs). Here I report the recapitulation of aspects of AD pathogenesis in iPSC-derived neurons from familial and sporadic AD patients. Purified neurons from both APP^{Dp} patients and one sporadic AD patient displayed significantly elevated levels of $Aß^{1-40}$, activated GSK3ß and phospho-tau, relative to controls. Neurons from a second sporadic AD patient were indistinguishable from controls in these assays. ß-secretase and γ-secretase inhibition both significantly reduced secreted Aß levels from iPSC-derived neurons. Only ß-secretase inhibition, however, significantly reduced active GSK3ß and phospho-tau levels. These results suggest a direct relationship between APP proteolytic processing and tau phosphorylation in human neurons. More generally, we demonstrate that iPSC technology can be used to model familial and sporadic forms of AD, even though it can take decades for overt disease to manifest in patients.

BACKGROUND AND SIGNIFICANCE

Alzheimer's disease (AD) is a fatal, incurable form of dementia that currently afflicts more than 35 million people worldwide (1). The primary neurological feature of AD is global cognitive decline, including deterioration of memory, orientation, judgment and reasoning (2). With the increasing longevity and aging of our population, the

devastation caused by AD on patients, families, societies and economies is growing. Currently, there is no approved treatment with a proven disease-modifying effect (3).

Two hallmark pathologies are used to diagnose AD and are both thought to be critically involved in disease pathogenesis. The first, amyloid plaques, are cerebral extracellular deposits primarily composed of Aß peptides (2, 4). Aß peptides are aggregate-prone protein fragments cleaved from the Amyloid Precursor Protein (APP), a process that involves the proteases ß-secretase and γ-secretase. Amyloid plaques are often present in the brains of individuals who die without dementia, but an unknown proportion of these individuals would have developed AD at a later timepoint.

The second hallmark pathology, neurofibrillary tangles, are filamentous accumulations of hyperphosphorylated tau protein located in the somatodendritic compartment of neurons (1). The abundance in brain autopsies of tangles or phosphorylated tau correlates with the severity of dementia better than the abundance of plaques (5, 6). In its normal state, tau is a microtubule associated protein primarily localized to the axonal compartment and has a well-characterized role in maintaining axonal microtubule stability (7, 8). Under disease conditions, tau is hyperphosphorylated by kinases such as GSK3ß and CDK5 (9), which causes its detachment from microtubules, its mislocalization to the somatodendritic compartment, microtubule instability, synaptic dysfunction, and possible disruption of axonal transport (10, 11). The mechanism responsible for activation of tau kinases is poorly understood. Although the predominant hypothesis is that Aß is the initial culprit, several lines of evidence suggest that other cleaved products of APP, especially the C-terminal fragments (CTFs), play a role (12-15).

AD can be subdivided into two categories: sporadic AD (sAD) and familial AD (fAD). The vast majority (~99%) of AD is sAD (16). sAD is heterogeneous on both the genetic level, with a non-Mendelian pattern of inheritance, and on the pathological level. Although called *sporadic*, sAD has a clear genetic contribution (17). Age of onset is generally late (> 65 years of age), but a high degree of variability also exists in this aspect. The rare fAD cases have fully penetrant, dominantly inherited forms of AD that are usually early onset (< 65 years). Although tau pathology more closely associates with disease severity, it is the Aß pathology that associates with fAD genetics (2). All known mutations that cause fAD involve either the *APP* gene, or the *Presenilin* genes, which encode proteolytic components of γ-secretase activity necessary to cleave Aß (and other derivatives) from APP. fAD caused by *APP* aberrations can either involve specific point mutations within the gene or a single duplication of the *APP* locus (18, 19). Since *APP* is located on chromosome 21, individuals with Down's syndrome invariably develop early onset AD pathologies. Despite detailed knowledge of the genetic causes of fAD and the pathological culmination of fAD and sAD, mechanistic understanding of pathogenesis and effective therapies remain elusive. A major reason for this is the failure of animal models to fully recapitulate AD pathogenesis.

Animal models harboring mutations found in fAD, although they have invaluably contributed to our current understanding of AD, do not recapitulate important pathological and neurological features of the disease (20). For example, the most common animal models of AD are mice that overexpress fAD mutant *APP* and/or fAD mutant *Presenilin*. Despite these extremely aggressive genetic paradigms, mice only develop plaque pathology and mild cognitive deficits, and escape tangle

pathology and neurodegeneration. Our current inability to model important aspects of AD is a major barrier separating us from a more complete understanding of AD and the development of novel therapies. Furthermore, the sporadic form of AD cannot be modeled in mice due to complex and unidentified genetics.

One obvious explanation for the shortcomings of animal models is species-specific differences. Indeed, Geula, *et al.* observed differences between rodents and primates in response to injected amyloid preparations, as well as between two different primate species (21). Additionally, important differences exist between rodent and human tau. An accurate *human* model of AD is therefore of extreme value. Unfortunately, human central nervous system biopsies are too limited in quantity and autopsy samples, though less limited, cannot be used to study live neurons or the critical early stages of pathogenesis. Human peripheral cells, such as skin fibroblasts, have been used as models for many years because they secrete Aß peptides into the culture media (22), but are incomplete models because they do not express tau and many other neuronal proteins. Additionally, fibroblast models have not been highly useful in elucidating the causes of sAD. Live, human, patient-specific neuronal models of AD, although of tremendous potential value, have not been reported.

In addition to the two hallmark pathologies, multiple additional defects have been observed in AD autopsies. Some, such as accumulations of endocytic and axonal vesicles, have been observed very early in disease pathogenesis (23, 24). Other pathologies detected more frequently in AD autopsies than control samples include reduction in synapse number, reduction in neurotrophin levels, damage to mitochondria, aberrant cell cycle reentry, calcium signaling dysregulation, and

activation of astrocytes and microglia (1). Another class of AD pathologies, including vascular disease, cholesterol dysregulation, and reduction of insulin-pathway components, are only observed in subsets of AD patients (1). Since animal models fail to fully recapitulate disease pathogenesis and AD autopsies represent endpoints of disease, the relative importance of all these pathologies to disease initiation and propagation, though of extreme interest, remains unclear. An abundant source of live, patient-specific neural cells could allow researchers to probe the contributions of these pathologies to overall pathogenesis.

The recent development of induced pluripotent stem cell (iPSC) technology has allowed the creation of live, patient-specific models of disease and the investigation of disease phenotypes *in vitro* (25-28). Currently, iPSCs are most commonly made by overexpressing the transcription factors *OCT4, SOX2, KLF4* and *cMYC* in primary fibroblasts, followed by culturing the transformed cells in human embryonic stem cell (hESC) culture conditions. Amazingly, the resultant *reprogrammed* cell lines, if high quality, are patient-specific stem cell lines that appear to divide indefinitely and can differentiate into theoretically any cell type of the human body. IPSC technology has been touted as a method to create “diseases in a dish,” as well as novel platforms for therapeutic development (29, 30).

Though the first report of human iPSCs occurred less than four years ago, a handful of research groups have already reported successful use of iPSCs in disease modeling. Ebert, *et al*. found that iPSC-derived motor neurons from two spinal muscular atrophy patients have a decreased survival rate relative to control neurons, and the undifferentiated iPSCs from affected patients have an increased number of intracellular gems, a marker of disease (28). Lee, *et al*. reported defects in neural

differentiation and cellular migration using iPSCs derived from patients with familial dysautonmia (31). Both studies reported that specific drugs could be used to partially rescue phenotypes.

Very recently, iPSCs have been made from a wide variety of diseases. However, not all reports include identification of a phenotype (32-34) and there is even one report of a disease that failed to be modeled with iPSCs even though hESCs could be used (35). It currently remains unreported if iPSC technology can be used to model AD or the sporadic form of any disease. A review by Saha and Jaenisch recently suggested that iPSCs may not be capable of modeling sporadic forms of disease (29). Additional limitations to the field include unexplained variability between patients within a disease, between cell lines within a patient, and between replicates within a cell line.

In this chapter I test the hypothesis that iPSC-derived neurons accurately recapitulate aspects of AD pathogenesis, such as increased Aß secretion and tau phosphorylation. Additionally, I test the hypotheses that products of APP other than Aß play a role in tau phosphoylation, and that iPSC-derived neurons can serve as a platform for therapeutic testing.

RESULTS

The predominant hypothesis in the AD field is that the initiating event of AD is elevation of Aß levels. It is unknown if iPSC-derived neurons from familial AD patients are capable of maintaining the elevated Aß production seen in their parental fibroblasts. To address this question, I differentiated 3 iPSC lines each from individuals NDC1, NDC2, sAD1, sAD2, $APP^{Dp}1$ and $APP^{Dp}2$ into purified neurons and

measured Aß$^{1-40}$ levels in media conditioned by the neurons for 48 hours (**Figure 3.1 A**). I found little variation in Aß levels in the neurons from both control individuals. Neurons from NDC1 and NDC2 were statistically equivalent to each other ($p = 1.0$). Neurons from patient sAD1 were also statistically indistinguishable from controls ($p = 1.0$). Similar to what I observed in fibroblast cultures, neurons from both APP^{Dp} patients secreted significantly higher levels of Aß than controls (APP^{Dp}1: $p < 0.05$ and APP^{Dp}2: $p < 0.0001$). Surprisingly, the neurons from patient sAD2 revealed an Aß phenotype that was not present in the parental fibroblasts. sAD2 neurons secreted significantly higher levels of Aß compared to controls ($p < 0.05$). These data are presented by patient in **Figure 3.1 A** and per iPSC line in **Figure 3.2 A**. Data from all neuronal assays are summarized in **Table 3.1**.

I observed two important differences between the neuronal and fibroblast Aß data sets (**Figure 3.1 B**). First, although fibroblasts and neurons from APP^{Dp} patients were both significantly higher than controls, the difference between controls and patients was markedly higher in the neuronal samples. While APP^{Dp} fibroblasts secreted on average 1.5-fold higher levels of Aß, neurons were elevated by 3-fold on average. The reason for this is unknown, but provides a possible explanation of why neurons are more vulnerable to aberrant Aß than fibroblasts. Second, as mentioned, patient sAD2 was significantly elevated only in neurons, not fibroblasts. In fact, fibroblasts from patient sAD2 secreted slightly lower levels of Aß on average than controls. This phenotype was present in all 3 iPSC lines from sAD2 (**Figure 3.2 A**), suggesting robustness. The surprising finding that the neurons of patient sAD2 revealed an Aß phenotype not present in the parental fibroblasts provides evidence that iPSC technology can be used to study aspects of sporadic AD pathogenesis in

way previously not possible. Furthermore these data suggest that fibroblasts are not fully predictive of neuronal phenotypes.

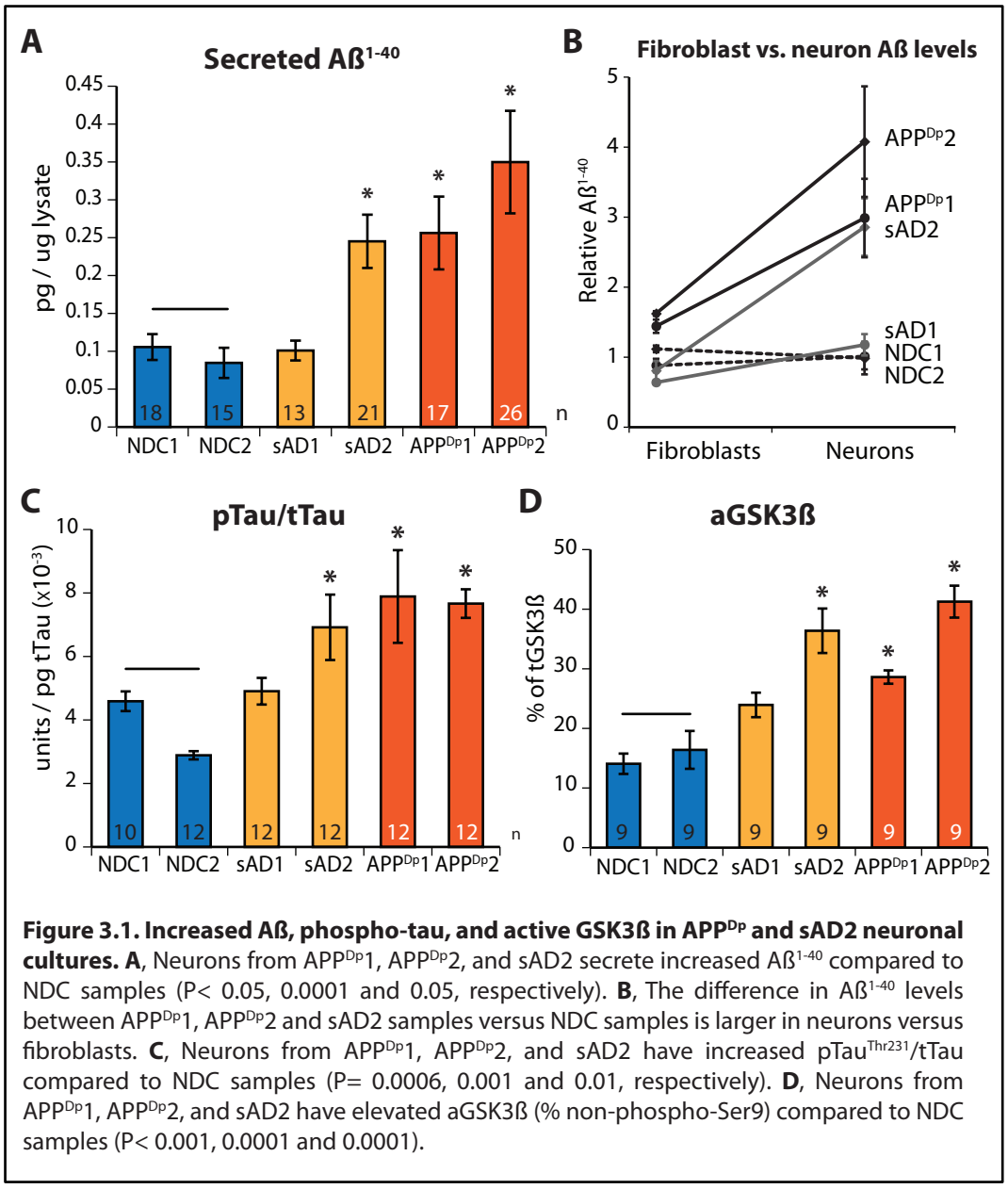

Figure 3.1. Increased Aß, phospho-tau, and active GSK3ß in APP^{Dp} and sAD2 neuronal cultures. A, Neurons from APP^{Dp}1, APP^{Dp}2, and sAD2 secrete increased Aß$^{1-40}$ compared to NDC samples (P< 0.05, 0.0001 and 0.05, respectively). **B**, The difference in Aß$^{1-40}$ levels between APP^{Dp}1, APP^{Dp}2 and sAD2 samples versus NDC samples is larger in neurons versus fibroblasts. **C**, Neurons from APP^{Dp}1, APP^{Dp}2, and sAD2 have increased pTau^{Thr231}/tTau compared to NDC samples (P= 0.0006, 0.001 and 0.01, respectively). **D**, Neurons from APP^{Dp}1, APP^{Dp}2, and sAD2 have elevated aGSK3ß (% non-phospho-Ser9) compared to NDC samples (P< 0.001, 0.0001 and 0.0001).

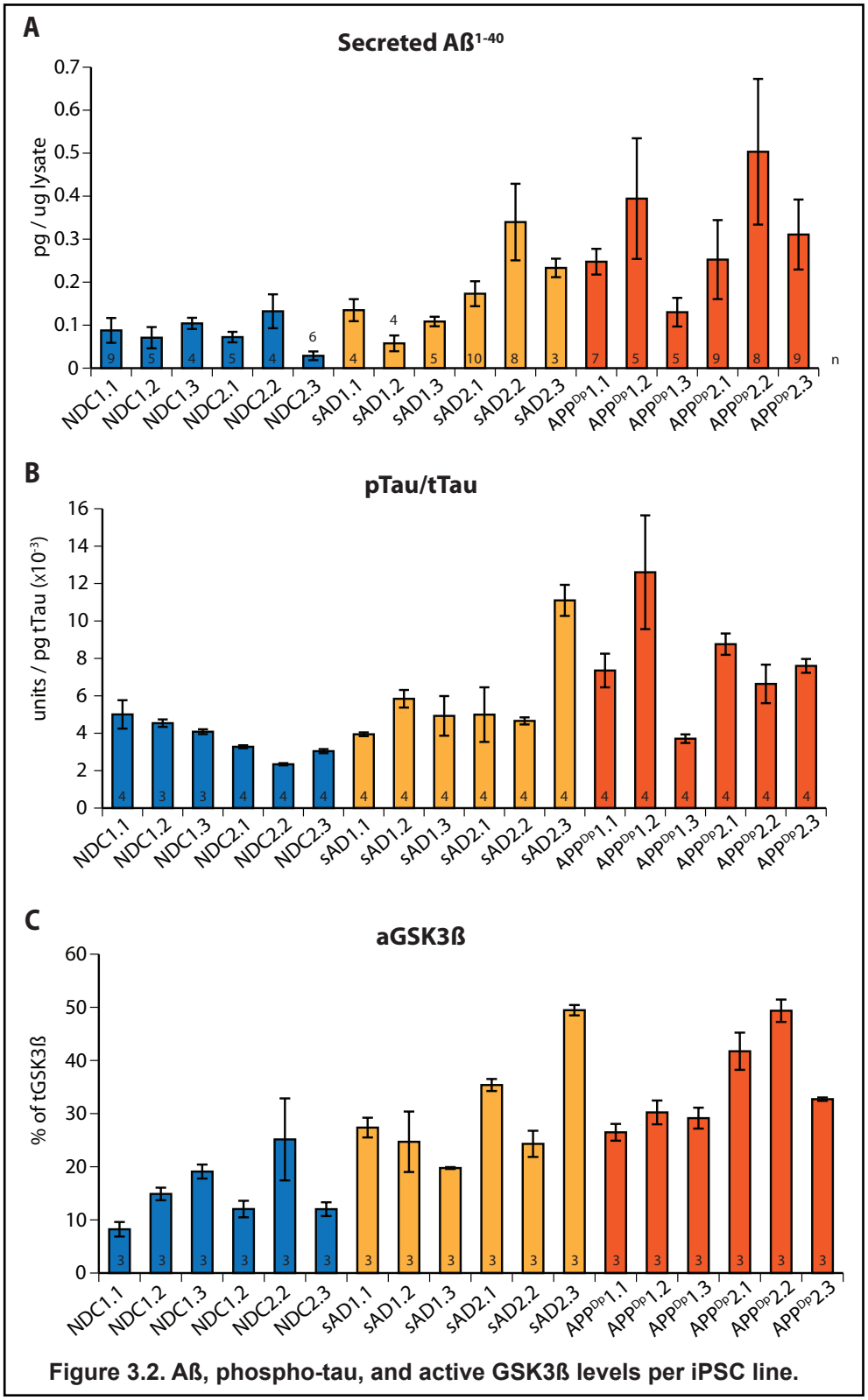

Figure 3.2. Aß, phospho-tau, and active GSK3ß levels per iPSC line.

Table 3.1. Summary of comparative analysis

	Aß1-40 (pg/ug)	aGSK3ß (%)	pTau/tTau (units/pg)	tTau (pg/mL)	Total protein (ug/mL)	VGLUT1	CHAT	GAD67
NDC1 mean	0.106	14.1	$4.6x10^{-3}$	3065	114.4	1.0	1.0	1.0
s.e.m.	0.017	1.7	$3.1x10^{-4}$	713	24.3	0.3	0.5	0.6
n	18	9	10	10	6	8	8	8
NDC2 mean	0.085	16.4	$2.9x10^{-3}$	3684	124.4	0.9	0.7	2.2
s.e.m.	0.020	3.2	$1.3x10^{-4}$	314	15.2	0.4	0.4	0.8
n	15	9	12	12	6	7	7	7
sAD1 mean	0.101	23.9	$4.9x10^{-3}$	6243	139.0	2.0	0.8	1.0
s.e.m.	0.013	2.1	$4.2x10^{-4}$	290	12.0	0.8	0.4	0.8
n	13	9	12	12	6	8	8	8
sAD2 mean	0.245	36.4	$6.9x10^{-3}$	6764	135.2	1.8	1.2	2.1
s.e.m.	0.035	3.7	$1.0x10^{-4}$	1067	15.0	0.7	0.6	0.4
n	21	9	12	12	6	9	9	9
$APP^{Dp}1$ mean	0.256	28.6	$7.9x10^{-3}$	5331	101.4	0.7	0.6	1.7
s.e.m.	0.048	1.1	$1.5x10^{-3}$	1791	14.1	0.3	0.2	1.1
n	17	9	12	12	6	6	6	6
$APP^{Dp}2$ mean	0.350	41.3	$7.7x10^{-3}$	7384	145.0	1.4	1.2	2.8
s.e.m.	0.068	2.7	$4.5x10^{-4}$	2753	17.8	0.2	0.7	0.7
n	26	9	12	12	6	7	7	7

Genetic evidence implicates altered or elevated APP processing and Aß levels as the driving agent behind familial AD (2) and, because of identical neuropathology, sporadic AD. However, tau, although not genetically linked to AD, forms NFTs, which correlate better with disease severity than amyloid plaque numbers. The mechanism by which altered APP processing might cause elevated pTau and NFT pathology is unclear. Tau phosphorylation at Thr231, one of several tau phosphoepitopes, regulates microtubule stability (10) and correlates with both neurofibrillary tangle number and degree of cognitive decline (6, 36). To determine if tau phosphorylation at Thr231 is elevated in APP^{Dp} and sAD neurons, I measured the amount of phospho-tau^{Thr231} relative to total tau levels (tTau) in lysates from purified neurons from three iPSC lines from each of the NDC, sAD and APP^{Dp} patients. Neurons from both APP^{Dp} patients had significantly higher pTau/tTau than neurons from NDC lines ($p < 0.001$ for each) (**Figure 3.1 C**). pTau/tTau in the two sAD patients mirrored the Aß findings: No difference was observed between sAD1 and NDC neurons while sAD2 neurons had significantly increased pTau/tTau ($p < 0.01$). These data provide evidence that a critical aspect of AD pathogenesis is recapitulated in iPSC-derived neurons. Since the increased levels of Aß and phospho-tau were present in purified neurons cultured in the absence of glia, the data further suggest that glia are not required to maintain these aberrations. Data are presented per patient in **Figure 3.1 C** and **Table 3.1**, and presented per iPSC line in **Figure 3.2 B**.

Tau can be phosphorylated by multiple kinases. The kinase GSK3ß (also known as tau protein kinase I) can phosphorylate tau at Thr231 *in vitro* and co-localizes with NFTs and pre-tangle phosphorylated tau in sAD postmortem neurons

(9). GSK3ß is thought to be constitutively active but is inactivated when phosphorylated at Ser9 (37). To determine if iPSC-derived neurons with elevated pTau have increased GSK3ß activity, the proportion of active GSK3ß (aGSK3ß) in purified neurons was calculated by measuring the amount of GSK3ß lacking phosphorylation at Ser9 relative to total GSK3ß levels. We observed that neurons from patients $APP^{Dp}1$, $APP^{Dp}2$ and sAD2 had significantly higher aGSK3ß than NDC neurons ($p < 0.001$, 0.0001 and 0.0001, respectively) (**Figure 3.1 D** and **Figure 3.2 C**). These data, in combination with the Aß and phospho-tau data sets, provide evidence that GSK3ß is present and active in iPSC-derived neurons and suggest that a biochemical pathway that is critically aberrant in AD brains is also aberrant in iPSC-derived neurons from AD patients.

Although Aß, pTau and GSK3ß clearly play roles in AD pathogenesis, their relationship is unclear. I observed that iPSC-derived neurons exhibited strong correlations between $Aß^{1-40}$, pTau/tTau and aGSK3ß levels (**Figure 3.3**). In contrast, correlation coefficients were much weaker between these measurements and levels of neuronal subtype marker expression, tTau, total protein, or transgene expression, with the exception of aGSK3ß and tTau (**Table 3.2**). These data are consistent with recapitulation of the Aß cascade in iPSC-derived neurons. Furthermore, since these experiments were performed in purified neurons in the absence of other cell types, these data suggest a direct relationship between the APP processing and tau phosphorylation pathways, with elevated levels of APP processing products as the initiating factor(s).

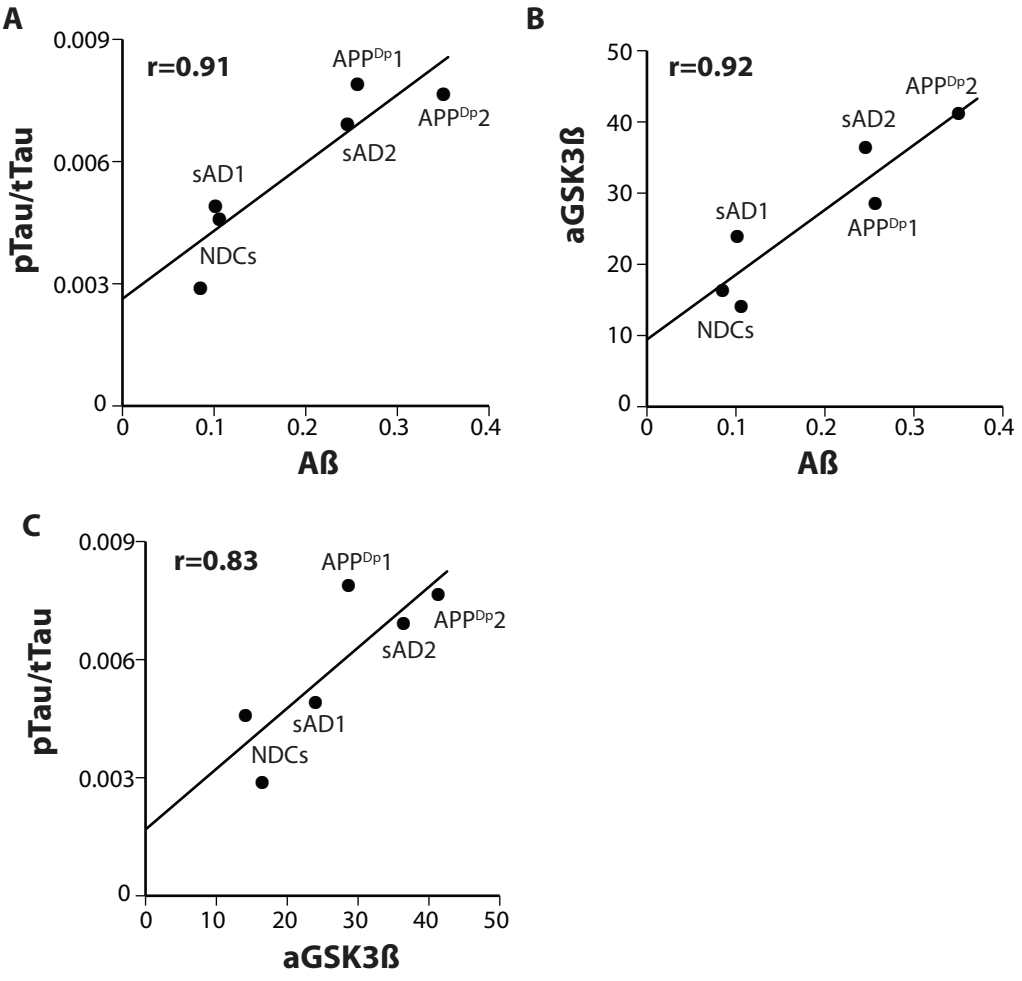

Figure 3.3. Strong correlations between Aß, phospho-tau and aGSK3ß levels in iPSC-derived neurons. A-B, $Aß^{1-40}$ levels strongly correlate with both pTau and aGSK3ß levels (r= 0.91 and r= 0.92, respectively). **C**, aGSK3ß and pTau also strongly correlate (r= 0.83).

Table 3.2. Correlation coefficients

Pearson r	Aß1-40 (pg/ug)	aGSK3ß (%)	pTau/tTau (units/pg)	tTau (pg/mL)	Total protein (ug/mL)	VGLUT1	CHAT	GAD67	iPSC tg expr'n*
Aß	1	0.92	0.91	0.55	0.21	0.03	0.43	0.68	0.28
aGSK3ß	0.92	1	0.83	0.93	0.50	0.39	0.53	0.65	0.31
pTau/tTau	0.91	0.83	1	0.71	0.01	0.08	0.31	0.34	0.05

Very strong correlations (r> 0.9) indicated in red, strong correlations (0.9 >r> 0.7) in greeen, moderate correlations (0.7 >r> 0.5) in blue, and weak or no correlations (r< 0.5) in black.
* iPSC tg expr'n = % of cells expressing the EGFP transgene

I reasoned that if APP proteolytic products, such as Aß, play a causative role in pTau and aGSK3ß elevation, then inhibiting γ- and ß-secretase activity should reduce pTau and aGSK3ß. To further probe this relationship, I treated purified neurons from patient APP^{Dp}2's three iPSC lines with γ-secretase inhibitors (200nM CPD-E or 200nM DAPT) and ß-secretase inhibitors (10μM BACEi-II or 750nM OM99-2) for 24 hours and measured Aß, pTau/tTau and aGSK3ß levels compared to vehicle-treated samples. All inhibitors reduced $Aß^{1-40}$ by similar levels (36-45%) (**Figure 3.4 A**). Intriguingly, I observed that, while neither γ-secretase inhibitor significantly differed from control samples, both ß-secretase inhibitors significantly reduced pTau/tTau and aGSK3ß levels (**Figure 3.4 B-C**). Data are presented per patient in **Figure 3.4** and per iPSC line in **Figure 3.5**. A likely explanation for this finding is that products of ß-secretase cleavage play a larger role in GSK3ß activation and tau phosphorylation than products of γ-secretase cleavage. APP CTFs are

potential culprits, since they are products of ß-secretase cleavage and have a previously defined role in axonal pathology (12, 13).

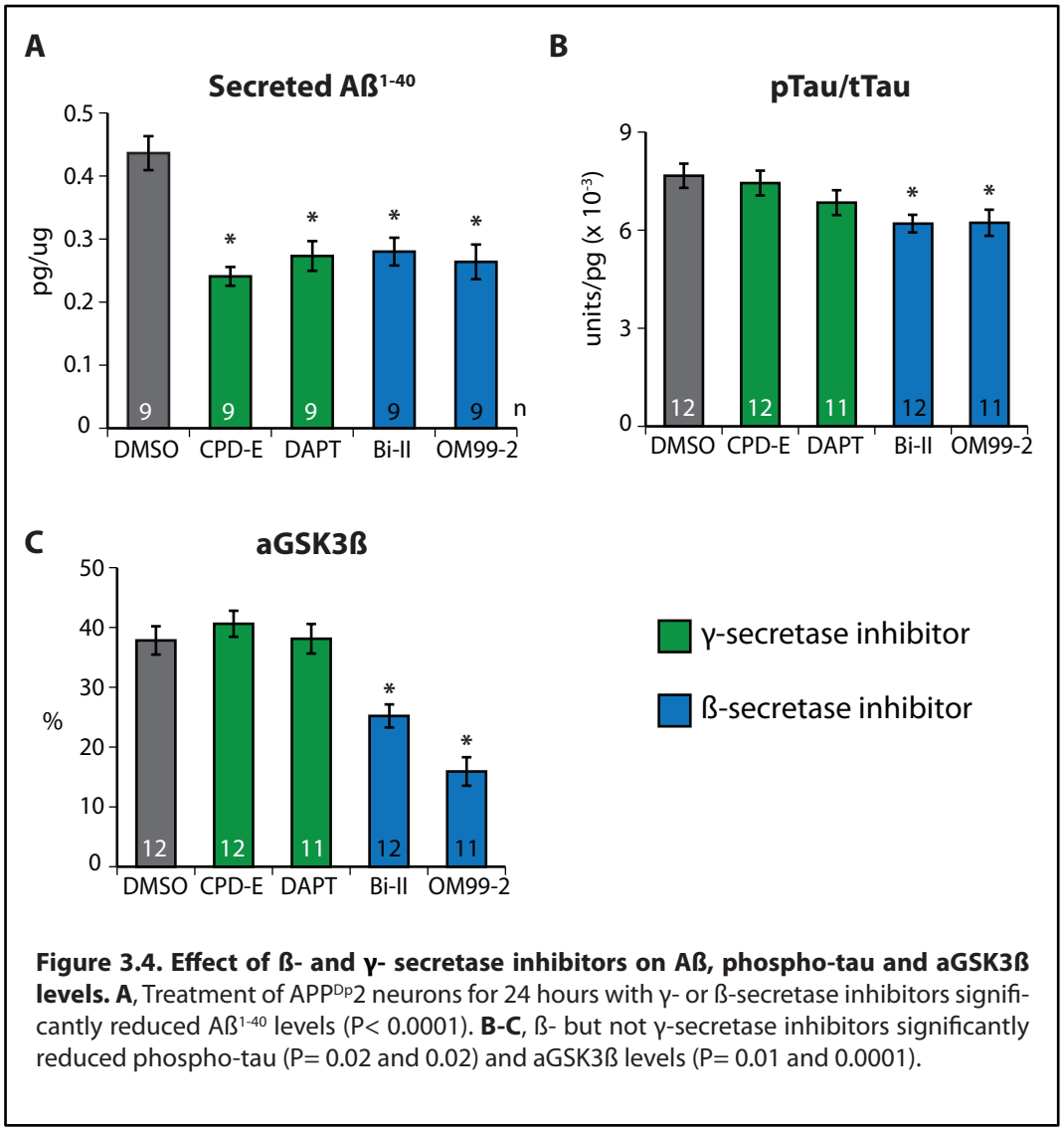

Figure 3.4. Effect of ß- and γ- secretase inhibitors on Aß, phospho-tau and aGSK3ß levels. A, Treatment of APP^{Dp}2 neurons for 24 hours with γ- or ß-secretase inhibitors significantly reduced Aß$^{1-40}$ levels (P< 0.0001). **B-C**, ß- but not γ-secretase inhibitors significantly reduced phospho-tau (P= 0.02 and 0.02) and aGSK3ß levels (P= 0.01 and 0.0001).

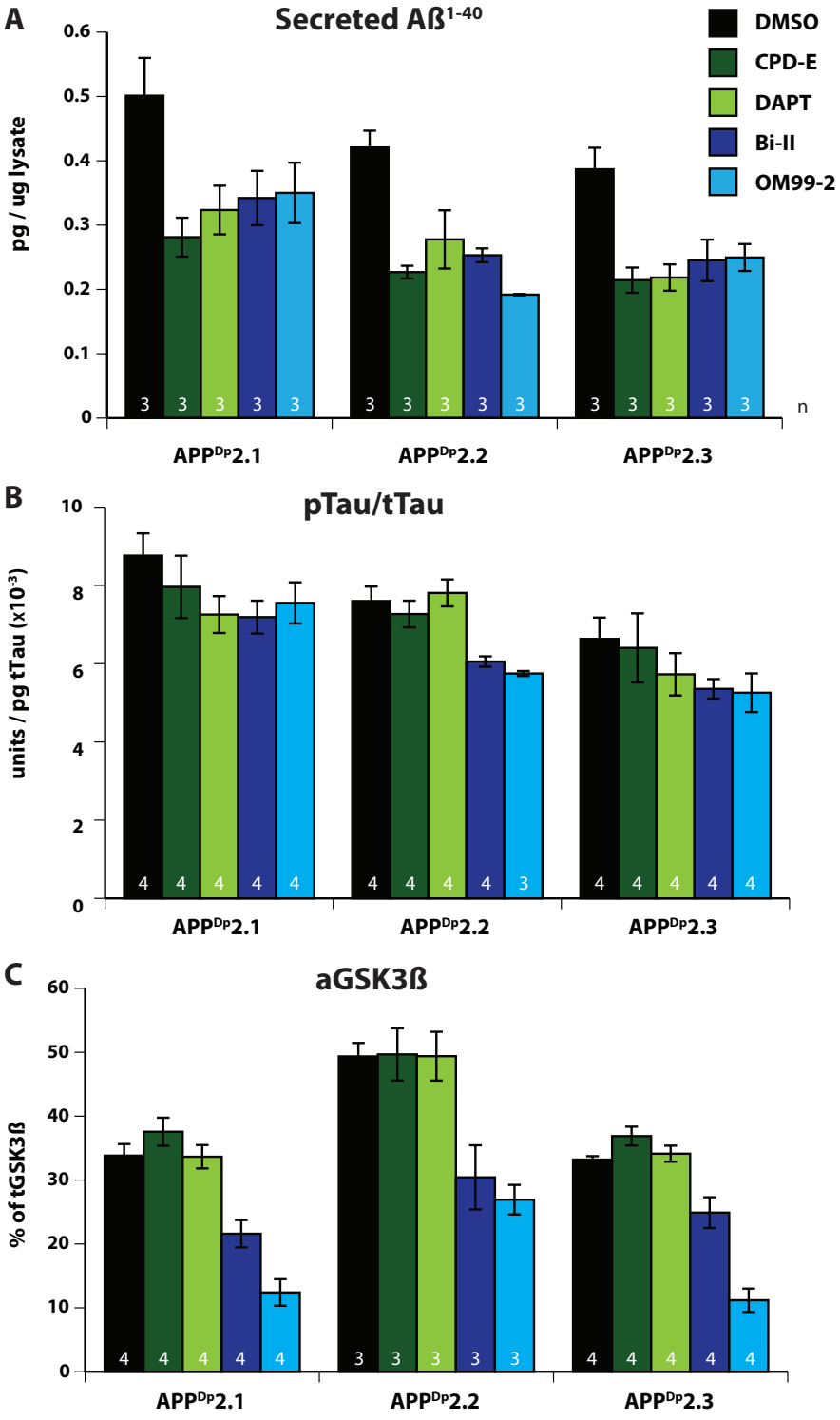

Figure 3.5. Effect of secretase inhibitors for each iPSC line. γ-secretase inhibitors are colored green, ß-secretase inhibitors are colored in blue.

CONCLUSION AND DISCUSSION

Relative to controls, I observed that iPSC-derived neurons from both APP^{Dp} patients and one sporadic AD patient had significantly elevated levels of secreted Aß, phospho-tau and active GSK3ß. Measurements were made on FACS-purified neurons that were less than one month old. These data rest on a solid foundation, as each individual was represented by 3 independently derived iPSC lines, and each line was analyzed in biological replicates. Since elevated levels of Aß and phospho-tau are primary features of the two hallmark pathologies of AD, this strongly suggests that critical aspects of AD pathogenesis are recapitulated in iPSC-derived neurons.

Comparing APP^{Dp} fibroblast Aß levels to Aß from iPSC-derived neurons demonstrated that iPSC-derived neurons are capable of accurately maintaining a disease-specific phenotype. Since it has been reported that not all diseases are accurately modeled with iPSC technology, and AD has yet to be modeled with iPSCs, these data provide important evidence that iPSC technology can be used to model AD. Comparing fibroblast versus neuronal Aß from sporadic AD patients revealed a surprising finding that the neurons of patient sAD2 possess an Aß phenotype not present in the parental fibroblasts. This finding provides important initial evidence that iPSC technology can be used to study aspects of *sporadic* AD pathogenesis (and sporadic diseases in general) in a way previously not possible. Furthermore these data suggest that fibroblasts are not fully predictive of neuronal phenotypes. This observation may explain why studies of sporadic AD using fibroblasts have not been highly fruitful.

This study focused primarily focused on $Aß^{1-40}$ levels, the predominant species of Aß. The levels of other Aß species were generally below the detection range of our

assay. It will be interesting in the future to additionally analyze other Aß species, especially $Aß^{1-42}$, which is commonly thought to be the most pathogenic species. Although in all six individuals the Aß 1-42/1-40 ratios were statistically identical in fibroblasts, it is possible that these ratios could be different in neuronal samples, especially from sporadic patients.

I observed that three out of the four AD patients (*i.e.* $APP^{Dp}1$, $APP^{Dp}2$ and sAD2) had significantly elevated aGSK3ß and phospho-tau levels. These findings are significant not only because phospho-tau is the primary component of a hallmark pathology of AD, but also because aberrant tau behavior is generally not found in mouse models harboring AD mutations. This observation is an important addition to the body of evidence suggesting important species-specific differences in tau biochemistry and AD pathogenesis in general.

Important future experiments are required to determine if the elevated levels of Aß and phospho-tau seen in iPSC-derived neurons from AD patients develop into advanced AD pathologies, such as plaques and tangles. Creating plaques and tangles *in vitro* may require extended periods of culture, but this should be possible with differentiated neurons under the right conditions. An *in vitro* model of tangle formation, derived from human, endogenous genetics, is likely to be highly valued by the AD and dementia fields.

The same three individuals with elevated Aß levels also had significantly elevated aGSK3ß and phospho-tau levels (*i.e.* $APP^{Dp}1$, $APP^{Dp}2$ and sAD2). These data provide new evidence suggesting a close relationship between the APP processing pathway and tau phosphorylation in human neurons. The other three

individuals all had statistically identical levels of Aß, aGSK3ß and phospho-tau, further supporting this close relationship.

I further probed the relationship between APP and tau by treating purified neurons from patient $APP^{Dp}2$ with inhibitors of ß-secretase and γ-secretase. Interestingly, while all inhibitors lowered secreted Aß levels by statistically identical amounts, only the two ß-secretase inhibitors lowered aGSK3ß and phospho-tau levels. These findings support a growing body of evidence that products of the APP processing pathway, other than Aß, drive AD pathologies. As an example, Jiang, *et al*. reported that endosomal pathology in human Down's syndrome fibroblasts was reduced by lowering the expression levels of BACE (the proteolytic subunit of ß-secretase), but was not significantly affected by γ-secretase inhibition (15). My findings are further mirrored in Salehi, *et al.*, where it was reported that axonal phenotypes in a mouse model of Down's syndrome correlated better with levels of ß-secretase products than with γ-secretase products (13). IPSC-derived neurons are likely to be an excellent *in vitro* model to continue elucidating the effects of various derivatives of the APP processing pathway, as well as non-APP products of ß- and γ-secretase cleavage, on AD pathologies, such as aberrant phospho-tau, axonal transport and autophagy.

One important unresolved issue is if different neuronal subtypes would have performed differently in any of the assays. My experiments were performed on purified neuronal cultures that primarily consisted of GABAergic and glutamatergic subtypes. It is commonly thought that forebrain cholinergic neurons are one of the most susceptible neuronal subtype in AD. Although multiple neuronal subtypes degenerate in AD, including GABAergics and glutamatergics, it will be important in

the future to verify findings in cholingeric neurons. This goal will require improved methods of cholingeric differentiation.

Since I observed elevated Aß, aGSK3ß and phospho-tau levels in neurons FACS-purified away from other cell types, such as glia, an important conclusion is that glia and other cell types are not required to maintain these phenotypes. Future studies that mix and match iPSC-derived neurons and glia from controls and patients can further elucidate whether specific aspects of AD pathogenesis are cell autonomous. For example, is a secreted factor causing increased tau phosphorylation?

The close resemblance of the neurons of patient sAD2 to the neurons of the familial AD patients, as opposed to the control neurons, demonstrates that it may be possible to model features of sporadic AD pathogenesis with iPSC-technology. This finding argues against published speculation that iPSC technology may not be able to model sporadic forms of disease (29). This finding also raises multiple new scientific questions. In iPSC-derived neurons, what percentage of sporadic AD patients resemble sAD2 and what percentage resemble sAD1? Since the degree of heterogeneity behind sporadic AD is unclear, addressing this question is an important initial step. Dissecting the heterogeneity of sAD with iPSCs will require a much larger number of iPSC lines than my current study, especially considering the facts that patients are misdiagnosed about 10% of the time and non-demented individuals can develop AD later in life. By power calculations our lab estimates that such an experiment should include 50 sAD patients and 50 controls. A second important question is why did the neurons of sAD2, but not the neurons of sAD1, resemble

familial AD neurons? The genetic cause(s) of aberrant Aß and phospho-tau levels in sAD2 is currently unknown.

An interesting observation that warrants further investigation is that variability in Aß and phospho-tau measurements was greater in the familial AD neurons compared to the control neurons. I hypothesize that this is caused by some familial AD neurons beginning to degenerate while other neurons remain healthy at this early timepoint. Harvesting neurons at multiple timepoints would test this hypothesis.

IPSC technology has been touted as a novel method to validate drugs on human cells. The finding that treatment of iPSC-derived neurons with two different ß-secretase inhibitors partially rescued aberrant Aß, aGSK3ß and phospho-tau levels suggests that this speculated strength of iPSC technology may apply to AD. For diseases that show clear differences between patients and animal models, such as AD, iPSC technology has the potential to serve as an important link between therapeutic development in animal models and clinical trials in patients.

Above all, the findings from this set of experiments demonstrate that iPSC technology can be used to model features of AD pathogenesis, including both the familial and sporadic forms, probe the relationship between APP and tau, and serve as a novel platform for therapeutic validation.

MATERIALS AND METHODS

Purified neuron culture conditions. Refer to chapter 4.

Harvesting of conditioned media and protein. Purified neurons received a full media change at day 3 and conditioned media and protein lysate were harvested 48 hours later (day 5). Cells were in 96-wells with 100μL of neuron media. Harvested

conditioned media was immediately added to cold tubes containing protease inhibitors (Calbiochem) and kept on ice at all times. Samples were centrifuged at 4 degrees to remove detached cells (although few or no floating cells were visible in all of these cultures), and immediately stored at -80 degrees until time of analysis. For protein lysate, 75μL of cold complete MSD lysis buffer (Meso Scale Diagnostics) was added to cultures immediately after conditioned media was removed. Lysates were homogenized by scraping, pipetting and storage on ice for 30 minutes. Samples were then clarified by spinning for 10 minutes at 10,000g. Supernatant was immediately stored at -80 degrees until analysis.

Aß, pTau/tTau and aGSK3ß measurements. Aß was measured with MSD Human (6E10) Abeta3-Plex Kits (Meso Scale Discovery). pTau/tTau was measured with a MSD Phospho(Thr231)/Total Tau Kit. aGSK3ß was measured with MSD Phospho/Total GSK-3b Duplex Kit. For these assays, each patient was represented by 3 iPSC lines, and for each iPSC line, multiple biological replicates were studied. For MSD assays a standard curve was generated and only samples that fell on the linear range were analyzed. Each data point represents an independent biological replicate. Fibroblast and neuronal Aß levels were normalized to total protein levels determined by BCA assay (Thermo Scientific). pTau/tTau was determined by dividing the calculated concentration of pTau by the calculated concentration of tTau. aGSK3ß (the percent of unphosphorylated GSK3ß at Ser9) was calculated by manufacturer's recommendations: [1-(2*phospho signal)/(phospho signal + total signal)]*100.

Inhibitor treatments. CPD-E (Compound-E) and DAPT were used at a final concentration of 200nM. BACEi-II and OM99-2 were used at 10μM and 750nM,

respectively. One µL of inhibitor or vehicle was added to the existing culture media of parallel cultures on day 4 and cultures were harvested on day 5. All inhibitors were from EMD Chemicals.

Statistics. Data were analyzed using JMP software (SAS Institute). $P<0.05$ was considered statistically significant. To compare individuals, ANOVA was used followed by Tukey's HSD posthoc test. For comparison between individuals, biological replicates from all iPSC lines were pooled. To compare drug treatments versus control samples, ANOVA was used followed by Dunnett's posthoc test. Correlations were determined by calculating the Pearson correlation coefficient (r). For MSD experiments, samples that did not fall into the linear range of standard curves were excluded from statistical analysis.

ACKNOWLEDGEMENTS

Chapters 3 contains work submitted for publication by authors: Mason A. Israel, Shauna H. Yuan, Sol M. Reyna, Yangling Mu, Christian T. Carson, Fred H. Gage, Anne M. Remes, Edward H. Koo, Lawrence S. B. Goldstein. The dissertation author was the primary investigator and author of this material.

REFERENCES

1. Querfurth HW & LaFerla FM (2010) Alzheimer's Disease. *New England Journal of Medicine* 362(4):329-344.

2. Tanzi RE & Bertram L (2005) Twenty Years of the Alzheimer s Disease Amyloid Hypothesis: A Genetic Perspective. *Cell* 120(4):545-555.

3. Citron M (2010) Alzheimer's disease: strategies for disease modification. *Nat Rev Drug Discov* 9(5):387-398.

4. Alzheimer A (1907) About a peculiar disease of the cortex (German). *Allg. Z. Psychiat. Med.* 64:146-148.

5. Arriagada PV, Growdon JH, Hedley-Whyte ET, & Hyman BT (1992) Neurofibrillary tangles but not senile plaques parallel duration and severity of Alzheimer's disease. *Neurology.* 42(3 Pt 1):631-639.

6. Buerger K, Teipel SJ, Zinkowski R, Blennow K, Arai H, Engel R, Hofmann-Kiefer K, McCulloch C, Ptok U, Heun R, Andreasen N, DeBernardis J, Kerkman D, Moeller H-J, Davies P, & Hampel H (2002) CSF tau protein phosphorylated at threonine 231 correlates with cognitive decline in MCI subjects. *Neurology* 59(4):627-629.

7. Cleveland DW, Hwo S-Y, & Kirschner MW (1977) Purification of tau, a microtubule-associated protein that induces assembly of microtubules from purified tubulin. *Journal of Molecular Biology* 116(2):207-225.

8. Ballatore C, Lee VMY, & Trojanowski JQ (2007) Tau-mediated neurodegeneration in Alzheimer's disease and related disorders. *Nat Rev Neurosci* 8(9):663-672.

9. Cho J & Johnson G (2003) Glycogen Synthase Kinase 3ß Phosphorylates Tau at Both Primed and Unprimed Sites. *J. Biol. Chem.* 278(1):187-193.

10. Cho J-H & Johnson GVW (2004) Primed phosphorylation of tau at Thr231 by glycogen synthase kinase 3ß (GSK3ß) plays a critical role in regulating tau's ability to bind and stabilize microtubules. *J. Neurochem.* 88(2):349-358.

11. Hoover BR, Reed MN, Su J, Penrod RD, Kotilinek LA, Grant MK, Pitstick R, Carlson GA, Lanier LM, Yuan L-L, Ashe KH, & Liao D (2010) Tau Mislocalization to Dendritic Spines Mediates Synaptic Dysfunction Independently of Neurodegeneration. *Neuron* 68(6):1067-1081.

12. Gunawardena S & Goldstein LSB (2001) Disruption of Axonal Transport and Neuronal Viability by Amyloid Precursor Protein Mutations in Drosophila. *Cell* 32(3):389-401.

13. Salehi A, Delcroix J-D, Belichenko PV, Zhan K, Wu C, Valletta JS, Takimoto-Kimura R, Kleschevnikov AM, Sambamurti K, Chung PP, Xia W, Villar A, Campbell WA, Kulnane LS, Nixon RA, Lamb BT, Epstein CJ, Stokin GB, Goldstein LSB, & Mobley WC (2006) Increased App Expression in a Mouse Model of Down's Syndrome Disrupts NGF Transport and Causes Cholinergic Neuron Degeneration. 51(1):29-42.

14. Nikolaev A, McLaughlin T, O/'Leary DDM, & Tessier-Lavigne M (2009) APP binds DR6 to trigger axon pruning and neuron death via distinct caspases. *Nature* 457(7232):981-989.

15. Jiang Y, Mullaney KA, Peterhoff CM, Che S, Schmidt SD, Boyer-Boiteau A, Ginsberg SD, Cataldo AM, Mathews PM, & Nixon RA (2010) Alzheimer's-related endosome dysfunction in Down syndrome is Aß-independent but requires APP and is reversed by BACE-1 inhibition. *Proceedings of the National Academy of Sciences* 107(4):1630-1635.

16. Campion D, Dumanchin C, Hannequin D, Dubois B, Belliard S, Puel M, Thomas-Anterion C, Michon A, Martin C, Charbonnier F, Raux G, Camuzat A, Penet C, Mesnage V, Martinez M, Clerget-Darpoux F, Brice A, & Frebourg T (1999) Early-Onset Autosomal Dominant Alzheimer Disease: Prevalence, Genetic Heterogeneity, and Mutation Spectrum. *American journal of human genetics* 65(3):664-670.

17. Gatz M, Reynolds CA, Fratiglioni L, Johansson B, Mortimer JA, Berg S, Fiske A, & Pedersen NL (2006) Role of Genes and Environments for Explaining Alzheimer Disease. *Arch. Gen. Psychiatry* 63(2):168-174.

18. Remes AM, Finnila S, Mononen H, Tuominen H, Takalo R, Herva R, & Majamaa K (2004) Hereditary dementia with intracerebral hemorrhages and cerebral amyloid angiopathy. *Neurology* 63(2):234-240.

19. Rovelet-Lecrux A, Frebourg T, Tuominen H, Majamaa K, Campion D, & Remes AM (2007) APP locus duplication in a Finnish family with dementia and intracerebral haemorrhage. *J. Neurol. Neurosurg. Psychiatry* 78(10):1158-1159.

20. Duyckaerts C, Potier M-C, & Delatour B (2008) Alzheimer disease models and human neuropathology: similarities and differences. *Acta Neuropathologica* 115(1):5-38.

21. Guela C, Wu C-K, Saroff D, Lorenzo A, Yuan M, & Yankner BA (1998) Aging renders the brain vulnerable to amyloid ß-protein neurotoxicity. *Nat. Med.* 4(7):827-831.

22. Citron M, Vigo-Pelfrey C, Teplow DB, Miller C, Schenk D, Johnston J, Winblad B, Venizelos N, Lannfelt L, & Selkoe DJ (1994) Excessive production of amyloid ß-protein by peripheral cells of symptomatic and presymptomatic patients carrying the Swedish familial Alzheimer disease mutation. *Proc. Natl. Acad. Sci. U.S.A.* 91(25):11993-11997.

23. Cataldo AM, Peterhoff CM, Troncoso JC, Gomez-Isla T, Hyman BT, & Nixon RA (2000) Endocytic pathway abnormalities precede amyloid beta deposition in sporadic

Alzheimer's disease and Down syndrome: differential effects of APOE genotype and presenilin mutations. *Am J Pathol.* 157(1):277-286.

24. Stokin GB, Lillo C, Falzone TL, Brusch RG, Rockenstein E, Mount SL, Raman R, Davies P, Masliah E, Williams DS, & Goldstein LSB (2005) Axonopathy and Transport Deficits Early in the Pathogenesis of Alzheimer's Disease. *Science* 307(5713):1282-1288.

25. Takahashi K & Yamanaka S (2006) Induction of Pluripotent Stem Cells from Mouse Embryonic and Adult Fibroblast Cultures by Defined Factors. *Cell* 126(4):663-676.

26. Takahashi K, Tanabe K, Ohnuki M, Narita M, Ichisaka T, Tomoda K, & Yamanaka S (2007) Induction of Pluripotent Stem Cells from Adult Human Fibroblasts by Defined Factors. *Cell* 131(5):861-872.

27. Yu J, Vodyanik MA, Smuga-Otto K, Antosiewicz-Bourget J, Frane JL, Tian S, Nie J, Jonsdottir GA, Ruotti V, Stewart R, Slukvin II, & Thomson JA (2007) Induced Pluripotent Stem Cell Lines Derived from Human Somatic Cells. *Science* 318(5858):1917-1920.

28. Ebert AD, Yu J, Rose FF, Mattis VB, Lorson CL, Thomson JA, & Svendsen CN (2009) Induced pluripotent stem cells from a spinal muscular atrophy patient. *Nature* 457(7227):277-280.

29. Saha K & Jaenisch R (2009) Technical Challenges in Using Human Induced Pluripotent Stem Cells to Model Disease. *Cell stem cell* 5(6):584-595.

30. Marchetto MCN, Winner B, & Gage FH (2010) Pluripotent stem cells in neurodegenerative and neurodevelopmental diseases. *Human Molecular Genetics* 19(R1):R71-R76.

31. Lee G, Papapetrou EP, Kim H, Chambers SM, Tomishima MJ, Fasano CA, Ganat YM, Menon J, Shimizu F, Viale A, Tabar V, Sadelain M, & Studer L (2009) Modelling pathogenesis and treatment of familial dysautonomia using patient-specific iPSCs. *Nature* 461(7262):402-406.

32. Dimos JT, Rodolfa KT, Niakan KK, Weisenthal LM, Mitsumoto H, Chung W, Croft GF, Saphier G, Leibel R, Goland R, Wichterle H, Henderson CE, & Eggan K (2008) Induced Pluripotent Stem Cells Generated from Patients with ALS Can Be Differentiated into Motor Neurons. *Science* 321(5893):1218-1221.

33. Soldner F, Hockemeyer D, Beard C, Gao Q, Bell GW, Cook EG, Hargus G, Blak A, Cooper O, Mitalipova M, Isacson O, & Jaenisch R (2009) Parkinson's Disease Patient-Derived Induced Pluripotent Stem Cells Free of Viral Reprogramming Factors. *Cell* 136(5):964-977.

34. Park I-H, Arora N, Huo H, Maherali N, Ahfeldt T, Shimamura A, Lensch MW, Cowan C, Hochedlinger K, & Daley GQ (2008) Disease-Specific Induced Pluripotent Stem Cells. *Cell* 134(5):877-886.

35. Urbach A, Bar-Nur O, Daley GQ, & Benvenisty N (2010) Differential Modeling of Fragile X Syndrome by Human Embryonic Stem Cells and Induced Pluripotent Stem Cells. *Cell Stem Cell* 6(5):407-411.

36. Buerger K, Ewers M, Pirttila T, Zinkowski R, Alafuzoff I, Teipel SJ, DeBernardis J, Kerkman D, McCulloch C, Soininen H, & Hampel H (2006) CSF phosphorylated tau protein correlates with neocortical neurofibrillary pathology in Alzheimer's disease. *Brain* 129(11):3035-3041.

37. Dajani R, Fraser E, Roe SM, Young N, Good V, Dale TC, & Pearl LH (2001) Crystal Structure of Glycogen Synthase Kinase 3ß: Structural Basis for Phosphate-Primed Substrate Specificity and Autoinhibition. *Cell* 105(6):721-732.

APPENDIX I. Recipes for cell culture media

Media name	Cell type	Plate coating	Base media	Serum	Supplements	Growth factors
MEF	MEFs	Gelatin	DMEM	10% FBS	Penicillin/Streptomycin, L-glutamine	None
hFibro	Human fibroblasts	None	DMEM	15% FBS	Penicillin/Streptomycin, L-glutamine, non-essential amino acids	None
iPSC	iPSCs and hESCs	MEFs	KO-DMEM	10% KO serum replacement, 10% Plasmanate (Talecris Biotherapeutics)	Penicillin/Streptomycin, L-glutamine, non-essential amino acids, ß-mercaptoethanol	30ng/mL bFGF (R&D Systems)
PA6	NPC generation	Gelatin	GMEM	10% KO serum replacement	Penicillin/Streptomycin, Sodium pyruvate, ß-mercaptoethanol	None
NPC	NPCs	0.002% poly-ornithine (Sigma), 5ug/mL laminin (Sigma)	DMEM/F12+ Glutamax	1X N2 supplement, 1X B27 supplement	Penicillin/Streptomycin	20ng/mL bFGF (R&D Systems)
Neuron	Differentiating NPCs, purified neurons	0.002% poly-ornithine (Sigma), 5ug/mL laminin (Sigma)	DMEM/F12+ Glutamax	1X N2 supplement, 1X B27 supplement	Penicillin/Streptomycin	20ng/mL BDNF (Peprotech), 20ng/mL GDNF (Peprotech), 0.5mM cAMP (Sigma)

* All reagents from Invitrogen unless noted

APPENDIX II. Sequences of PCR primers

Gene	Application	Orientation	Sequence (5'-)
APP exon17	RT-QPCR	F	TGCATCTGCTCAAAGAACTTG
APP exon17	RT-QPCR	R	CCTTGGTGATGCTGAAGAAGA
APP exon18	Genomic QPCR	F	GCCACAGCAGCCTCTGAAG
APP exon18	Genomic QPCR	R	CACCGATGGGTAGTGAAGCA
APP intron1	Genomic QPCR	F	CGCCTTCCACAGGCAAAC
APP intron1	Genomic QPCR	R	CCATTTCTCGCAAGTTACACAAAA
ChAT	RT-QPCR	F	GGA GGC GTG GAG CTC AGC GAC ACC
ChAT	RT-QPCR	R	CGG GGA GCT CGC TGA CGG AGT CTG
GABA	RT-QPCR	F	TGG CTG ATG GCT CTG TCT TC
GABA	RT-QPCR	R	ACA GTG TCT TGG CTG GGC TG
nanog	RT-PCR	F	TGAACCTCAGCTACAAACAG
nanog	RT-PCR	R	TGGTGGTAGGAAGAGTAAAG
NONO	RT-QPCR	F	GAT GGA ACT TTG GGA TTG ACC
NONO	RT-QPCR	R	TAG TAT CGG CGA CGT TTG TTT

pCX4 transgene	RT-QPCR	F	TCATGTGGGAGCGGCAATTCG
pCX4 transgene	RT-QPCR	R	TGCACTACCAATCGCAATGGCT
SOX2 endogenous	RT-PCR	F	CCCAGCAGACTTCACATGT
SOX2 endogenous	RT-PCR	R	CCTCCCATTTCCCTCGTTTT
ß-globin	Genomic QPCR	F	TGGGCAACCCTAAGGTGAAG
ß-globin	Genomic QPCR	R	GTGAGCCAGGCCATCACTAAA
TBP	RT-QPCR	F	GAACCACGGCACTGATTTTC
TBP	RT-QPCR	R	CCCCACCATGTTCTGAATCT
VGLUT (SLC17a7)	RT-QPCR	F	ACG TGA ACC ACC TGG ACA TAG
VGLUT (SLC17a7)	RT-QPCR	R	CCG TAG AAG ATG ACA CCT CCA

APPENDIX III. Antibody details

Antibody	Conjugation	Species	Dilution	Vendor	Application
α-fetoprotein (AFP)	Unconjugated	Rabbit	1:1000	Millipore	Immunocytochemistry
APPCTF (Zymed)	Unconjugated	Rabbit	1:500	Invitrogen	Western blot
APPFL (22C11)	Unconjugated	Mouse	1:1000	Millipore	Western blot
CD15	FITC	Mouse	1 test per 1x106 cells	BD Biosciences	FACS
CD184	APC	Mouse	1 test per 1x106 cells	BD Biosciences	FACS
CD24	PE-Cy7	Mouse	1 test per 1x106 cells	BD Biosciences	FACS
CD271	PE	Mouse	1 test per 1x106 cells	BD Biosciences	FACS
CD44	PE	Mouse	1 test per 1x106 cells	BD Biosciences	FACS
ChAT	Unconjugated	Goat	1:200	Millipore	Immunocytochemistry
GFAP	Unconjugated	Rabbit	1:1000	Dako	Immunocytochemistry
MAP2a/b	Unconjugated	Mouse	1:500	Millipore	Immunocytochemistry

Nanog	Unconjugated	Rabbit	1:200	Abcam	Immunocytochemistry
Nestin	Unconjugated	Rabbit	1:1000	Santa Cruz	Immunocytochemistry
OCT4	Unconjugated	Mouse	1:1000	Santa Cruz	Immunocytochemistry
PAX6	Unconjugated	Mouse	1:2000	Developmental Studies Hybridoma Bank	Immunocytochemistry
smooth muscle actin (SMA)	Unconjugated	Mouse	1:50	Millipore	Immunocytochemistry
SOX1	Unconjugated	Chicken	1:2000	Millipore	Immunocytochemistry
SOX2	Unconjugated	Rabbit	1:2000	Millipore	Immunocytochemistry
tubulin, α	Unconjugated	Mouse	1:10,000	Sigma	Western blot
tubulin, ßIII (TUJ1)	Unconjugated	Rabbit	1:1000	Millipore	Immunocytochemistry
Tau, total	Unconjugated	Rabbit	1:500	Sigma	Western blot
Tau, total (Tau5)	Unconjugated	Mouse	1:500	Invitrogen	Western blot
TauPHF1	Unconjugated	Mouse	1:500	Pierce	Western blot
TauTHR231	Unconjugated	Rabbit	1:500	Sigma	Western blot

TRA1-81	APC	Mouse	1 test per 1x106 cells	BD Biosciences	FACS
TRA1-81	Unconjugated	Mouse	1:500	Millipore	Immunocytochemistry
anti-mouse secondary antibody	Alexa Fluor 488	Goat	1:200	Invitrogen	Immunocytochemistry
anti-mouse secondary antibody	IR dye 680	Goat	1:2500	Licor	Western blot
anti-rabbit secondary antibody	Alexa Fluor 568	Goat	1:200	Invitrogen	Immunocytochemistry
anti-rabbit secondary antibody	IR dye 800CW	Goat	1:2500	Licor	Western blot